Project N. 037110

NEAREST

Integrated observations from NEAR shore sources of Tsunamis: Towards an early warning system

Instrument: STREP

Thematic priority: 1.1.6.3 GOCE (Global Change and Ecosystems)

D9: broad band OBS data analysis

Due date of deliverable: September 2009
Actual submission date: October 2009

Start date of the project: 01/10/2006   Duration: 36 + 6 months

Organisation name of the lead contractor for this deliverable: AWI

Revision: Final

Project Co founded By the European Commission within the Sixth Framework Programme (2002-2006)		
Dissemination Level		
PU	Public	
PP	Restricted to other programme participants (Including Commission Services)	
RE	Restricted to a group specified by the Consortium (Including Commission Services)	
CO	Confidential, only for members of the Consortium (Including Commission Services)	**CO**

Content

1 Introduction
1.1 Knowledge at the beginning of the NEAREST project

Seismicity summary in the Gulf of Cadiz

The seismicity in the Gulf of Cadiz has been investigated by Fernando Carrilho in his MsC thesis (2005). The main characteristics of the seismicity were: i) an absence of any clear relationship between active faults and seismic activity, only active patches can be identified, related to the Guadalquivir Bank, S. Vicente Canyon and Gorringe Bank; ii) the dominant stress regime is compressive and its average orientation, N30ºE, is rotated northwards from the inferred convergent direction between the Eurasia and Africa plates (Carrilho, 2005). Interpreting the epicentre distribution for the period between 1995 and 1999, when a dense seismic network operated in southern Portugal, the diffuse pattern was attenuated and a few broad aseismic areas could be outlined by Carillho (2005). However, due to the absence of seismic sensors offshore, the seismic activity did not allow a clear association with the known active geological structures in the area.

In his work, Carrilho (2005) made a thorough study of the best-constrained seismic events and the results are shown in figure 1.1. There seems to exist a good correlation between seismicity and the decollement surface interpreted in the AR-10 seismic profile by Zitellini et al. (2001). The number of outliers observed indicates that some caution should be used. Only a long term seismic monitoring with OBS should be able to clarify this relationship between earthquakes and the active faults. Given the above considerations, and the knowledge of the active structures in the Gulf of Cadiz, we proposed the deployment of OBS to clarify the relationship between active structures and seismic events. The most important active faults to be monitored are, from E to W: i) Guadalquivir Bank fault structure; Marquês de Pombal Fault; Horseshoe Fault; Gorringe Bank fault structures. Due to limitations in the number of OBS and deployments in water depths >2000 m (because of fishery and increased noise level), only the last two structures were finally investigated by the NEAREST-OBS array.

1.2 Objectives & planned activities within WP3

The geophysical and geological investigations conducted so far in the Gulf of Cadiz provided an excellent overview on the largest active faults that could generate destructive earthquakes and tsunamis in the future. However, their kinematics and seismic activity were poorly known because the land-based seismic networks do not allow a precise hypocentre location. The event magnitude detection threshold is also very large (greater than 2.5) considering the tsunamigenic sources in the central and western Gulf of Cadiz. Thus, the objectives of WP3 were to characterise the potential tsunamigenic sources in the area through seismological monitoring of natural seismicity by means of 24 Broadband (BB) seismometers deployed for around 9 months. The results obtained were planned to be used for assessment of the location reliability of the seismic node of a future early warning system for tsunamis.

Objectives

Characterisation of tsunamigenic sources through seismological monitoring of natural seismicity by means of 24 BB seismometers deployed for around a year in selected locations of the area.

Description of work

Task 3.1 – Application for the broadband OBS instruments of the German instrument pool (write a proposal, keep application updated) and secure ship time, which is essential for this WP.
Task 3.2 – Preparation of the cruises; ordering of consumables (anchor, batteries, etc.); ordering of sub-contracted technicians for deployment and recovery ordering of mobilisation, demobilisation, transportation and insurance; quality checks at any level of preparation.
Task 3.3 – Cruise for deployment of the broadband OBS; OBS preparation onboard the ship; deployment of the OBS; writing a cruise report

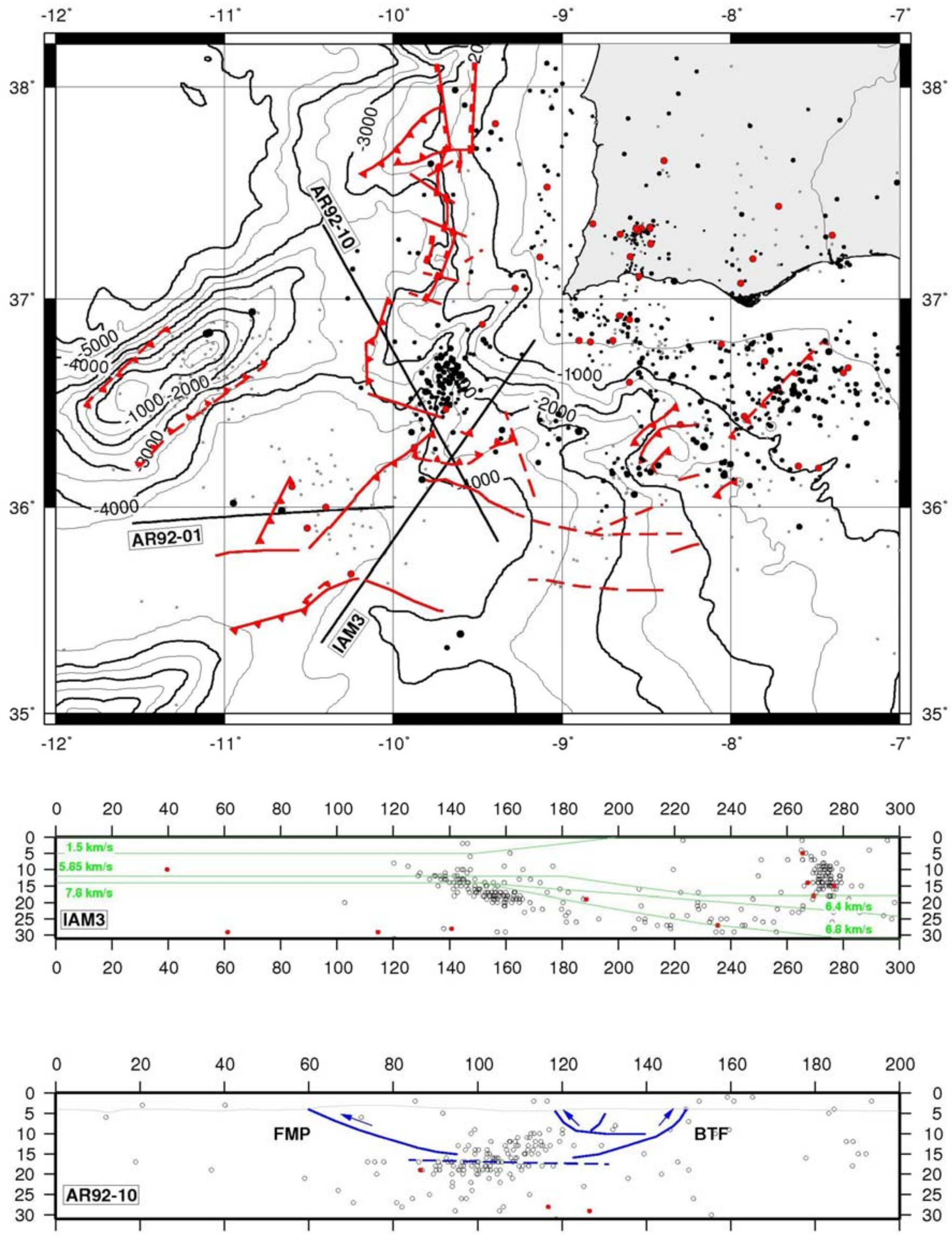

Figure 1.1 – Revised epicentre and hypocentre distributions from Carrilho (2005). One suggestion is that the decollement surface identified in AR-10 profile (Zitellini et al., 2001, 2003) is seismically active. Furthermore, this decollement surface seems to dip to the NE, following the crust-mantle boundary.

Task 3.4 – Cruise for recovery of the broadband OBS; recovery of the OBS download, backup and quality control of data; preparation of the OBS for transportation; writing a cruise report
Task 3.5 – Pre-processing and database compilation; store data in the database of the instrument pool; convert data into desired formats; distribution of the data to the different partners
Task 3.6 – Processing of the OBS data

Deliverables
D7 - Deployment of the broadband OBS: cruise report
D8 - Recovery cruise of broad band OBS, pre-processing data and data base compilation report
D9 – Report of the broad band OBS data analysis

Milestones11 and expected result
M3 - End of the processing of the OBS data and of data quality checks of deep-sea platform

Task 3.6 – Processing of the OBS data
Because of the long deployment of the OBS, only 6 months remained within the life-time of the NEAREST project to analyse the data. This is very a very short time for the huge amount of data collected. Though, the seismic data were processed in parallel among several partners, we recognize that the full exploitation of these data will be completed only after the end of the project. Thus, the tasks that are considered below represent the most important ones regarding the objectives of the project.
(i) Preliminary identification and hypocenter locations of local seismic events
(ii) Precise hypocenter location using: (a) relative and joint techniques; (b) modelling of deeper seismic phases like pP and sS; (c) earthquake taxonomy for the recognition of seismic sequences with the same source area.
(iii) Computation of source mechanism and (when possible) seismic moment tensor for a selection of the largest local events; update of stress indicators
(iv) Preliminary evaluation of a seismic tomography study with local and regional events
(v) Extraction of waveforms for a selection of teleseismic events and preliminary computation of receiver functions
(vi) Integration of land recorded waveforms for a set of the best-located local seismic events
(vii) Computation of station delay corrections for the land network using a set of the best located local seismic events
(viii) Relocation of events using a sub-set of the marine instruments to simulate the performance of future warning systems

2 Activities carried out (OBS and land station deployments, OBS recovery)
2.1 Instrumentation of OBS

In total, 24 DEPAS LOBSTER (**L**ongterm **O**cean **B**ottom **S**eismometer for **T**sunami and **E**arthquake **R**esearch, see figure 1) K/MT 510 manufactured by K.U.M. Umwelt- und Meerestechnik Kiel GmbH, Germany, were used during the experiment. These instruments are equipped with a Güralp CMG-40T broadband seismometer hosted in titanium pressure housing, a hydrophone, and a GEOLON MCS (**M**arine **C**ompact **S**eismocorder) data logger from SEND GmbH Hamburg, Germany. The electric power supply for the recorder and the seismometer was provided by 132 lithium power cells. Each sensor channel was sampled with 100 Hz, preamplifier gain of the hydrophone channel was 4 and 1 for the three seismometer components. The total disk space of the stations is 20 GB. Depending on the local seismic activity and active seismic surveys in the region the disk space can normally cover a recording time of 11 to 12 months. The clock of the data loggers were synchronized by GPS time before deployment, and will be synchronized again after recovery of the instruments. The time difference during the recording period is corrected linearly. The seismometers are equipped with a cardanic levelling mechanism, which will be initiated a few hours after deployment, when the OBS has settled on the seafloor, and then repeated every 15 days (see figure 2.1).

2.2 Deployment cruises in 2007, R/V "Urania", fisher boat "Mario Luis"

The OBS deployment cruise took place from Faro, Portugal (date of departure: 28.08.2008) to Faro, Portugal (date of arrival: 04.09.2008) just after the deployment cruise of the GEOSTAR deep sea observatory. Previous to the deployment, the release units of the OBS were tested under field conditions in 3500m water depth using a winch of R/V Urania. During the test the release code were transmitted three times. After recovery onboard all release hooks were open; thus, the test confirmed the proper function of the releaser at the average operation depth of the survey. During the cruise 22 of 24 OBS were deployed. OBS 24 could not be deployed because the power connector to the recorder pressure tube was damaged. The OBS 07 was deployed for a test measurement (comparison with GEOSTAR) on the 29.08.2007, and recovered successfully two days later. At November 27th, 2007 during another cruise with the fisher boat "Mario Luis" from Portimao (P), the last two OBS were finally deployed (OBS 24 and OBS 25) (see Table 2.2). The OBS network covered an area of about 50.000 km^2 (Figure 2.2). When starting the recording the internal clock was synchronized with a GPS time signal.

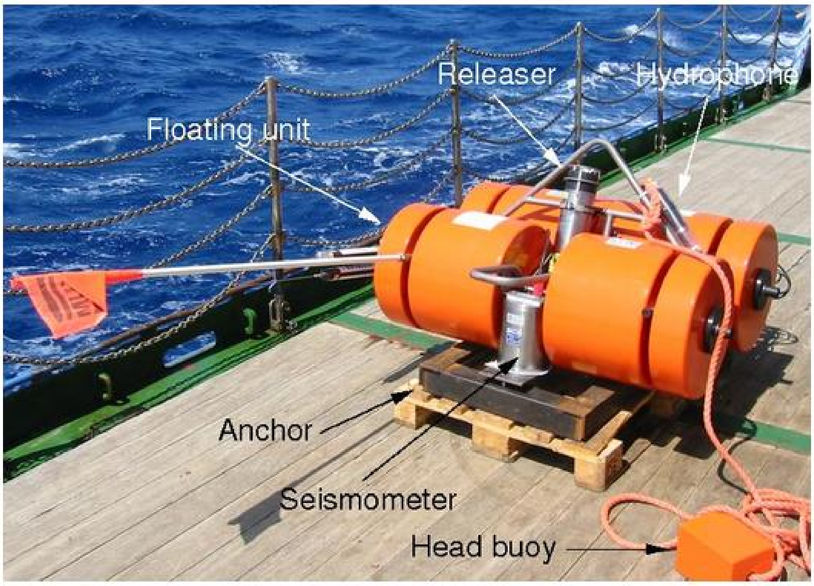

Figure 2.1 – OBS details

Table 2.1 – Technical details Ocean Bottom Seismometer (OBS)

Geophone, gimbal-mounted:	Güralp CMG-40T, 60 sec - 50 Hz
Hydrophone:	HighTechInc HTI-04-PCA/ULF, 100 sec - 8 kHz
Digital data recording unit:	Send Geolon MCS, 24 bit, 1 - 1000 Hz, 20 GB
Acoustic release transponder:	Kum K/MT 562 and Kum K/MT 8011M onboard unit
VHF radio beacon:	Novatec RF-700A1 + Seimac DR500 bearing receiver
Xenon flash:	Novatec ST-400A
Flotation:	Syntactical foam
Frame and pressure tubes:	Titanium alloy
Anchor:	Iron
Max. deployment depth:	6000 meters
Max. deployment duration:	16 months
Dimensions (excl. flag and beacons):	1.65 m x 1.30 m x 0.72 m
Dimensions (incl. flag and beacons):	2.80 m x 1.30 m x 0.72 m
Weight (excl. anchor) in air / in water:	340 kg / -30 kg
Weight (incl. anchor) in air / in water:	405 kg / 27 kg

Test measurement: OBS07 close to GEOSTAR site

To test the operation of the seismic acquisition system of the GEOSTAR observatory OBS07 was deployed close to the GEOSTAR position for only 2 days to allow parallel recording of the seismic activity. The deployment on August 29th and the recovery on August 31st 2007 were conducted without any problems. Levelling of the seismometer was performed 4 hours after recording started and again one day later. The sample rate was 100 Hz, preamplifier gain was 4 for the hydrophone, and 2 for the seismometer channels. The instrument operated without any errors. About 134 MB of data were recorded during this test. Data retrieval from MCS recorders was performed using send2x software. However, airgun signals from an active seismic survey of Spanish scientists onboard the French R/V L'Atalante performed during that time dominated the recorded signals. Nevertheless, two small local earthquakes were detected.

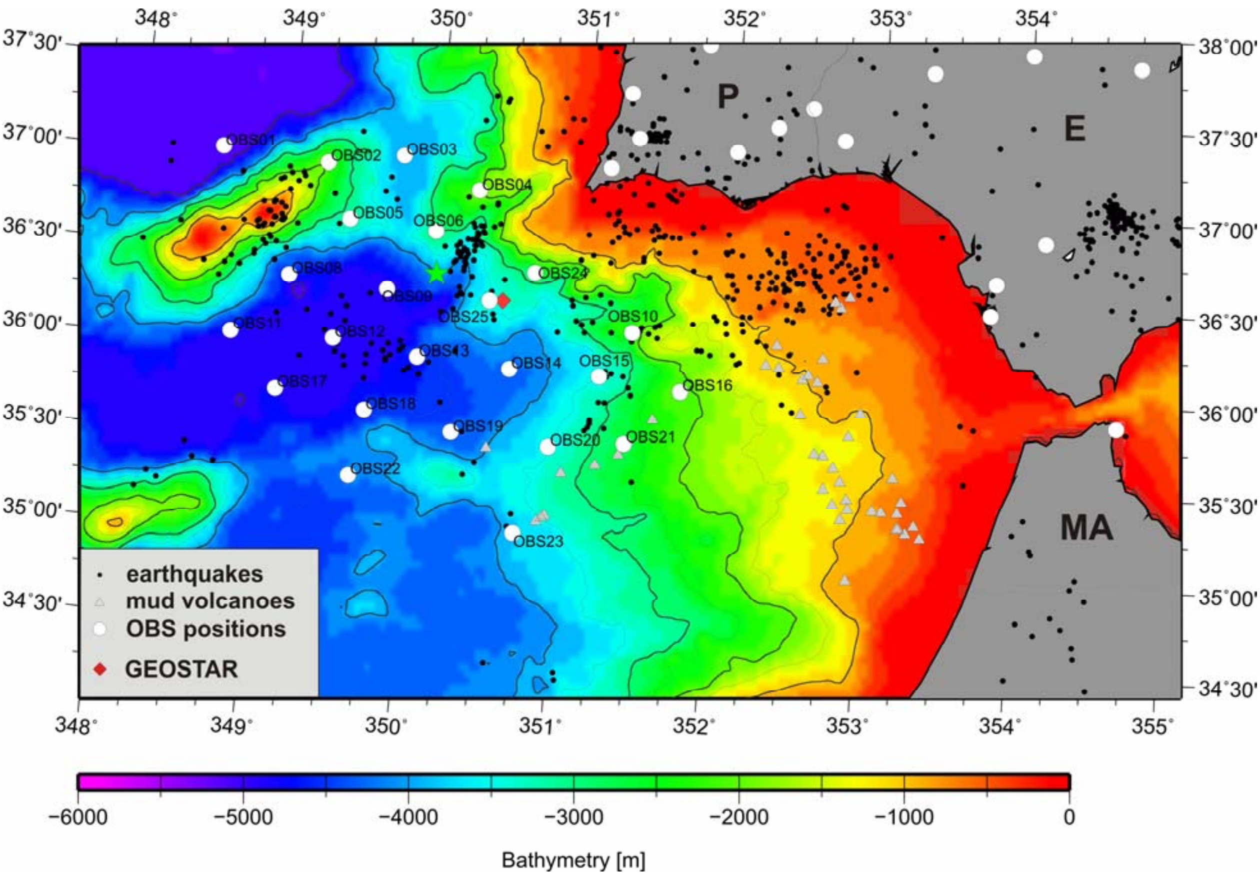

Figure 2.2 – Location of the NEAREST OBS network. Depth contours every 1000m.

2.3 Recovery cruise in 2008, R/V "Urania"

The recovery cruise started in Palermo, Italy (date of departure: 01.08.2008) and terminated in Faro, Portugal (date of arrival: 12.08.2008). All deployed OBS (24) were recovered without any damage. Previous to the recovery, the ship was stopped at 1nm for shallow OBS (2000 to 3000 m water depth) and at 2 nm from the deployment positions to send the release code. For the first two OBS on the track (OBS 16 and 21) a complete set of range measurements was performed. During rise of OBS 16 and 21 we continued to measure the range, and estimated an OBS rise velocity of 1.2 m/s. The rise velocity was used to calculate the time for all the remaining stations. With the remaining stations there were big problems to detect the responding acoustic code, which was already observed during the releaser test 2007. Possible causes might be a strong layering (stratification) of the water column or the noise of R/V Urania itself. Sometimes after sending the release code, we tried to get the range close to the expected recovery position to monitor the rise of the OBS. In most cases we got answers from the releaser units starting from a distance of at about 3600 m from the rising OBS. After transmitting the release code the ship was positioned a few hundred meters away from the expected position of emergence at the surface. In most cases the station was located by eye. A flag attached to each OBS was helpful at day, the flash light at night.

Table 2.2 – Mean station coordinates.

OBS Nr.	deployment			recovery			mean		deviation		water depth
	date (UTC)	lat [°]	lon [°]	date (UTC)	lat [°]	lon [°]	lat [°]	lon [°]	lat [°]	lon [°]	[m]
OBS 01	30.08.2007	37.050	-11.450	10.08.2008	37.060	-11.445	37.055	-11.448	0.005	0.002	5100
OBS 02	30.08.2077	37.026	-10.734	10.08.2008	37.024	-10.734	37.025	-10.734	0.001	0.000	2270
OBS 03	30.08.2007	37.100	-10.230	10.08.2008	37.100	-10.228	37.100	-10.229	0.000	0.001	3932
OBS 04	29.08.2007	36.950	-9.700	09.08.2008	36.954	-9.704	36.952	-9.702	0.002	0.002	1993
OBS 05	29.08.2007	36.730	-10.550	11.08.2008	36.730	-10.553	36.730	-10.552	0.000	0.002	3095
OBS 06	29.08.2007	36.710	-9.969	09.08.2008	36.707	-9.969	36.708	-9.969	0.002	0.000	2956
OBS 07	29.08.2007	36.365	-9.497	31.08.2007	36.366	-9.495	36.366	-9.496	0.000	0.001	3205
OBS 08	30.08.2007	36.400	-10.920	10.08.2008	36.395	-10.922	36.398	-10.921	0.002	0.001	4671
OBS 09	29.08.2007	36.370	-10.260	09.08.2008	36.373	-10.262	36.372	-10.261	0.002	0.001	4811
OBS 10	01.09.2007	36.250	-8.600	11.08.2008	36.250	-8.603	36.250	-8.601	0.000	0.001	2067
OBS 11	30.08.2007	36.069	-11.270	10.08.2008	36.062	-11.276	36.066	-11.273	0.003	0.003	4855
OBS 12	31.08.2007	36.080	-10.590	09.08.2008	36.081	-10.590	36.081	-10.590	0.001	0.000	4860
OBS 13	31.08.2007	36.020	-10.020	07.08.2008	36.023	-10.020	36.022	-10.020	0.002	0.000	4494
OBS 14	02.09.2007	36.000	-9.400	11.08.2008	36.001	-9.401	36.001	-9.400	0.001	0.000	2439
OBS 15	01.09.2007	36.000	-8.800	11.08.2008	35.997	-8.799	35.999	-8.800	0.001	0.000	3357
OBS 16	01.09.2007	35.950	-8.250	06.08.2008	35.949	-8.251	35.950	-8.251	0.000	0.001	2069
OBS 17	30.08.2007	35.780	-10.939	09.08.2008	35.778	-10.940	35.779	-10.939	0.001	0.000	4765
OBS 18	31.08.2007	35.710	-10.340	07.08.2008	35.713	-10.338	35.711	-10.339	0.001	0.001	4605
OBS 19	31.08.2007	35.630	-9.750	07.08.2008	35.635	-9.751	35.633	-9.751	0.003	0.001	4287
OBS 20	01.09.2007	35.600	-9.100	06.08.2008	35.596	-9.099	35.598	-9.100	0.002	0.000	3449
OBS 21	01.09.2007	35.650	-8.600	06.08.2008	35.641	-8.601	35.646	-8.600	0.004	0.000	2566
OBS 22	31.08.2007	35.350	-10.400	07.08.2008	35.348	-10.403	35.349	-10.402	0.001	0.002	4095
OBS 23	01.09.2007	35.117	-9.285	06.08.2008	35.118	-9.289	35.117	-9.287	0.000	0.002	3747
OBS 24	27.11.2007	36.532	-9.283	11.08.2008	36.531	-9.281	36.531	-9.282	0.001	0.001	2439
OBS 25	27.11.2007	36.361	-9.573	11.08.2008	36.358	-9.570	36.360	-9.571	0.001	0.002	3234

Unknown regular signals (one ping about every 10 seconds) were recorded as "answers" by the deck unit at stations OBS23 and later at OBS14 (The signals disappeared at station OBS14 during the ranging).

The recovery onto the deck was possible in most cases within 10 to 15 min after the appearance of the OBS at the sea surface due to the good work of the bridge and the deck crew. During the recovery an entering hook and a crane was used. The position of recovery at deck was taken to calculate the mean coordinate of the OBS at depth from deployment and recovery coordinates. In most cases the difference in coordinates between deployment and recovery is very small (0.001° to 0.003°).

Immediately after recovery of the OBS on deck, we tried to manually stop the recording and synchronize the internal clock with GPS time signal using a SENDCOM-3 interface. With only few exceptions, all stations stopped recording already before recovery due to the following reasons: "disk full" and "battery low". The first cause was expected due to the length of the period of operation and the high sampling rate. All recorders of the 9 stations with full disks stopped recording properly and allowed a GPS synchronisation without any problems. The "battery low" message at 9 stations was unexpected, since the capacity of the 132 Li cells was estimated to be enough for 12 month recording. The battery low was that severe (with only one exception), that even there was not enough power left to keep the clocks running (although there is a safety mode, which worked for one station). Therefore, the recorder lost the synchronisation, and we were not able to measure the time shift of the internal clock.

After stopping the recording, the stations were cleaned and dismounted. All removable components were stored in boxes, the LOBSTER itself were stacked and stored onboard. With the exception of two stations (OBS16, OBS21) the stations were in very good conditions after recovery. These two stations showed corrosion at the power connectors of the recorder tube. Similar corrosion was maybe the cause of the failure of one power connector during the first deployment cruise in 2007. There was almost no carbonate patina as it was observed before in the Mediterranean Sea during the EGELADOS experiment.

Table 2.3 – Recording parameters.

OBS Nr.	Recorder SN	Start Recording (UTC)	Stop Recording (UTC)	data recorded	Synchronized (UTC)	synchtime (secs)	skew time (UTC)	skew time (sec)	skew [µs]	recalibration	comments
OBS 01	050919	30.08.2007 07:52:52	12.06.2008 21:59:37	16071096 kb	30.08.2007 07:51:45	236677905	-		not synchronized		battery low, recorder off
OBS 02	050916	30.08.2007 03:47:35	22.05.2008 14:16:42	15305614 kb	30.08.2007 03:45:31	236663131	-		not synchronized		battery low, recorder off
OBS 03	060741	29.08.2007 23:53:25	31.07.2008 16:10:57	18469887 kb	29.08.2007 23:51:33	236649093	-		not synchronized		battery low, recorder off
OBS 04	050901	29.08.2007 22:10:32	25.06.2008 17:42:20	19513715 kb	29.08.2007 22:08:09	236642889	09.08.2008 07:39:37	266485177	+1456156	183	disk full, sleeping mode
OBS 05	050924	29.08.2007 16:59:04	23.06.2008 16:37:44	16570501 kb	29.08.2007 16:57:35	266493923	-		not synchronized		battery low, recorder off
OBS 06	050910	29.08.2007 18:56:59	20.07.2008 07:14:42	19513715 kb	29.08.2007 18:55:54	236631354	09.08.2008 10:05:23	266493923	+1427375	477	disk full, sleeping mode
OBS07	050904	29.08.2007 10:35:26	31.08.2007 09:54:12	133668 kb	29.08.2007 10:33:14	872418794	31.08.2007 09:55:39	872589339	+156	47	
OBS 08	050923	30.08.2007 13:09:59	10.08.2008 08:37:04	18758201 kb	30.08.2007 13:01:55	236696515	10.08.2008 08:37:26	266575046	+494781	40	still recording, stop by END
OBS 09	050921	29.08.2007 14:02:56	29.04.2008 20:20:08	13172897 kb	29.08.2007 14:01:42	236613702	-		not synchronized		battery low, recorder off
OBS 10	050912	01.09.2007 20:32:16	29.06.2008 16:07:25	19513716 kb	01.09.2007 20:30:45	236896245	12.08.2008 00:28:45	266718525	-116438	-79	disk full, sleeping mode
OBS 11	050913	30.08.2007 18:03:02	02.05.2008 15:51:21	12288701 kb	30.08.2007 18:02:10	236714530	10.08.2008 03:43:48	266557428	+996218	203	batt. low, recording ended, sleeping mode
OBS 12	050915	30.08.2007 23:12:43	21.07.2008 09:09:57	19513715 kb	30.08.2007 23:11:28	236733088	09.08.2008 17:57:09	266522229	+280875	-6	disk full, sleeping mode
OBS 13	050909	31.08.2007 10:52:51	14.07.2008 23:52:24	17458792 kb	31.08.2007 10:51:47	236775107	-		not synchronized		battery low, recorder off
OBS 14	050926	02.09.2007 02:50:51	04.08.2008 15:34:01	19513715 kb	02.09.2007 02:49:51	236918991	11.08.2008 18:06:13	266695573	-3671407	-497	disk full, sleeping mode
OBS 15	050917	01.09.2007 19:36:09	07.04.2008 06:54:36	19513715 kb	01.09.2007 19:35:10	236892910	11.08.2008 22:02:11	266709731	-80907	-129	disk full, sleeping mode
OBS 16	050927	01.09.2007 10:40:59	07.07.2008 04:02:47	19513715 kb	01.09.2007 10:40:08	236860808	06.08.2008 07:46:16	266226376	-4257563	-595	disk full, sleeping mode
OBS 17	050906	30.08.2007 21:24:09	28.05.2008 21:00:33	15023160 kb	30.08.2007 21:14:35	236726075	-		not synchronized		battery low, recorder off
OBS 18	050905	31.08.2007 14:41:10	18.07.2008 03:13:29	19513716 kb	31.08.2007 14:39:18	236788758	07.08.2008 12:09:52	266328592	-2592782	-471	disk full, sleeping mode
OBS 19	060743	31.08.2007 19:03:44	17.07.2008 17:03:37	19513716 kb	31.08.2007 19:02:53	236804573	07.08.2008 03:44:13	266298253	-3357407	-304	disk full, sleeping mode
OBS 20	050907	01.09.2007 03:40:33	12.07.2008 10:31:17	19513716 kb	01.09.2007 03:39:41	236835581	06.08.2008 16:06:03	266256363	-3239282	-769	disk full, sleeping mode
OBS 21	050928	01.09.2007 07:28:02	09.07.2008 06:01:13	19513715 kb	01.09.2007 07:27:05	236849225	06.08.2008 11:55:51	266241351	-2494594	-312	disk full, sleeping mode
OBS 22	050925	31.08.2007 17:02:54	24.07.2008 17:54:03	17827192 kb	31.08.2007 17:01:55	236797315	-		not synchronized		battery low, recorder off, no END mark
OBS 23	050918	31.08.2007 23:21:49	28.06.2008 21:03:08	16435417 kb	31.08.2007 23:20:35	236820035	-		not synchronized		battery low, recorder off
OBS 24	050903	27.11.2007 03:21:27	11.08.2008 11:15:32	17422768 kb	27.11.2007 03:20:46	244351246	11.08.2008 11:15:53	266670953	+266562	-333	still recording, stop by END
OBS 25	050904	24.11.2007 12:00:04	11.08.2008 14:09:54	16620292 kb	24.11.2007 11:57:58	244123078	11.08.2008 14:10:01	266681401	-70750	33	still recording, stop by END

After the recorder tube was cleaned, the recorder was taken off from the tube and connected to the Desktop PC by FireWire. Data retrieval from MCS recorders was performed using send2x software (*mcscopy*). Afterwards the raw data were decompressed into s2x format using *mcsread*. The final stage of first data conversion on the ship was the conversion into mseed format (*seedwrite*) to allow the very first quality check of the data. Two copies of the raw data were saved on external hard disks (less than 500 GB disk space), a third one on DLT tapes. Furthermore, one copy of the uncompressed s2x-files (altogether more than 1 TB) and two copies of mseed data (500 GB) were save on external hard disks.

The first checks onboard showed that 9 stations lost the time (the clock wasn't running anymore) because of problems with the battery voltage and the recording was terminated. So it wasn't possible to get the time shift (skew) of the internal clock. At 11 stations the disk was full and the recording was normally ended. These stations allowed synchronization with the GPS time without any problems. Three stations were still recording during recovery. A result of the onboard data evaluation was that most probably not all seismometer components levelled well. The hydrophones seemed to work properly.

2.4 Installation of land stations MESJ, PDRG

Within the frame of NEAREST project two new very-broadband seismological stations were installed in southern Portugal by IGIDL in cooperation with CGUL to complement the existing seismic onshore network. The best sites we have found are on public lands with nearby power and away from significant sources of cultural noise (roads, highways, railroads, etc). Data will be available trough the University of LISbon SEISmic network using a standard ftp protocol.

MESJ – Messejana, Pêro Beco, Portugal

Geology: dolerite

Site description: A hole was dig, with approximately 60 cm depth, which was large enough to contain two boxes, one with the sensor and the other one with the recording system (Figure 2.4). The loose weathered material was removed until an approximately level and flat piece of solid rock, large enough to hold the seismometer, was exposed. Thermal insulation has then been done using blue insulation foam. The recording system was installed in a separated box, together with two batteries, for protection against humidity. To have the sensor in its own box and the recorder apart avoid disturbing the sensor when servicing to the equipment is done. The vault was then covered and solar panels installed.

Figure 2.3 – Geographical location of the *MESJ VBB seismic station

Figure 2.4 - The hole with 60 cm deep and the two boxes, and the pier with the rock outcropping surrounding by the insulating box.

Station Instrumentation:
1. *Seismometer Type***:** Streckeisen tri-axial STS2.
2. *Seismic Data Acquisition System:* Reftek 130-01 (6 channels running at 100 sps and 20 sps).
3. *Network*: LX - University of LISbon SEISmic network
Centro de Geofisica da Universidade de Lisboa
4. *Operation:* 04 Jul 2007 to present.

Tab. 2.4 – Station Information MESJ

Code	Latitude	Longitude	Altitude (m)	Depth of Sensor (m)
MESJ	37º50.3743´N	08º13.1959´W	230	-0.6

Figure 2.5 – The Reftek 130-01 station and the two batteries (12 V –each other) were placed in another box. The batteries are powered by one solar panel (60 w).

PDRG – Pedrógão, Sítio do Borlão, Portugal

In this installation we concentrated on two main aspects, which have the largest impact on the overall performance of a seismic station housing a broadband seismometer. The aspects of the installation, which most influence the overall performance of the broadband seismometer, are the construction of the seismic pier and the application of thermal insulation around the sensor and pier.

Figure 2.6 – Geographical location of the PDRG VBB seismic station.

Geology: granite

Site description: A hole was excavated, with a depth of 60, large enough to deploy the boxes containing the sensor and the recording system. The loose weathered material was removed until an approximately level and flat piece of solid rock, large enough to hold the seismometer, was exposed (figure 2.7).

After setting up the seismometer, it was covered with an insulating box made of blue insulation foam. The Reftek 130-01 station and the two batteries (12V - each other) were placed in another box, to avoid sensor perturbation, each time we have to exchange station hard disks. The batteries are powered by solar panel (60W). The vault was closed and the whole area was fenced regarding better protection.

Figure 2.7 – The pier with the rock outcropping and the box that insulated the sensor.

Station Instrumentation:
1. Seismometer Type: Streckeisen tri-axial STS2
2. Seismic Data Acquisition System: Reftek 130-01 (3 channels running at 100 sps and 20 sps)
3. Network: LX - University of LISbon SEISmic network
Centro de Geofisica da Universidade de Lisboa
4. Operation: 28 Jun 2007 to present.

Figure 2.8 – The Reftek 130-01 station and the batteries were placed in another box. The batteries are powered by solar panel.

Tab. 2.5 – Station Information PDRG

Code	Latitude	Longitude	Altitude (m)	Depth of Sensor (m)
PDRG	38º06.4721´N	07º38.2956´W	102	-0.6

3 Data
3.1 OBS data, quality checks, orientation, problems etc.

Most of the data quality control was done using software SEISMIC HANDLER (Stammler et al., 1995) and SEISAN (Havskov & Ottemöller, 2005). First of all, the correct levelling of the seismometer components were controlled. At the beginning of operation, normally all three components of the seismometer are not in the centre position. Therefore, the levelling was forced a few hour’s after the deployment and repeated regularly every 15 days during the deployment period. The levelling shown in figure 3.1 took about 85 seconds. The result of the check was that only at 9 stations all components levelled well from the beginning of the recording (Table 3.1; labelled green). OBS 4 and 14 showed a successful levelling in all components after 1 month and after 5 month all components of OBS 6 were levelled as well. Many times one component (mainly the X component) was clipped during the whole recording time (Table 3.1; labelled yellow). At station no. 2 and 11 two components were not levelled (Table 3.1; labelled red).

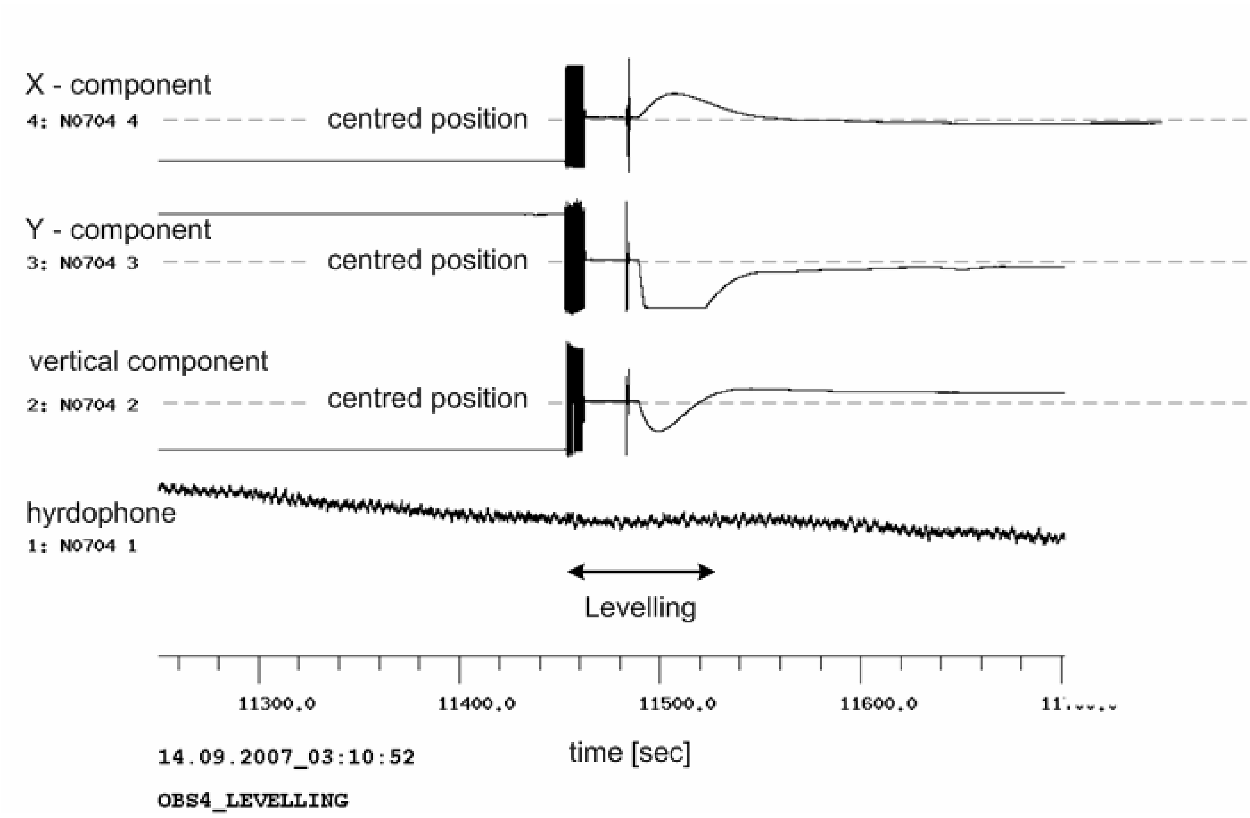

Figure 3.1 – Seismogram example of second levelling of OBS04 after the first levelling had failed 15 days before. The bottom trace shows the hydrophone channel. Above the three seismometer channels are shown.

Problems

Levelling problems

Unfortunately, not all of the seismometer components levelled properly during the deployment. The reason is still not exactly known. Most probably, it is related some internal parts of the seismometer. The sensors were sent to Guralp Ltd. after the experiment to solve the problem, and the modified sensors were successfully tested in summer 2009.

Table 3.1 – Results of data quality checks for timing and levelling.

		2007									2008														
		02/aug	01/sep	02/sep	01/oct	02/oct	01/nov	02/nov	01/dec	02/dec	01/jan	02/jan	01/feb	02/feb	01/mar	02/mar	01/apr	02/apr	01/may	02/may	01/jun	02/jun	01/jul	02/jul	01/aug
OBS 1	s	x																							
OBS 2	s	xz					z	xz	z				yz												
OBS 3	s	x																							
OBS 4		xyz																							
OBS 5	s	x																							
OBS 6		x																							
OBS 7																									
OBS 8		x																							
OBS 9	s	x																							
OBS 10																									
OBS 11		xz																							
OBS 12																									
OBS 13	s	x																							
OBS 14		x																							
OBS 15		y																							
OBS 16																									
OBS 17	s	x																							
OBS 18																									
OBS 19																									
OBS 20																									
OBS 21																									
OBS 22	s	x																							
OBS 23	s	x																							
OBS 24																									
OBS 25																									

	everything okay	OBS 1	battery low
	1 comp. Dead	OBS 4	time okay,stop by END
	2 comp. Dead	OBS 4	time okay, disk full
	3 comp. Dead	s:	not synchronized

Power problems

During the deployment 10 OBS failed in continuous operation until the end, since the batteries got unexpectedly low after several months. The manufacturer of the OBS (KUM Kiel GmbH) did tests to identify the source of increased power consumption. They found out that the problem is related to not-levelled seismometer components. If the components are not in the centre position, the seismometer needs more power since the electronics try to compensate for the offset.

The other problem with the increased power consumption was that the recorder did not stop recording before the batteries were empty. Normally, there is a safety switch in the software, which should stop operation when the battery voltage reaches a certain low level. But unfortunately, only one instrument went into the safety mode and kept the time information from the internal clock until recovery in August 2008. All the other instruments lost the internal clock, so that no time drift could be measured after recovery. The strong power consumption of the starting hard disks most probably leads to extreme power lows which finally lead to stop of all operations of the recording system. This is a major problem, because there might be time drifts of the internal clocks in the order of ±4 seconds, which is crucial for location of local events and also for teleseismic tomography.

Time correction

No time correction was actually done by conversion codes of SEND, which was only recovered during working on OBS data. Since the time drift can be in the order of 4s/year, this is crucial for the location of local earthquakes. Since no correction routine could be provided in time by the producer of the recording system, scripts had to be programmed. One script allows time correction of daily mseed files. The second corrects SEISAN waveforms and picks for the time drift.

OBS orientation

The OBS with its three-component seismometer have an unknown orientation on the seafloor. There is an electronic compass onboard; however, test showed that they cannot be used at the moment. The magnetic field around the compass is dominated by the anchor weight (made from steel). Therefore, the orientation of the OBS was estimated from the polarisation of teleseismic P phases in the period range 15 to 35 s. Results are shown in Table 3.3.

Table 3.3 – OBS orientation from polarisation analyses of teleseismic P phases

OBS	azimuth (mean)	n	σ
25	119	5	9
24	noisy		
21	338	3	18
20	29	6	11
19	132	5	4
18	12	5	5
16	noisy		
14	249	3	8
12	94	3	8
10	103	4	3
06	noisy		
04	342	3	10

3.2 GEOSTAR

During the NEAREST project there was a close cooperation with WP4 regarding the registration of seismic signals at GEOSTAR observatory and nearby OBSs. GEOSTAR was equipped with a GEOSTAR Guralp CMG-40T seismometer 30s-50 Hz (OBS), Guralp CMG-5T accelerometer DC-50 Hz (ACC), OAS hydrophone DC-50 Hz (HYD) and a DM24 GURALP digitizer (24 bit).

Data quality assessment has been performed both in time and frequency domain using SAC software. We report different types of data disturbances and their cause:

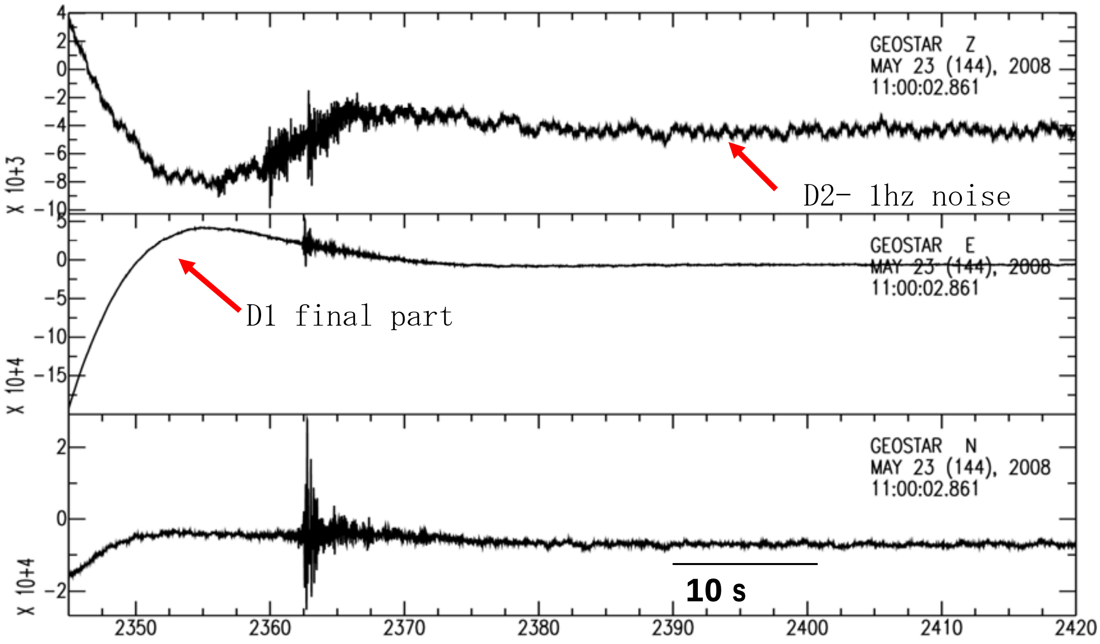

Figure 3.2 – Unfiltered recording of a local seismic event on the GEOSTAR-OBS, where disturbances D1 (final part) and D2 are visible.

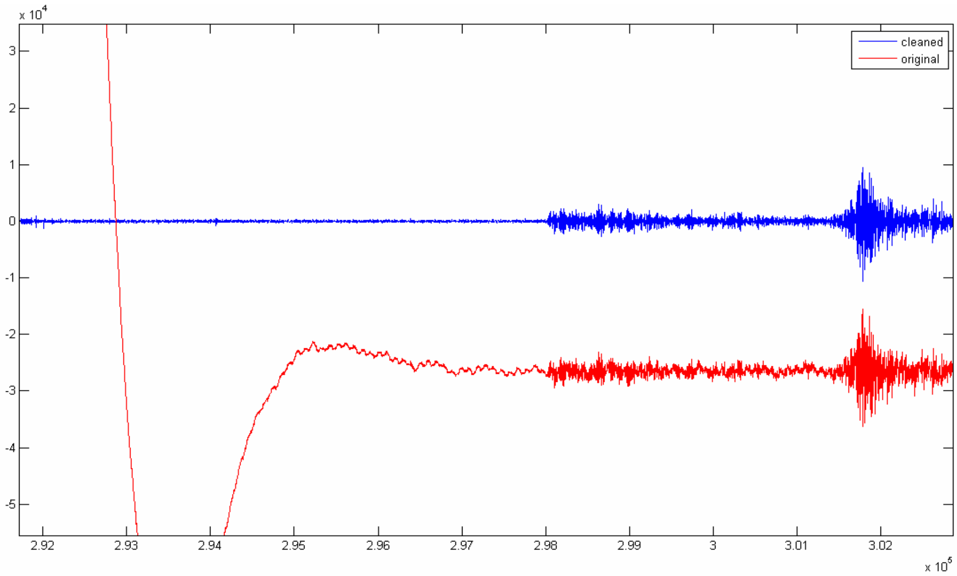

Figure 3.3 – Example of signal cleaning from disturbances D1 and D2 using the spline interpolation method. Original signal is in red, cleaned signal is in blue. A local event is included in the recording (on the horizontal scale are counts).

1) High amplitude disturbance (D1) visible on all 6 components of OBS and ACC. This disturbance is present during the entire mission time and recurs about every 145 s lasting about 50 s, and unfortunately it has energy at all frequencies. After tests and collaboration from Guralp LTD we discovered that the disturbance is caused by continuous re-centering of the levelling platform. This behaviour is due to the presence of a too small condenser (should be 100 times larger) in the levelling platform control line, based on an interrupt-control system, as Cansun Guralp explained. Such a small condenser made the system too sensitive to electronic spikes.

2) High frequency (~1 Hz) disturbance (D2) with amplitude a bit higher than the background noise (~2 times) in the frequency range 4-12 Hz where local events have greater energy.
3) A third type of disturbance (D3), associated with loss of data (~45 minutes), is caused by frequent rebooting of the SDU (Seismometer Data-Handling Unit) connected to the GURALP DM24 digitizer. D3 is present from the beginning of the mission, at very frequent rates (about every hour). After 24/10/08 D3 happens once a day at 21:15:04, and sporadically also at another hour. Another problem is the presence of gaps in data, due to loss of data packets during transmission from the DM-24 to the DAU (Data Acquisition Unit). Statistics show that data is in total (including loss of data due to D3) 95 % of total for both OBS and ACC. Unfortunately, the HYD was malfunctioning from the beginning of the mission due to failure caused very possibly by initial damage of the instrument during a rough deployment.

a)

b)

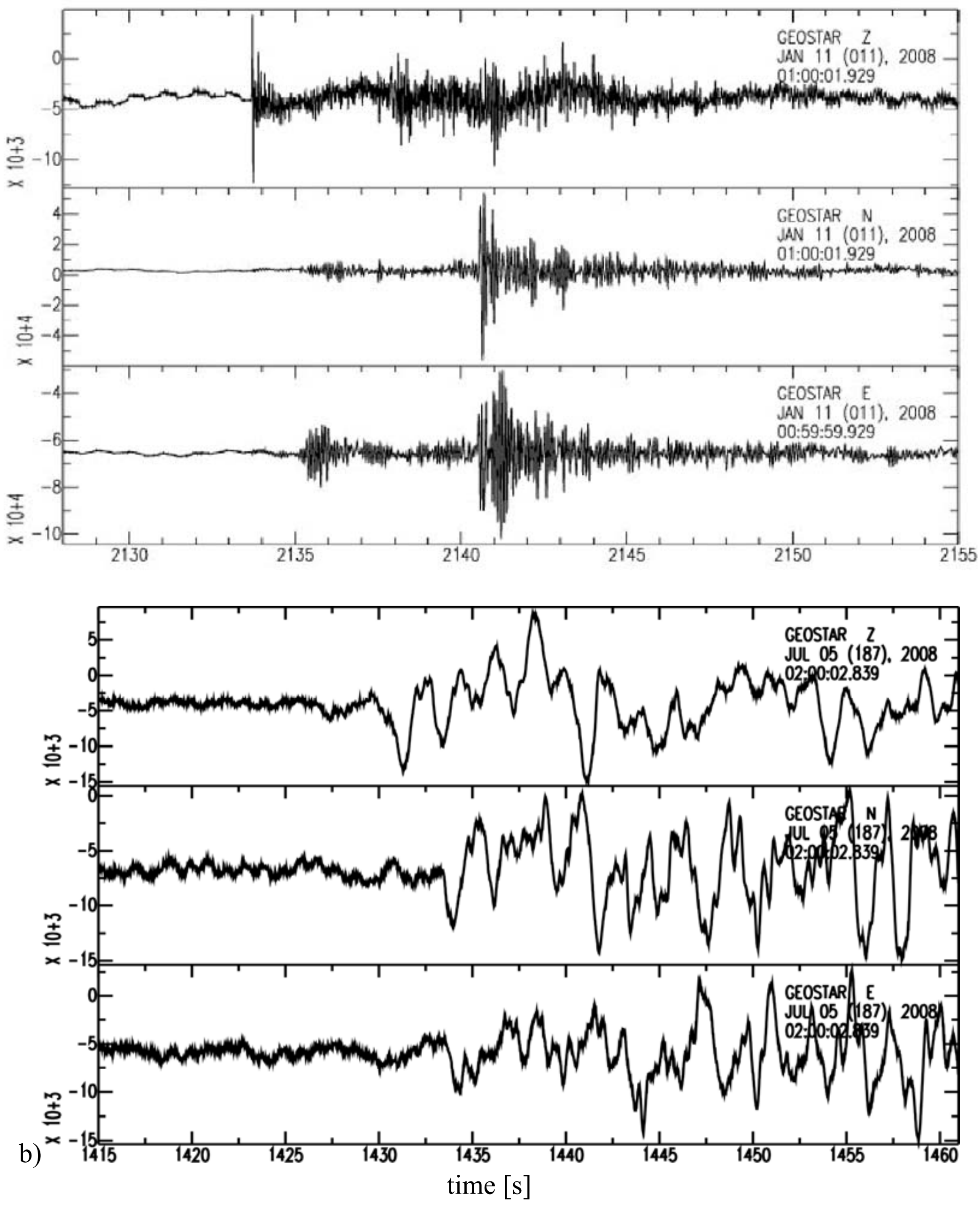

Figure 3.4 – Example of unfiltered recordings from the GEOSTAR OBS. A) Local event Ml2.4 from SW of Cabo S. Vicente. B) Teleseismic arrival Mw7.7 from the Sea of Okhotsk.

As a remedial action to improve the data quality the GEOSTAR group is developing methods to correct the disturbances (both D1 and D2), and the results look promising. Mainly we are testing two methods 1) An analytic reconstruction of the main disturbance D1, where the function is of the type describing a damped harmonic oscillator 2) Empirical reconstruction with a spline interpolation. Figure 3.3 shows an example of signal cleaning by using method (2).

Before data distribution to partners, a time drift correction for the entire period (359 days) of 184 ms (~0.51 ms/day for linear drift) was applied to the data. The entire GEOSTAR data-set for OBS and ACC, together with information for correct station orientation, and sensors and digitizer characteristics was delivered to the partners. Orientation was calculated thanks to GEOSTAR's main frame compass.

4 Recorded Signals ("from tide signals to whale calls")

Broadband seismic signals were recorded with 100 Hz sample rate in water depths between 2000 and 5000 m. We recorded signals from very long periods (tides), oceanic and atmospheric signals, teleseismic, regional and local earthquakes, active seismic surveys, ship noise, short duration events, “fish bumps”, up to low-frequency vocalizations of most probably fin and blue whales. A proper way to identify different sources of seismic signals is the use of spectrograms.

4.1 Long period signals/noise

4.1.1 Observations in seismograms

Already during the onboard data checking some very low frequency fluctuations were observed on some of the hydrophone recordings (see figure 4.1). We may see that 3 of the sensors recorded one low-frequency sinusoidal fluctuation that is interpreted as related to oceanic tides, showing that the instruments recorded all the frequency spectrum of the signal, even if there might be a phase shift. Two other sensors record some faster fluctuations that seem to propagate from one instrument to the other. We have checked the records of atmospheric pressure measured on land stations and we may discard this effect as the cause for the fast fluctuations observed. An alternative explanation could be the recording of non-linear internal waves in the water column.

With the all dataset available, we examined the signals recorded by the 24 instruments during one complete month, January 2008. We classified the recordings according to the amplitude of the anomalous fluctuations recorded as: No, Weak, Strong and Strange. To illustrate the meaning of this classification we show in figure 4.2 examples of these types of recordings. The location of the instruments that recorded each type of signal is shown in figure 4.3. The relationship between instrument depth and the type of signal is shown in Table 4.1.

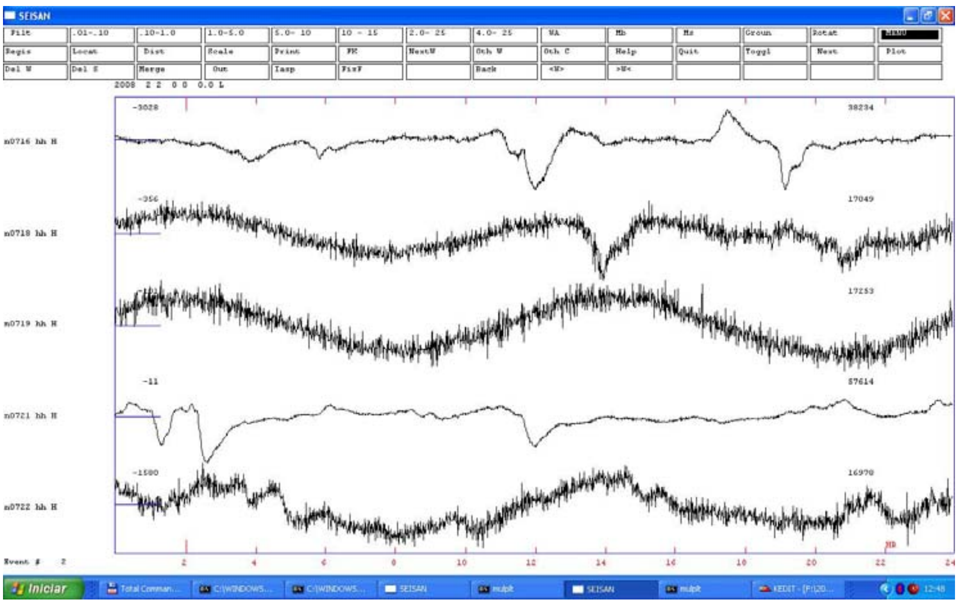

Figure 4.1 – One day recording of pressure data on 5 instruments.

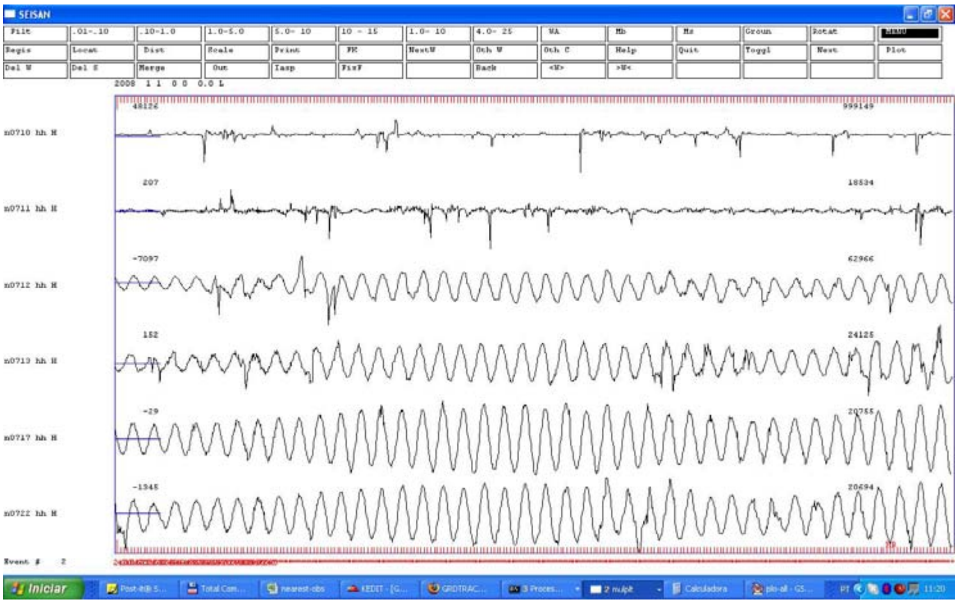

Figure 4.2 – One complete month of bottom pressure recorded by two instruments on each class: 10, 11 are “Strong”; 12, 13 are “Weak”; 17, 22 are “No”.

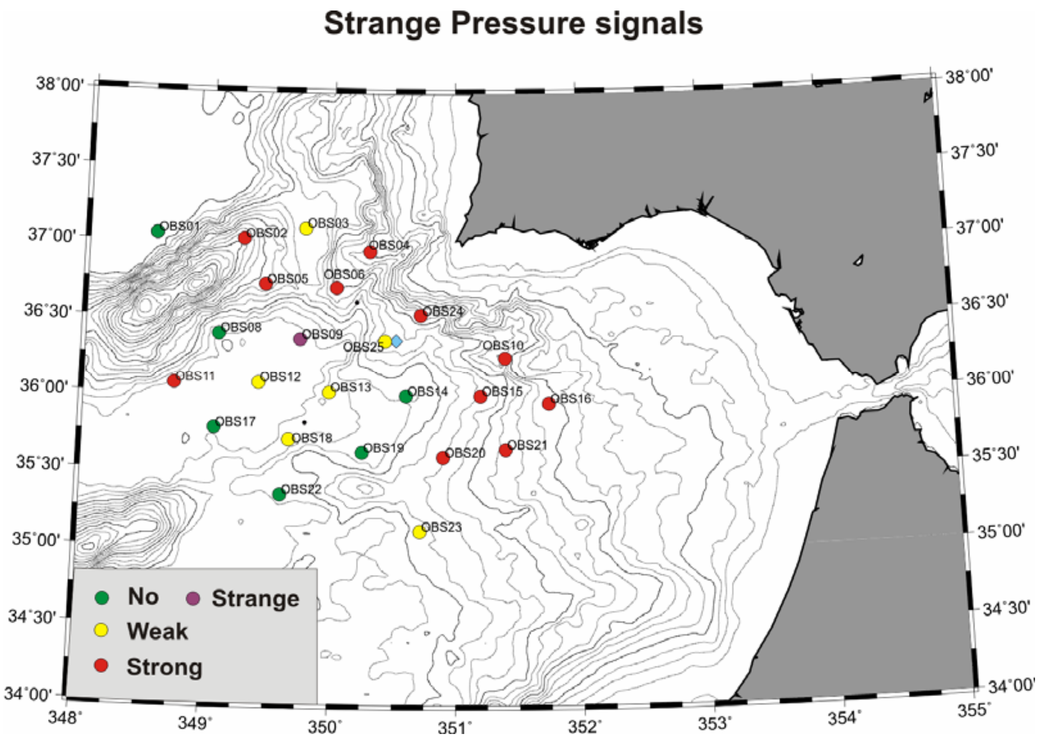

Figure 4.3 – Location of the instruments that recorded each type of anomalous pressure signal.

From the examination of table 4.1 we see that the shallowest instruments recorded strong anomalous pressure signals while the deeper ones normally not. Two deep instruments recorded strong fluctuations (OBS11) and “strange” fluctuations (OBS09). Regarding the amplitude of the fluctuations we may only estimate that they must be stronger than the tide signal, since we do not have the exact calibration information of the hydrophones. The question stands: are these signals originated in the water column or do they result from some instrumental malfunction? Further examination of these long-period signals revealed that they also affect the components of the broadband seismometer.

Table 4.1 – Classification of low-frequency pressure signals recorded at OBS

Code	Depth	I.-Waves	Code	Depth	I.-Waves	Code	Depth	I.-Waves
OBS04	1980	Strong	OBS25	3234	Weak	OBS18	4605	Weak
OBS10	2061	Strong	OBS15	3360	Strong	OBS08	4668	No
OBS16	2061	Strong	OBS20	3442	Strong	OBS23	4745	Weak
OBS02	2269	Strong	OBS03	3935	Weak	OBS17	4764	No
OBS24	2437	Strong	OBS22	4101	No	OBS01	4800	No
OBS21	2575	Strong	OBS14	4209	No	OBS09	4811	Strange
OBS06	2948	Strong	OBS19	4394	No	OBS11	4858	Strong
OBS05	3095	Strong	OBS13	4500	Weak	OBS12	4858	Weak

When a seismic wave hits the sensor from below, the seismometer records both the horizontal and vertical movement of the earth, but only the vertical movement is transmitted to the water layer above and recorded by the hydrophone as a pressure signal. This is illustrated in figure 4.4 where the P-phase recording of a local earthquake is shown. The pressure and vertical signals are almost identical at the beginning of the P-phase, but the polarities are reversed. The horizontal channels recordings show no clear correlation with the others. We will now examine the correlation between the recordings of the hydrophone (H), the vertical (Z) and one horizontal (X) component of the seismometer. To investigate the very low frequency signals the original records were decimated from 10 ms sampling interval to 10 s sampling interval. This was done by taking the median sample from each 20 s interval. This procedure is a non-linear filter with a cut-off frequency close the Nyquist frequency. We will show next several examples of the recordings obtained.

We begin with OBS01 (figure 4.5) that was classified not having recorded “strange signals”. The hydrophone records the tides quite well and we see that correlated with the tides we have bursts of higher frequency noise on the channels H and Z. On the Z channel we see also sudden downward deflections, not recorded by the hydrophone. These “strange signals” are not present in the whole record and disappear by the end of the month investigated (January 2008). We interpret the higher frequency bursts of energy as induced by currents near the sea bottom that show a regime clearly controlled by tides. This is a feature that we see systematically, particularly on the horizontal component records.

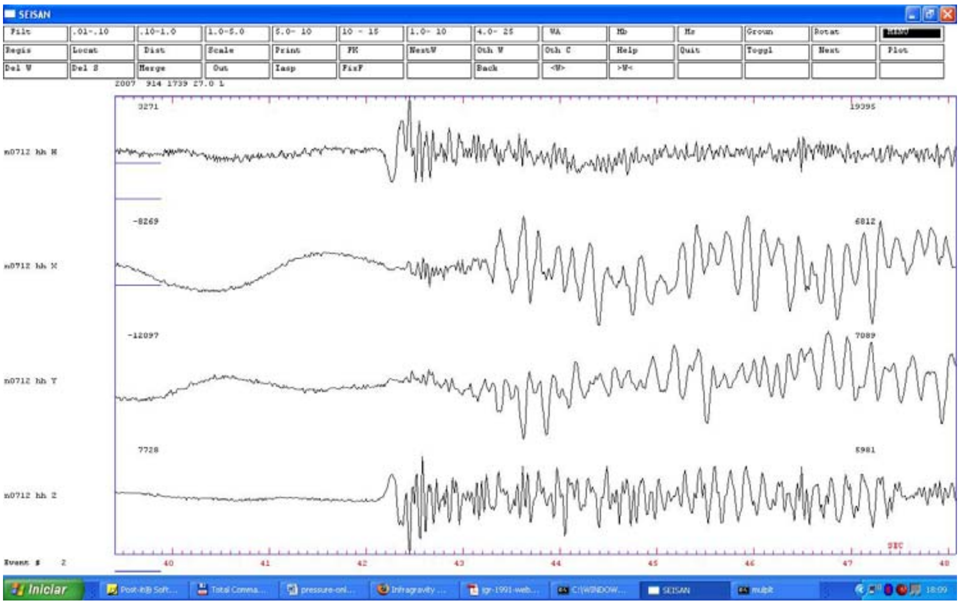

Figure 4.4 – Plot of the P-phase from a local earthquake recorded by OBS12. We see that the hydrophone and vertical component of the seismometer are correlated with a reversed polarity.

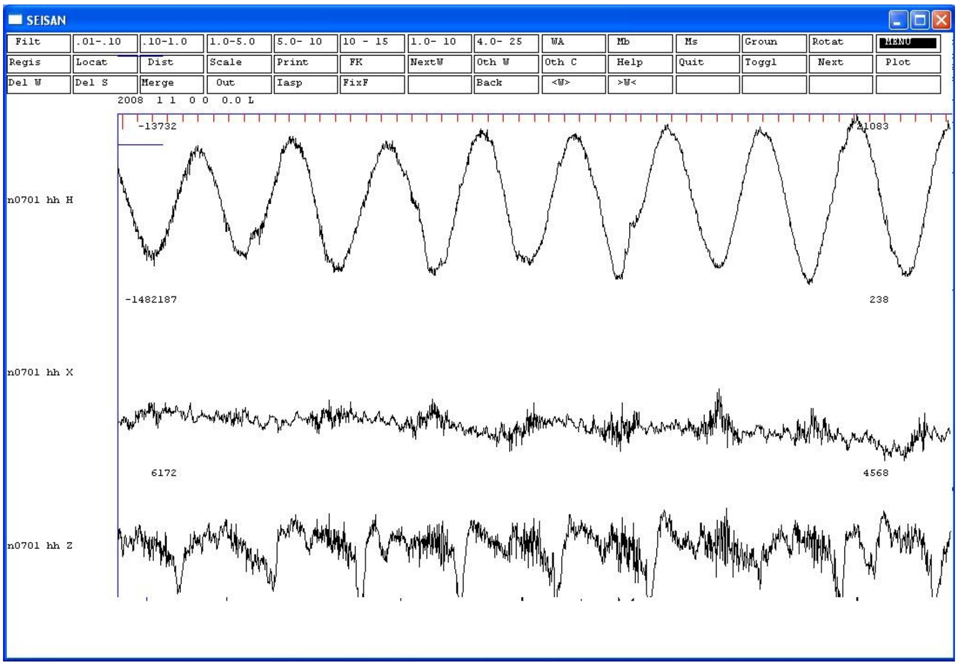

Figure 4.5 – Low frequency signals recorded by OBS01. Each red tick is 1 hour.

Next is OBS04 (figure 4.6) that was classified as having strong "strange signals". Here the hydrophone and Z-component record are correlated, with reversed polarity, just like we see on much higher frequencies for the seismic waves. The horizontal channel shows large bursts of energy that seem to be synchronized with the tide. The strange signals have not a very clear relationship with tides. This is typical of the "strong" observations. However, due to levelling problems, not all the instruments recorded properly the vertical or horizontal components.

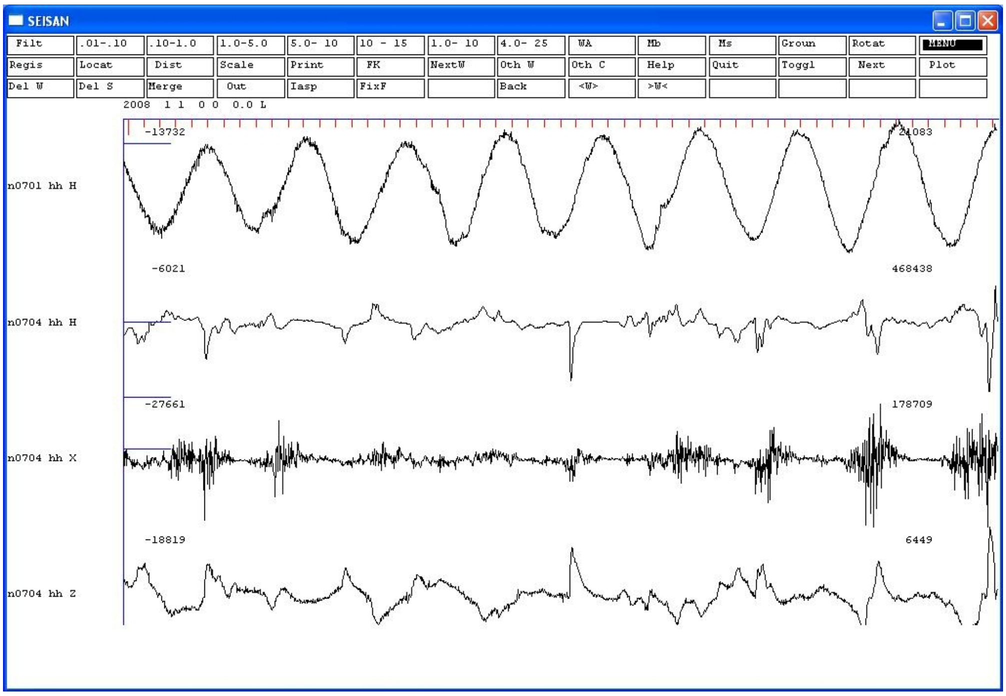

Figure 4.6 – Low frequency signals recorded by OBS04. H channel from OBS1 is included to provide the tide signal. Each red tick is 1 hour.

The recordings of OBS12 (figure 4.7) show what was considered as having weak “strange signals”. We see only a few of these signals on the hydrophone that have no correlation with the seismometer Z-component. The horizontal channel continues to show bursts of energy that seem to be synchronized with the tide. This is typical of the other recordings also considered as “weak”.

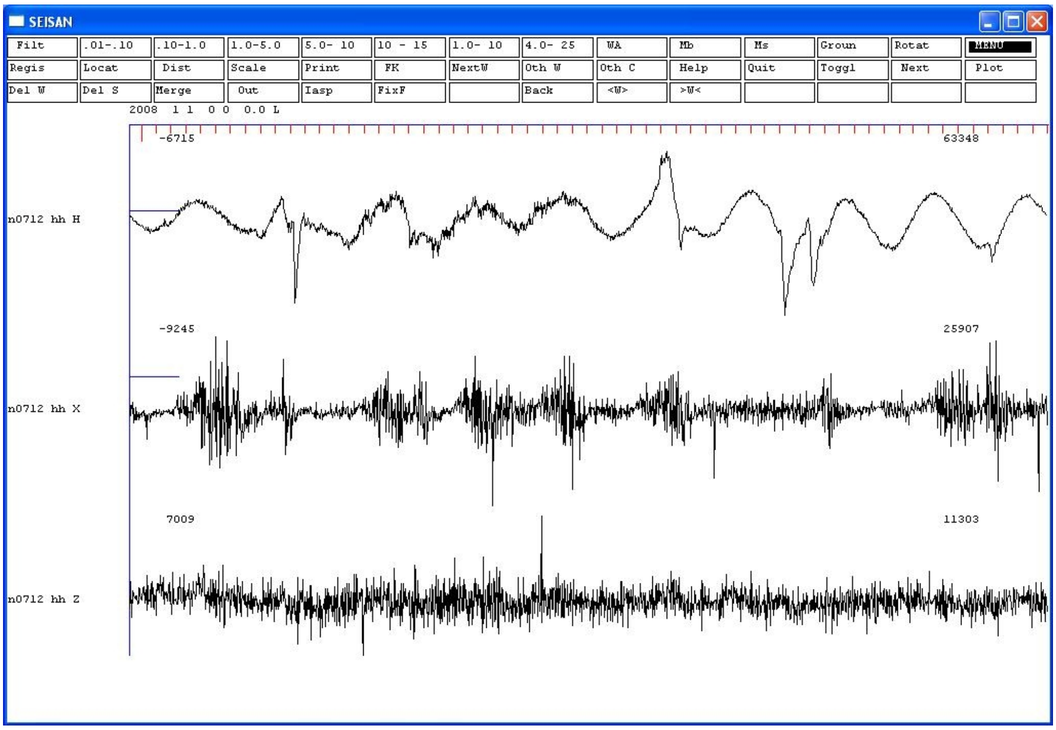

Figure 4.7 – Low frequency signals recorded by OBS12. Each red tick is 1 hour.

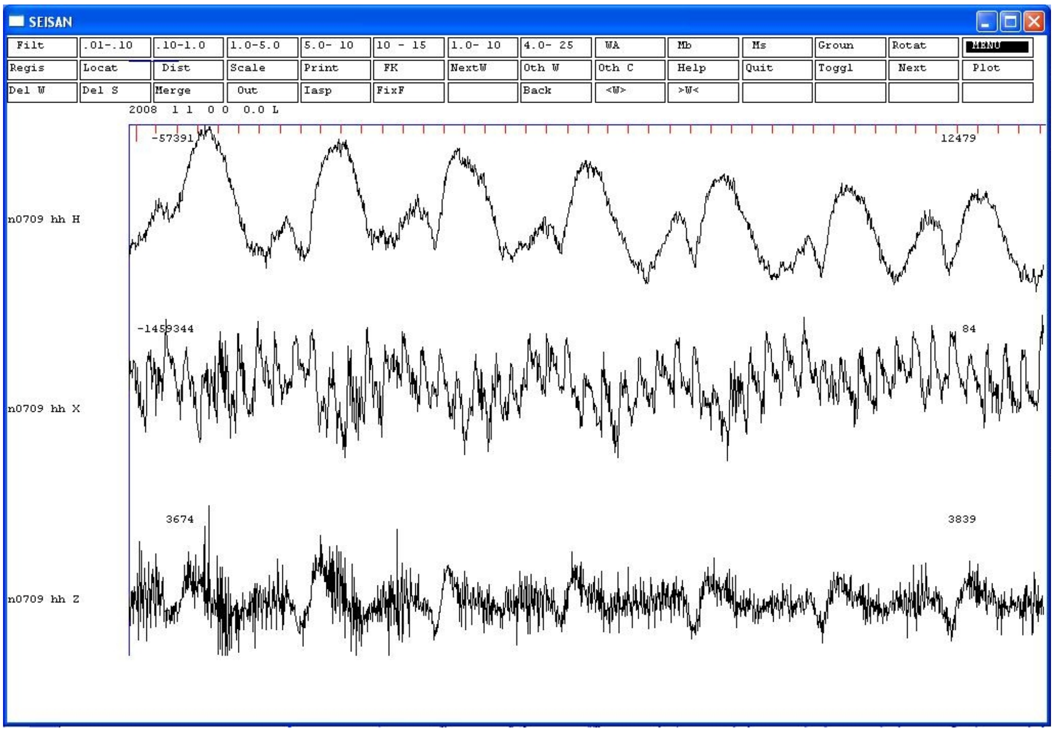

Figure 4.8 – Low frequency signals recorded by OBS09. Each red tick is 1 hour.

The recordings of OBS09 were classified as **strange**. We may see now on figure 4.8 what was meant by that classification. The hydrophone records show a strong interference between quasi-sinusoidal signals with frequencies that are close to the tide. There is some suggestion of correlation between the H and Z recordings, particularly on the “strange signals”. However, contrary to the previous observations, both signals are in phase. This is not due to some instrumental anomaly since this instrument recorded the high-frequency seismic phases with a reversed polarity, as for all the other instruments.

4.1.2 Power spectra of recorded long-period signals

The power spectra of pressure records from the seafloor are discussed in the literature of Physical Oceanography in terms of the oceanic and atmospheric processes that cause them (e.g. Filloux, 1980, Webb et al., 1991). Thus, we proceed by computing the power spectra from the recorded signals. To do this we use the algorithm suggest by Press et al. (1986) that, by using K overlapping segments of data, allows the reduction of the variance on the power estimates by $9K/11$. Since we wish to explore the entire spectrum from the M2 tide period to the sampling rate, we had to do the power spectra computations on two steps. On the first step I will show the spectra from 1×10^{-3} Hz to 10 Hz. The second step will show the spectra from 1×10^{-5} Hz to 0.03 Hz.

To investigate the noise at high frequencies we choose the 2nd January 2008 day, when there were no large teleseismic or local events reported in the catalogues. Five hours of continuous recording and 26 segments were used. The results are shown on figures 4.9, 4.10, and 4.11 for the H, Z and X channels respectively.

The pressure power spectra (figure 4.9) show several prominent features between 0.01 Hz and 10 Hz, namely two low noise bands, one in the middle and another at the high-frequency band. There are 3 clear power peaks with frequencies (and periods) given by: i) 0.0711 Hz (14 s); ii) 0.142 Hz (7 s); iii) 0.269 Hz (3.7 s). There is a clear octave relationship between these peaks that we don’t know how to interpret. They seem to be quite systematic and not very dependant on the water depth, that varies from 2000 m to 5100 m. In the middle low-noise band there seems to be no difference between the different types of “strange signals” recorded. There are “strong” recordings with very low and very high power levels on this band. However, when we go to lower frequencies, below 0.01 Hz, the “strong” instruments show a systematic higher level of noise power.

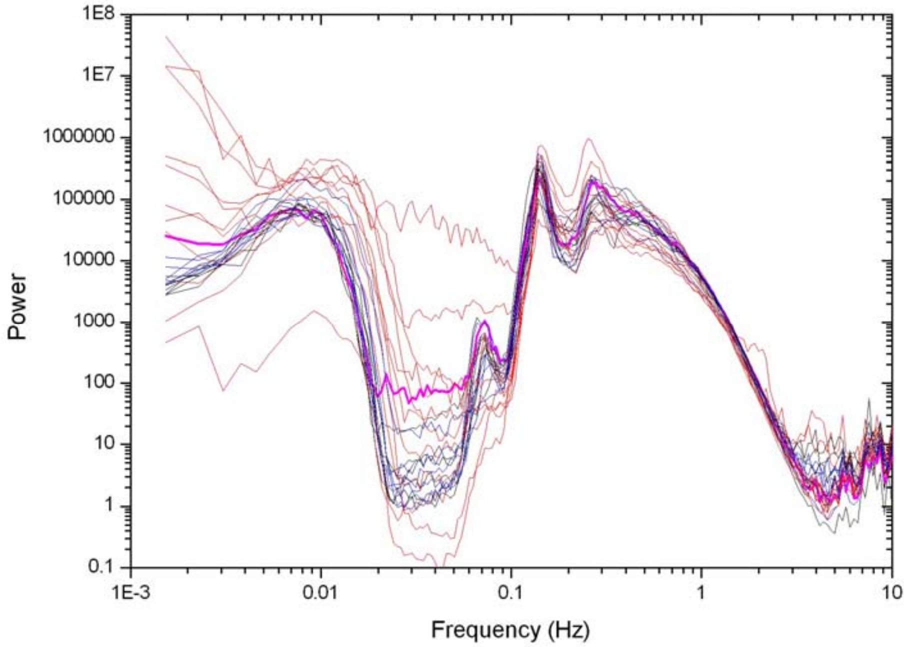

Figure 4.9 – Power spectra for the hydrophone records from all the 24 instruments used. The colour code indicates which type of strange signals was reported: red for strong, blue for weak, black for none and pink for strange.

The power spectra of the vertical movement recorded by the seismometer (figure 4.10) shows identical features to the pressure power spectra, for frequencies higher than 0.1 Hz. The middle low-noise band is considerably reduced and below 0.1 Hz (10 s period) the power noise has a clear f^{-3} variation. As we will see later, the noise cut-off near 0.01 Hz is partly due to the instrumental response of the seismometer.

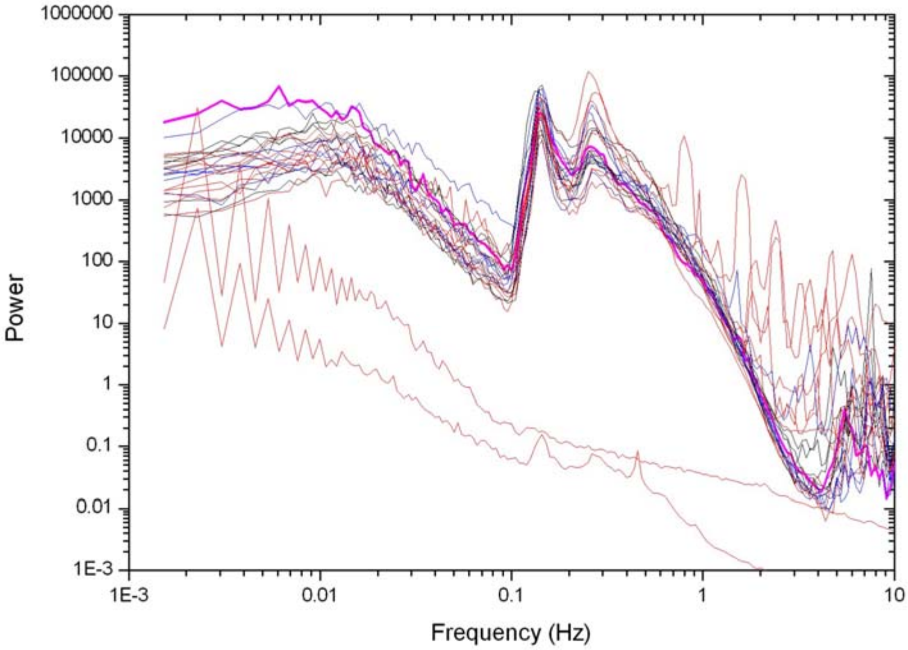

Figure 4.10 – Power spectra for the vertical seismometer component records from all the 24 instruments used. The colour code indicates, which type of strange signals was reported: red for strong, blue for weak, black for none and pink for strange. Abnormal spectra were calculated from OBS 02 and OBS 11 because Z was not levelled.

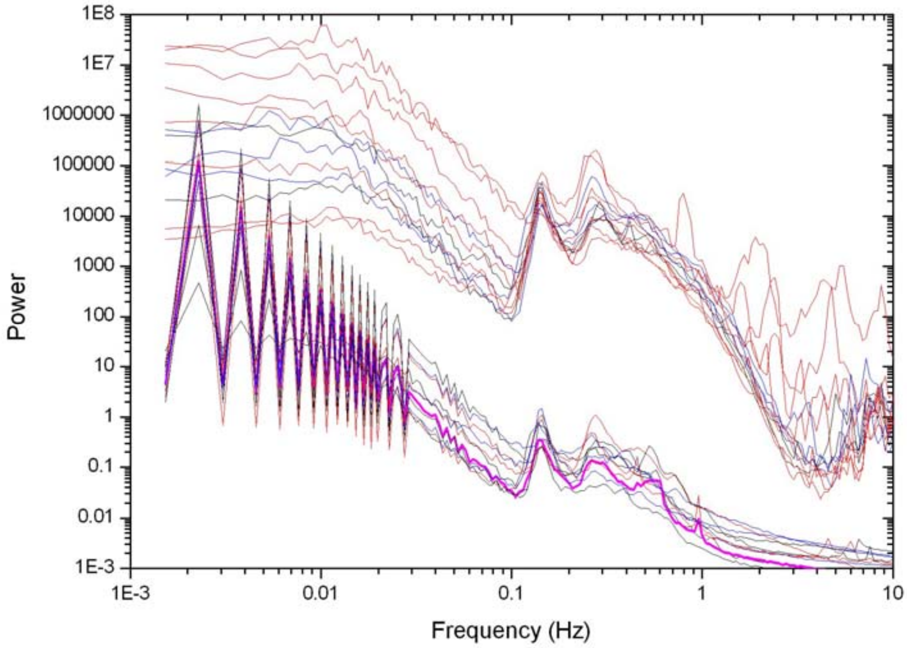

Figure 4.11 – Power spectra for the seismometer horizontal X component records from all the 24 instruments used. The colour code indicates, which type of strange signals was reported: red for strong, blue for weak, black for none and pink for strange. Some instruments have abnormal spectra (zig-zags) for the X component; they are not levelled.

In the high-frequency interval investigated there seems to be not a great difference between the several types of "strange signals" recorded. Many of the "strong" recordings are associated with high-frequency noisy records. It is also clear from the spectra in figure 4.10 that two of the vertical recordings look anomalous, probably due to not-levelling. The power spectra of the horizontal movement recorded by the seismometer X component (figure 4.11) are very similar the vertical component power spectra. For frequencies below 0.1 Hz there is a wider variation in the noise level. We see also a greater number of anomalous spectra, due to not-levelling. Given the records examined we suspect that the f^{-3} power noise that we observe below 0.1 Hz in the seismometer is induced by currents. Since currents do not affect the pressure measurements this explains the great differences between the hydrophone and seismometer spectra below 0.1 Hz observed.

To investigate the noise at low frequencies 20 days of continuous recordings were analysed, starting the 1st January 2008. The recordings were first decimated to 10 s sampling interval and then we used the same algorithm as before, this time with a total of 20 segments. The results are shown of figures 4.10, 4.11, and 4.12 for the H, Z and X channels respectively.

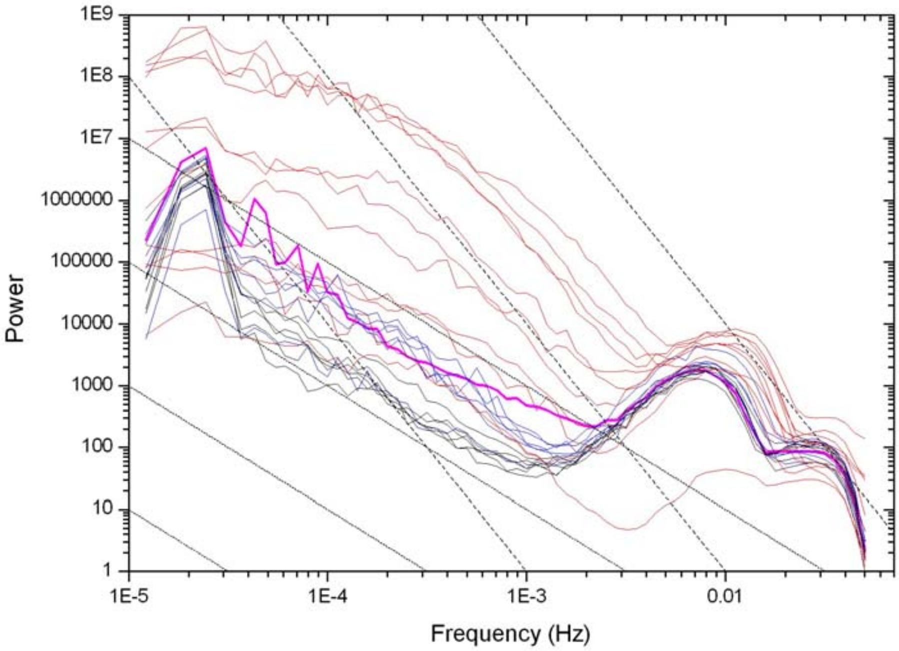

Figure 4.12 – Power spectra for the hydrophone records from all the 24 instruments used. The colour code indicates which type of strange signals was reported: red for strong, blue for weak, black for none and pink for strange. The dotted lines indicate an f^{-4} variation; the thin straight lines indicate an f^{-2} variation.

The power spectra of the signals recorded by the hydrophone (figure 4.12) show a very clear difference between the "strong" strange signals, the "weak" and the "no" strange signals. The "no" and "weak" spectra show a clear tide peak and the power spectra decreases with a f^{-2} variation up to 0.001 Hz. At higher frequencies all instruments record a bump in the spectra, centred at 0.01 Hz (100 s period). The "strong" recordings have a different variation with frequency, between f^{-3} and f^{-4}, and have so much energy that the tide peak is obscured. The "strange signals" power seems to flatten close to the M2 tide period.

The effect of the "strong" strange signals on the power spectra recorded by the seismometer vertical component is not as clear as for the hydrophone (figure 4.13). The spectra are mostly flat below 0.01 Hz and some of the signals show a slight increase in the noise power at the lowest frequencies, associated with the "strong" strange signals. If we interpret the flat spectra as the result of currents affecting the sensor, then the strange signals are only seen when their energy is higher than the one induced by the currents. No clear tidal peak is observed.

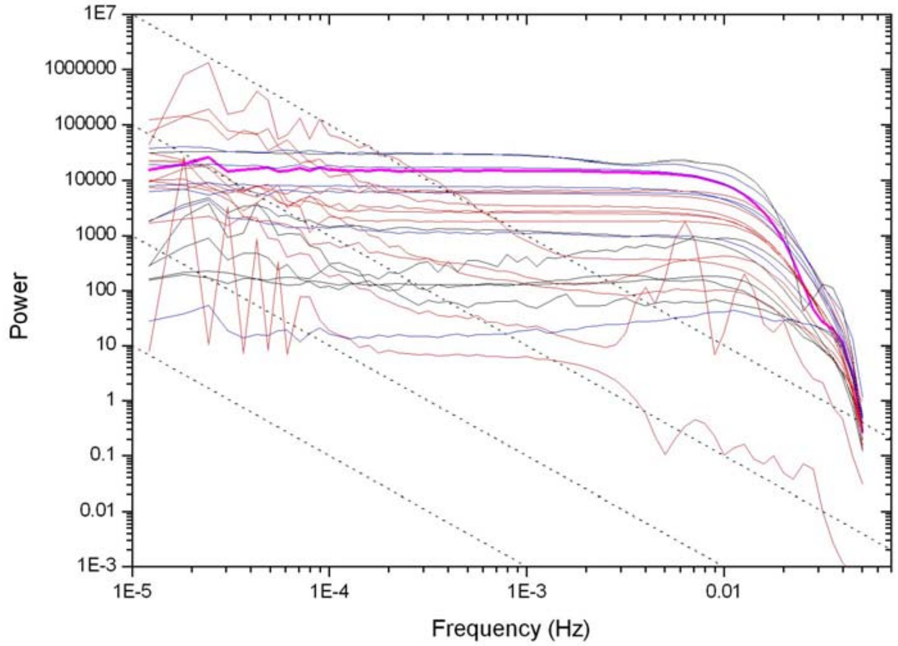

Figure 4.13 – Power spectra for the vertical component of the seismometer records from all the 24 instruments used. The colour code indicates, which type of strange signals was reported: red for strong, blue for weak, black for none and pink for strange. The dotted lines indicate an f^{-2} variation.

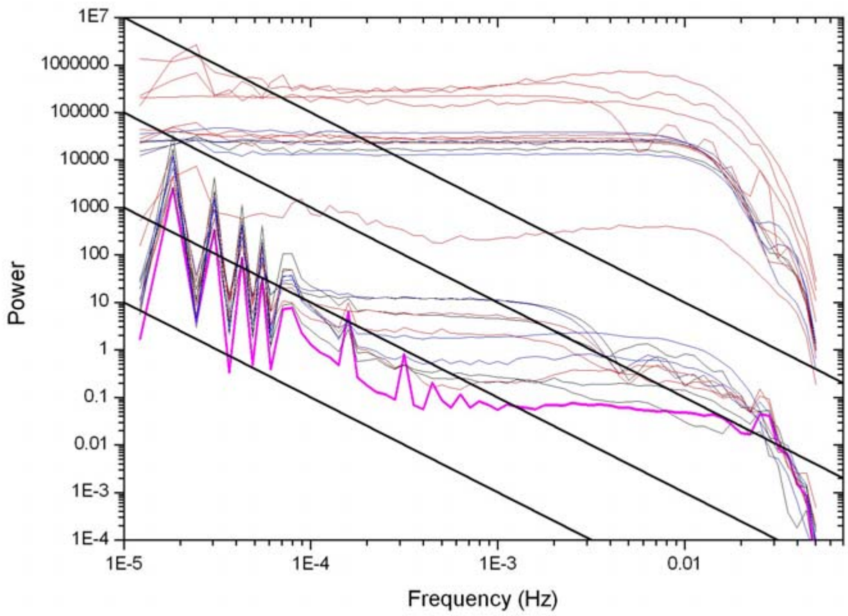

Figure 4.14 – Power spectra for the horizontal (X) component of the seismometer records from all the 24 instruments used. The colour code indicates, which type of strange signals was reported: red for strong, blue for weak, black for none and pink for strange. The thick lines indicate an f^{-2} variation. Strange looking spectra belong to not levelled X components.

The power spectra for the horizontal (X) component of the seismometer shows yet a different picture (figure 4.14). There is a considerable difference in noise levels that we cannot explain at the moment. They reflect either the local coupling of the sensors or levelling problems. The “strong” strange signals are associated mostly with high levels of noise power, and for many of them we see an upward rise of the power, when we approach the M2 tide frequency, like for the vertical component.

4.1.3 Deep ocean pressure spectra

There exist a lot of published information in Physical Oceanography that discuss the power spectra of pressure measurements recorded on the deep ocean floor. We will review here only 3 of the references found in the literature. Webb et al. (1991; their fig.1) show a power spectra of pressure fluctuations recorded on the seafloor in the Northwest Atlantic Ocean. It is obvious that this plot is very similar to the ones we computed for the Gulf of Cadiz, high-frequency band (figure 4.9). This implies that the interpretations made by Webb et al. (1991) for this frequency band, may be used also to the interpretation of our spectra. For frequencies lower than 0.02 we like to use the spectra published by Garret and Munk (1975, figure 2), and by Filloux (1980, figure 6).

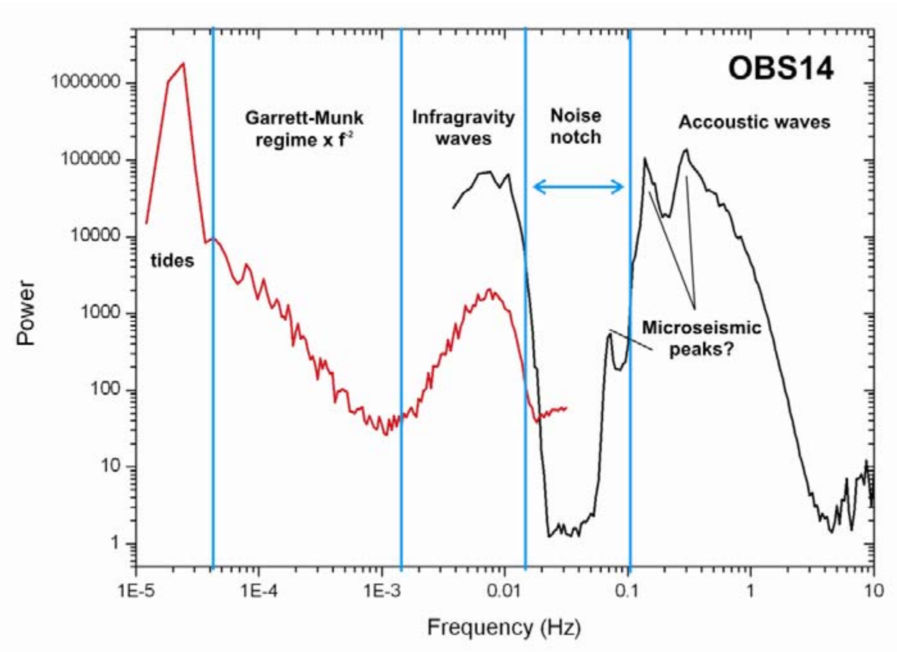

Figure 4.15 – Power spectra for the OBS14's hydrophone. The two frequency bands investigated are plot together. Interpretation of the features is taken from Webb et al. (1991) and Garrett and Munk (1975).

We use these references to make a very schematic interpretation of the spectra recorded. We use the recordings from OBS14 (that is classified as not recording strange signals) to illustrate the typical spectra observed, for a non-disturbed signal (figure 4.15). The large differences between the amplitudes computed using the low and high frequency bands might be explained by the large variance observed in noise. The low frequency power is an average computed from 20 days of data, while the high frequency only used 5 hours of data. Following Webb et al. (1991), when we go from the high to the low frequencies, we find first the "acoustic wave" band. Here, we find two noise peaks, classified as "microseismic peaks" and a 3rd one, separated by one octave, already in the following band.

Below approximately 0.02 Hz there is another high-noise band that is due to infra-gravity waves. Between the two there is a "noise notch" in the pressure power spectrum. According to Webb et al. (1991) the signal level in this band is probably very low, because hydrodynamic and acoustic scales are either too large (acoustic) or too small (hydrodynamic) for energy to be easily coupled into propagating waves. Below 0.002 Hz we enter a regime that, according to Garrett and Munk (1975), is controlled by internal waves with a very distinct f^2 variation. Finally, at 2.3×10^{-5} we enter in a tide dominated energy band. The shape of the bands recorded below 0.01 Hz in the Gulf of Cadiz by the NEAREST experiment may be distorted due to the band-limited instrumental response of the sensors, as we will see below. The bands themselves, despite the limitations by instrument response, are clearly identified by their different dependence with frequency.

4.1.4 Instrumental response

The seismometers deployed during the NEAREST experiment where the CMG-40T (60 s) broad band sensors. Its response to the soil velocity is very well described by the response of a single oscillator with the same natural frequency (ω_0) and dumping,

$$|\Phi(\omega)| = \frac{\omega^2}{\left[\left(\omega^2 - \omega_0^2\right)^2 + 4\varsigma^2\omega^2\right]^{1/2}}$$

where ς is the damping coefficient.

Using the appropriate values (natural period of 60 s and critical dumping), we obtain the amplitude response to soil velocity that is shown in figure 4.16. Here, we neglect the effects of the acquisition system that affect mostly the high-frequency response.

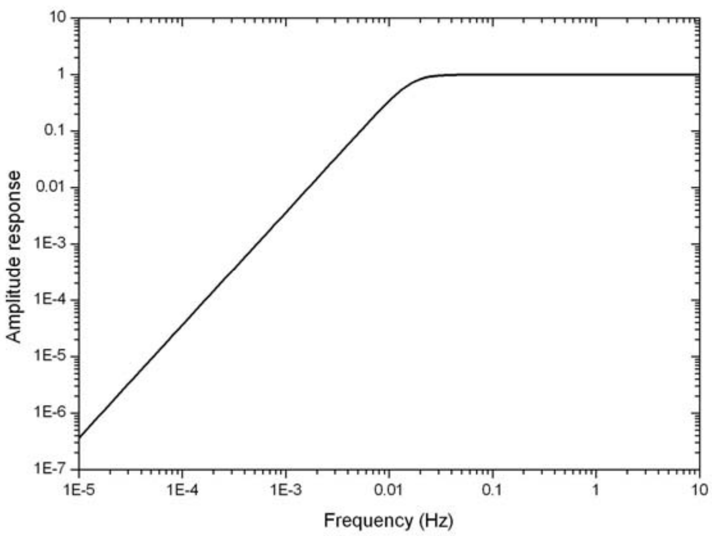

Figure 4.16 – Typical amplitude response of the CMG-40T broadband seismometer to the soil velocity.

The seismometer response is flat above the natural frequency (0.0167 Hz) and falls off with f^2 for frequencies below. This instrumental response is identical for all the three seismometer components and may distort the power spectra computed for frequencies below 0.01 Hz. As regards the hydrophone used in the NEAREST experiment, we have its general description, model HTI-04-PCA/ULF, made by High Tech Inc, and indicative flat response from 100 s to 8 kHz[1]. We have not yet its frequency response as for the seismometer, but we may estimate that the differences observed between the typical pressure power spectra and the spectra recorded by the NEAREST experiment below 0.01 Hz may be due to the 10 s cut-off reported in the sensor specifications. For this reason, we cannot compute the true amplitude of the strange signals on the hydrophone, but they could be computed for the Z component of the seismometer using the known instrumental response.

4.1.5 Discussion

The main question to be addressed regarding the “strange signals” recorded by the pressure transducers during the NEAREST experiment is if they have some natural origin or if they are pure instrumental artefacts. One argument for the artificial origin of these signals is the amplitude. We have seen that its power is larger than the power related to the tides in the deep ocean. If there is a physical process then it must be able to generate such large signals.

[1] http://www.awi.de/en/research/research_divisions/geosciences/geophysics/depas_german_instrument_pool_for_amphibian_seismology/

Another strong argument for an instrumental cause of the signals is their shape. In figure 4.17 we show the low frequency signals recorded by instrument OBS24 in comparison to the hydrophone recordings from OBS01 (note that there might be a phase shift in this periods because it is outside the normal operation frequency range of the hydrophone-recorder system). The signals are strongly locked to the tide signal and the X component records a very high noise level also synchronized with the tides. The signal shape is given by a very sharp rise and a slow decaying tail, similar to the charge/discharge of a capacitor in an electrical circuit. This could be indicative of the response of a system to a very fast change (step or Heaviside function) with a characteristic release time of 30 minutes. Mainly OBS close to strong gradients in bathymetry show this behaviour which might imply some effects of contour currents.

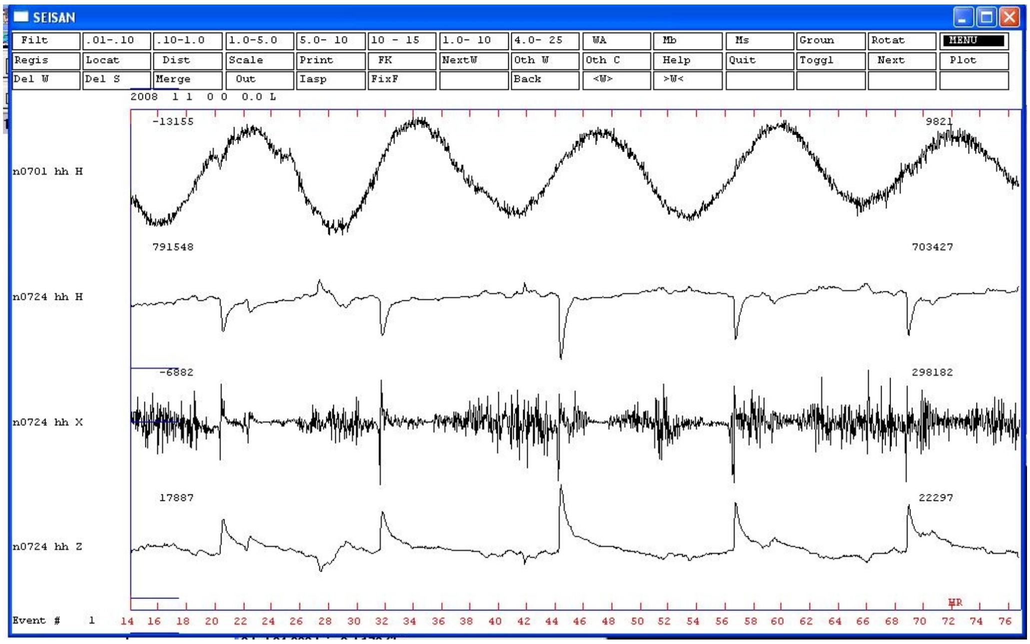

Figure 4.17 –Low frequency signals recorded by OBS24. Each red tick is 1 hour. H channel from OBS1 is included to provide the tide signal.

When we compare the recordings from several channels, we have seen that many times the vertical seismometer records exactly the same signals as the hydrophone, with an opposite phase (see also figure 4.17), like it is observed for high frequency seismic signals. But the horizontal components do not record these signals most of the time. Figure 4.17 shows an example of recordings, where the X seismometer component is clearly affected, but not so strongly as the Z component, by the signals on the hydrophone. Each "strange signal" is recorded in the X component as a fast flip-flop transient. On the other cases the signals may be below the S/N ratio on the horizontal channels that are dominated by noise induced by the currents interfering with the instruments. If it is some sort of power fluctuation effect, we do not see the reason with the polarity should be reverse between the H and Z channels. It is also difficult to understand, why near half of the instruments would be subjected to these anomalies and the other half not.

John Hutnance (Proudman Oceanographic Laboratory, Liverpool) suggested that the anomalies found may be due to the instrument response to some changing environmental variable like the temperature. He reported to have seen some pressure anomalies that were later attributed to this effect. If so, again we do not see the reason why the seismometer would record exactly the same signal with an opposite phase. However, the idea that the anomalies are caused by some environmental interference deserves further investigation.

As we can infer from the instrument assembly the seismometer and hydrophone are rigidly connect to the main frame. These sensors will thus record all the mechanical effects that the instrument may receive from the environment, like currents. The head buoy is connected to the frame with a 4-meter long rope. It is used to help the recovery of the instrument as soon as it reaches the surface. When the instrument falls on the sea bottom, it has a total weight in the water of 27 kg[1]. The head buoy, due to its buoyancy, will stand upright pulling the frame according to the currents 4 meters above the sea floor. Pulling the frame at high frequencies may generate in the hydrophone and seismometer the correlated signals that we have seen for seismic waves. The question is that if the same effect could also be observed when the head buoy is affected by tides and currents generated by internal waves. Could this mixture of instrumental and environmental causes be the explanation for the strange signals observed in the Gulf of Cadiz? Or is there a pure physical oceanography explanation for them?

This question has to be answered before any big investment is made on deep-ocean systems for tsunami early warning that are based on pressure measurements.

4.2 Earthquake signals (teleseismic, regional, local)

4.2.1 Check for known events

The quality check of the OBS data included the visibility of known teleseismic and local events. The Sichuan event on the 12.05.2008 is the largest recorded teleseismic earthquakes within in the period of OBS operation. Seismograms are shown in figure 4.18. The length of this recording is about 90 min. The Sichuan event showed a strong P-onset and strong Love and Rayleigh waves. The epicentral distance is about 88° or 9800 km.

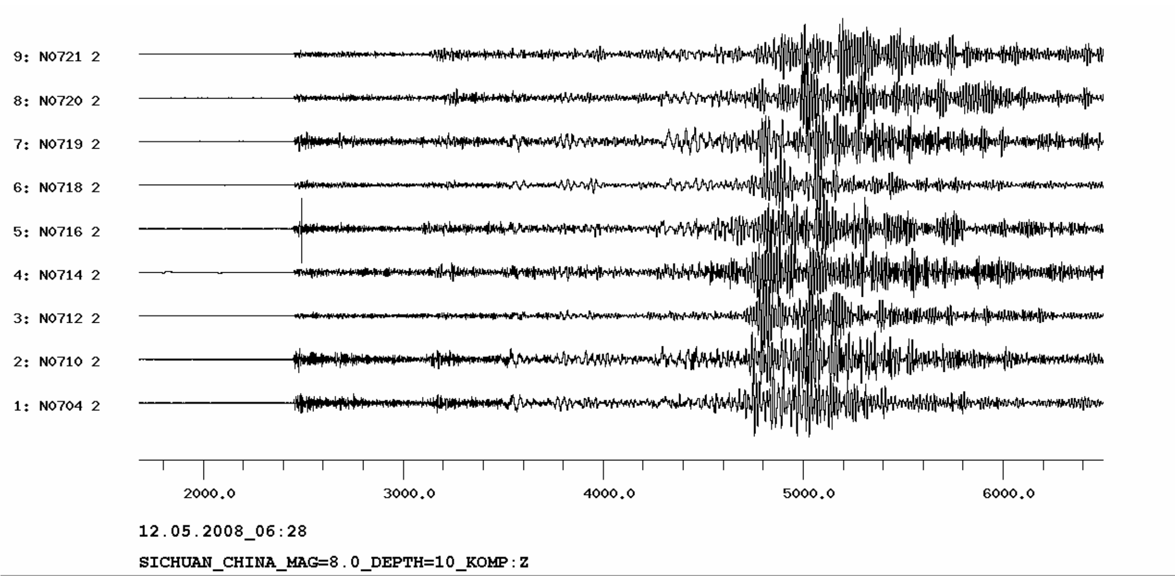

Figure 4.18 – Seismogram of the Sichuan event, 12.05.2008. Z components.

In figure 4.19 we show seismograms from a strong earthquake at intermediate distance (30°) in Greece (M=6.5; 08.06.2008). The used filter is a high-pass 0.1 Hz to eliminate low noise frequencies. The seismogram, especially the hydrophone and the vertical component showed a strong P-onset. The length of the recording is about 30 min.

Furthermore, the data was screened for 168 teleseismic events recorded at stations in central and southern Portugal mainland with Mag. ≥6.0, which should also be recorded by the OBS network. The quality of the visibility has been subdivided into 3 categories: ”Good visible” (38%) as the best category means that there is a visible P- and S- onset with the following surface waves. As ”visible, but not clear” (34%) events were classified, where no clear P-onset, but at least the surface waves are visible. And when the recording showed no remarkable recording the event was classified as ”not visible” (27%). About 72% of teleseismic events might be useful for further analyses. While screening, the data was filtered with a band-pass 15-35s with an order 4.

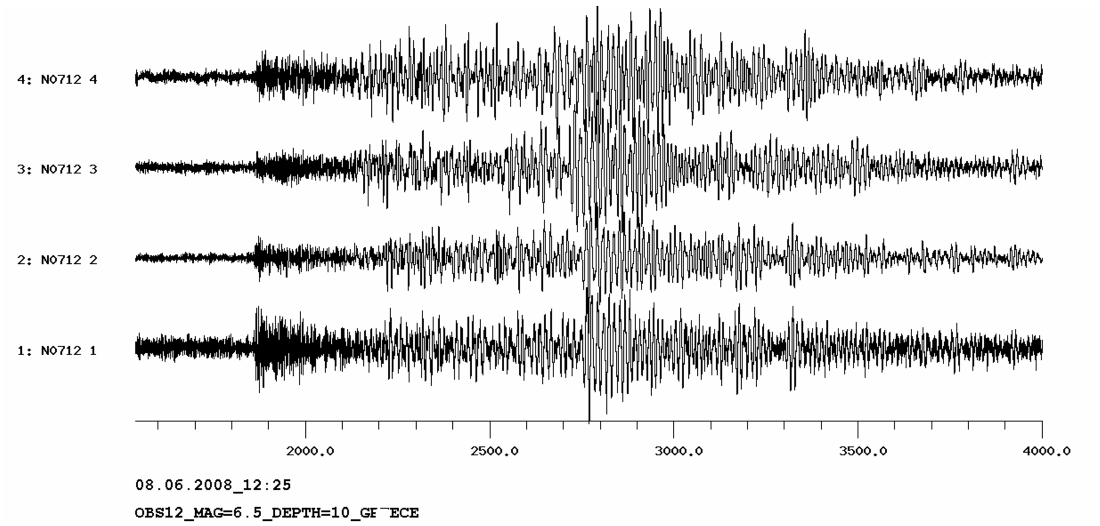

Figure 4.19 – Seismogram of an earthquake in Greece. 1, hydrophone; 2, vertical component (Z); 3,4, horizontal components (Y,X).

An example of a local earthquake in the Sea of Morocco (M=4.1; 10.05.2008) is shown in figure 4.20. The seismograms are filtered with a high-pass filter (1 Hz, order 4). A first evaluation of local events including 257 known events resulted in 52% of events fully useable for location; 17% will also contribute for the determination of source mechanism using P-wave polarity. Just 27% were expected to be useless for location. During the analysis the recorded seismograms showed some characteristic problems concerning the behaviour of the seismometer components. For example the clipped components, especially the X component (see chapter 4.1.1 Levelling). Another probably problematic behaviour is the transient signals following impulsive phases. The horizontal components are often affected by these signals. Figure 4.7 shows these problems on the basis of the event from the 11.01.2008 recorded on OBS 5. The epicentral distance to OBS 5 is 0.55° or 61km. The transient signals are supposed to be caused by an instrument-related mechanical problem or by the "bad" coupling of the OBS to the muddy ground.

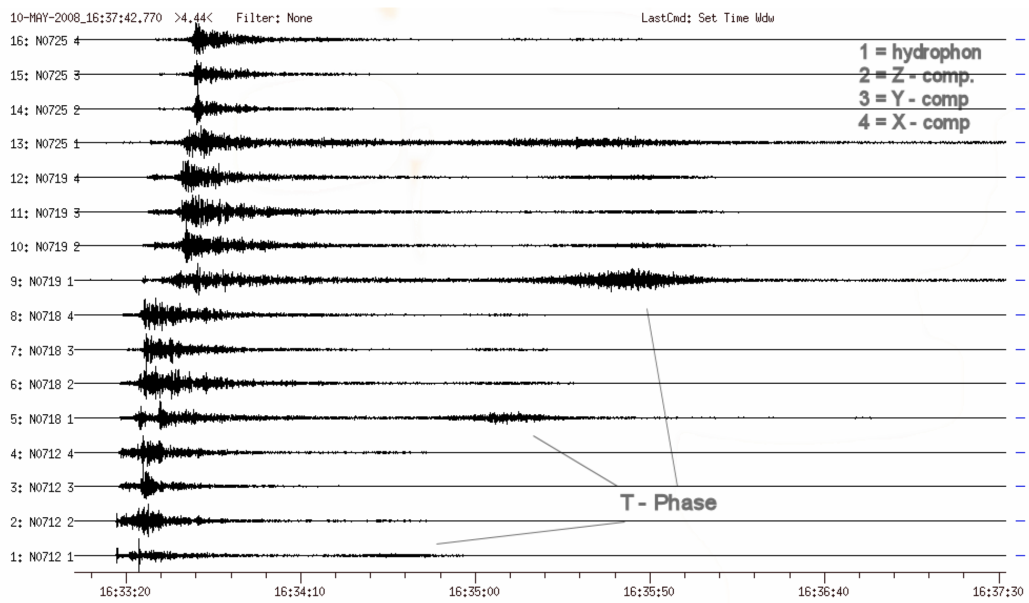

Figure 4.20 – Seismograms of a local event in the Sea of Morocco, 10.05.2008. 1, hydrophone; 2, vertical component (Z); 3,4, horizontal components (Y,X).

4.2.2 Comparison OBS – GEOSTAR recordings

OBS25 was deployed close to the GEOSTAR deep sea observatory. This allows us to compare the waveforms and, therefore, the seismic data quality of both systems. It is especially interesting, since similar seismometers and recording parameters were used.

About the cause of the resonance-like behaviour of the OBS seismometer components we can only speculate so far. Most probably it might be related to the overall construction of the system or it is related to underground effects, since most of the instruments are grounded in muddy layers. No resonance is observed at GEOSTAR; the observatory is well coupled to the underground, since it is also significant heavier. It sunk about 14 cm into the mud at the sea-bottom.

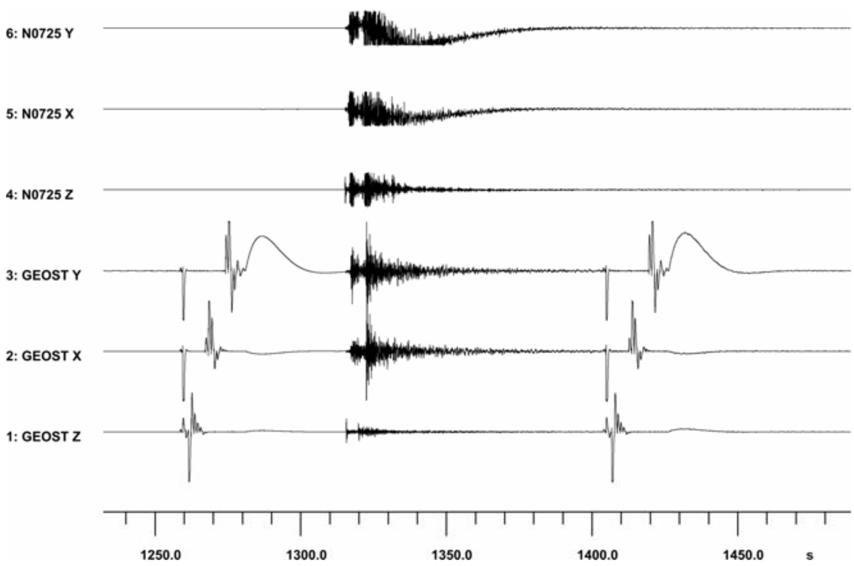

Figure 4.21 – Comparison of seismometer components from OBS 25 and GEOSTAR deep sea observatory for the strongest local event (Jan 11th, 2008 00:21). Clearly the specific problems of both platforms can be seen: There is a strong transient signal observed at OBS 25 which is also responsible for clipping of the seismic signal. GEOSTAR recordings are dominated by the repeated levelling sequences.

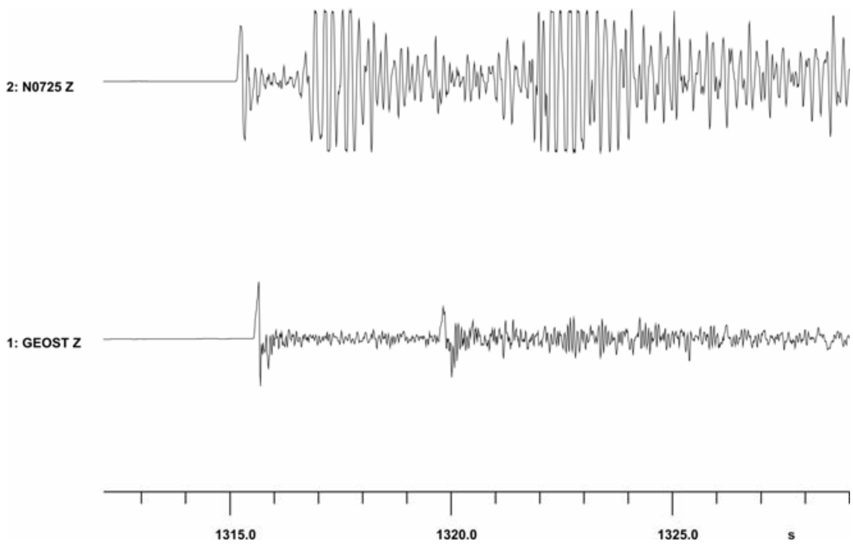

Figure 4.22 – Comparison of Z components from OBS 25 and GEOSTAR deep sea observatory for the strongest local event (Jan 11th, 2008 00:21). There is a strong ringing at the OBS for the P onset. Also S phases (Ps converted and direct S phases) are visible on the OBS, but not on the GEOSTAR recording. Water multiple is more clear at GEOSTAR, but also observed at OBS25. The recordings from the OBS look mono-frequently.

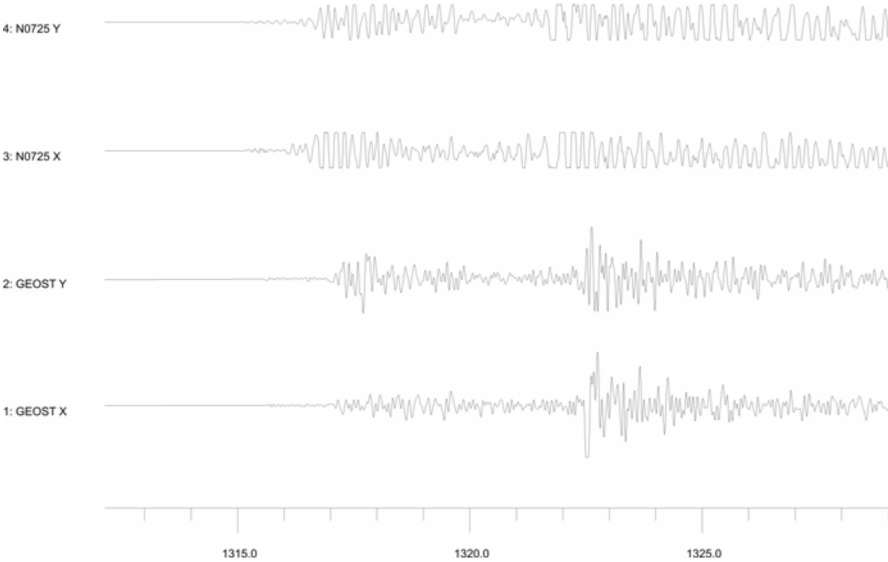

Figure 4.23 – Comparison of horizontal components from OBS 25 and GEOSTAR deep sea observatory for the strongest local event (Jan 11th, 2008 00:21). Obvious is the clipping at OBS 25, even for the Ps converted phases in front of the direct S phases. The recordings from the OBS have a monofrequent appearance.

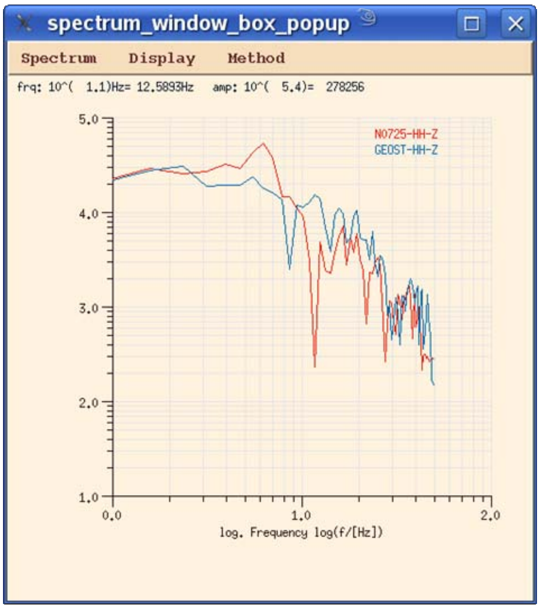

Figure 4.24 – spectra of vertical components from OBS 25 and GEOSTAR seismometers for the strongest local event (Jan 11th, 2008 00:21). The OBS shows a maximum between 5 and 6 Hz, which explains the mono-frequent character of the seismograms (Figures 4.22, 4.23)

4.2.3 Magnitude of completeness

The following figure shows the dependency between the magnitude of an event and its distance to a station. The visibility was checked for local-and teleseismic events. Full and clearly visible events are marked with green dots, which means that the P-wave-onset can be used for localization. The yellow dots are events, which were not clear concerning their onset. However, they can be used for the analysis of surface waves. With a proper filter perhaps a P-or S-onsets can be picked. The black line is the interpretation of the boundary between events, which were visible and those which were not visible. Every mark shown in figure 4.14 represents an earthquake. The colour of the mark expresses the quality of the recording of the event (green -the event is visible in the recording; yellow -the event is visible but not clear; red -the event is not visible in the recording). The events were divided into local events (dots) and events, which occurred far away from the OBS-Network (expressed by squares). The dashed line of best fit tries to divide the visible events from the not visible events. Above a distance of 70° the boundary between ”visible” and ”not visible” cannot be defined very well. It strongly depends on the direction of the event if it is visible or not. Figure 4.14 shows that events above a magnitude of 6.5 are visible in general.

Land-stations are able to detect teleseismic events of a lower magnitude in a better quality than seafloor stations because they don’t have the noise of low frequency caused by the ocean surface, and they can properly be grounded. The ocean is an important source of broadband seismic noise, so that high noise levels limit the types of seismic measurements (Webb, 1998). Because of this the minimum magnitude for the visibility of world-wide occurred events around 6.5 is higher than the most continental arrays. The average distance between the OBS stations is 48 km. With a minimum depth of an earthquake of around 15 km the minimum distance of a station is 28 km (=0.25◦). That means that, based on figure 4.14, the minimum magnitude of a visible earthquake has to be 1.0. Above a minimum magnitude of 2.0 the recording of local earthquakes should be clear enough to pick P-and S-Phase and allow location of the event.

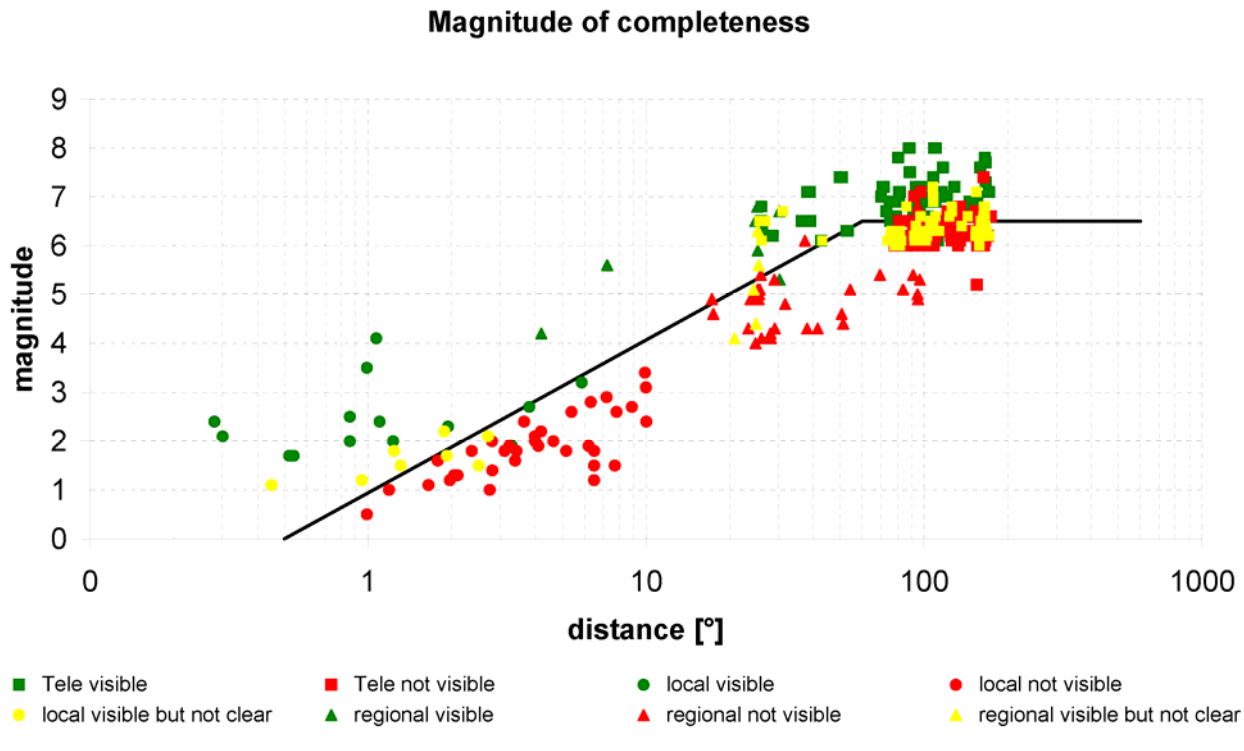

Figure 4.14 – Magnitude of completeness

4.2.4 Unidentified events

Beside the known signals recorded by the OBS (earthquakes, ocean noise, whales etc.), there is a wide variety of signals, which cannot be classified as biological or earthquakes.

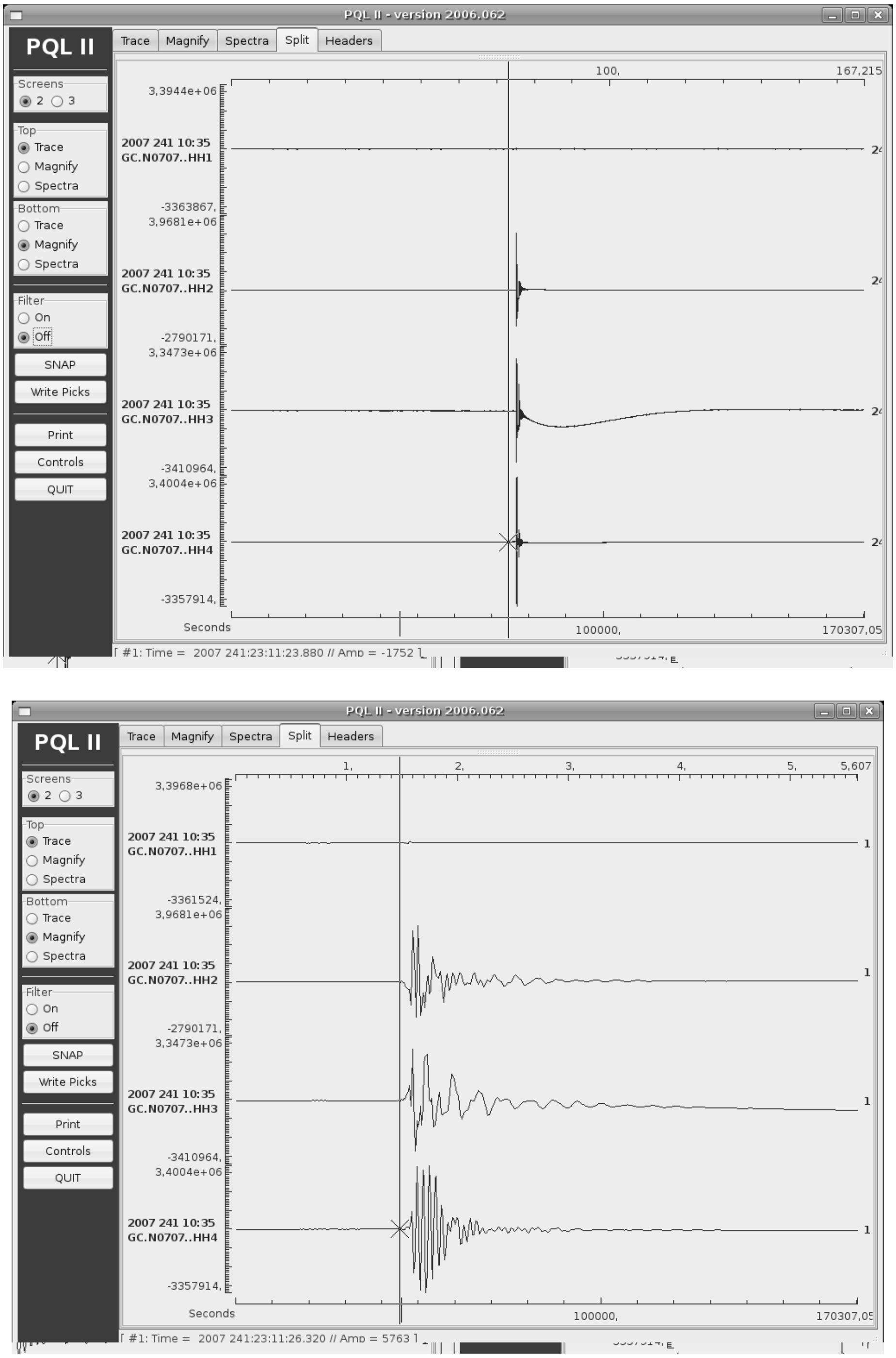

Figure 4.15 – Example of unclassified event recorded by OBS07.

4.3 High-frequency signals/noise

4.3.1 Seismic survey, R/V L'Atalante Sep. 2007

During and immediately after the deployment of the OBS, there was a seismic survey by Spanish colleagues onboard R/V Atalante (Somoza et al., 2007). The shots could be recorded throughout the OBS array. One of the seismic profiles was finally designed to cross the OBS from west to East (OBS17 to OBS21) (see figure 4.16). This profile might be useful to validate the velocity models obtained by WP2 during the NEAREST-SEIS campaign in 2008 along P1 and P2.

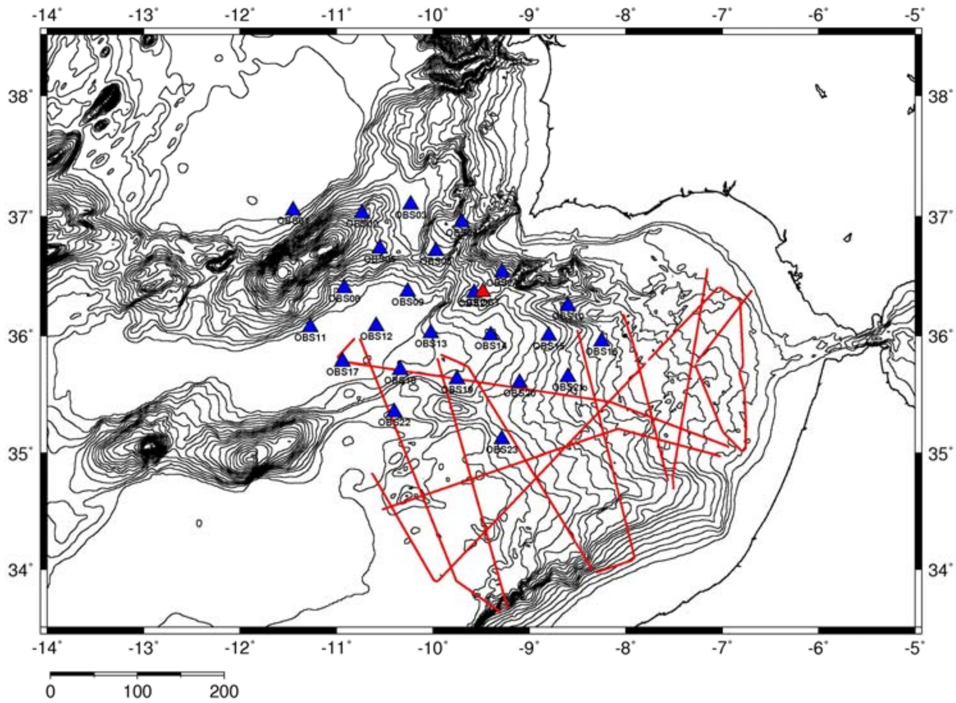

Figure 4.16 – Location of the shots for MCS acquisition during the Moundforce cruise, August/ September 2007 (Somoza et al., 2007).

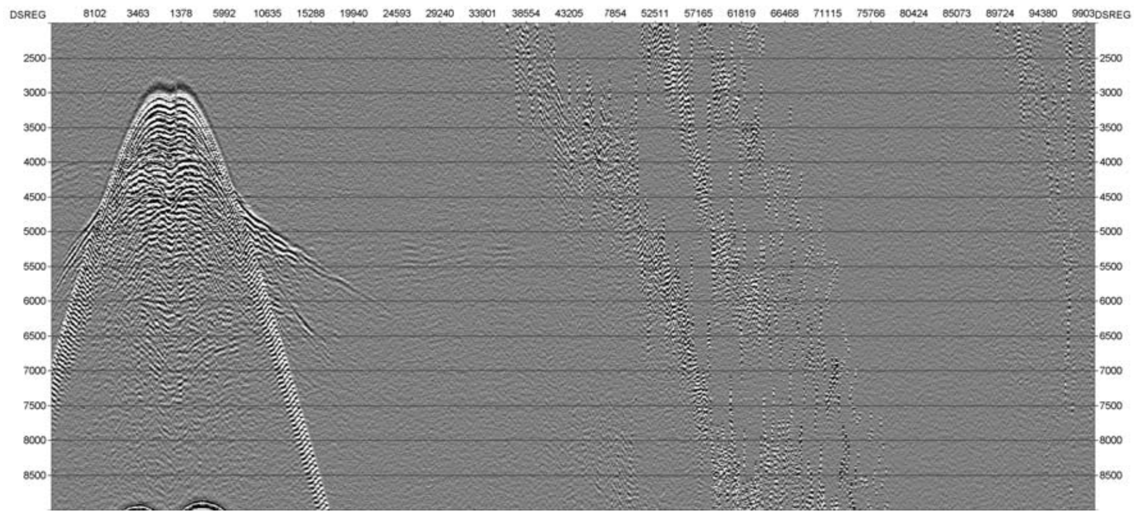

Figure 4.17 – Wide-angle record section for OBS18 recording the W-E Moundforce profile. Reducing velocity is 6 km/s.

4.3.2 Whale vocalizations

To facilitate the analysis of the one-year continuous recording made by 24 BB OBS from the AWI pool on behalf of the NEAREST project, it has been proposed to use the visual inspection of spectrograms. It was soon apparent that other signals have been recorded by the bottom instruments, as it is shown in figure 4.18. Some of these signals could be identified as mammal vocalizations, namely the ones produced by fin whales (figure 4.19). This report shows the work that has been done by the NEAREST-WP3 working group on the analysis of this type of signals. It is hoped that a more thorough examination of the complete data set can follow by some interested party.

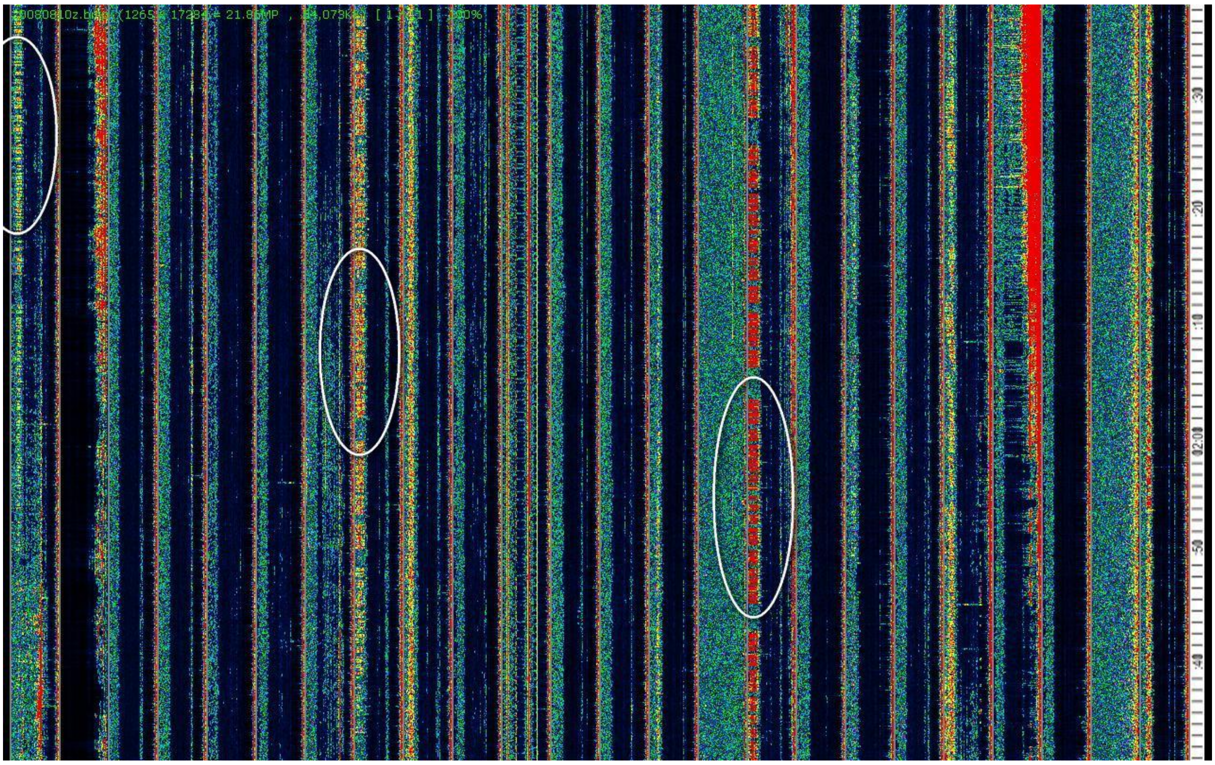

Figure 4.18 – Sample of the spectrograms from the Z component computed for the 24 OBS belonging to the NEAREST network. The day is at the beginning of July 2008. The white ellipses show the suspected mammal vocalizations.

Basics on fin whale vocalizations

Fin whale is the common name for the *Balaenoptera physalus*[2]. This whale has the particularity to make vocalizations that are easily identified on ocean sound records due to its low frequency, narrow band and periodicity. In this text we will follow the nomenclature proposed by Watkins et al. (1987) to characterize the sounds generated by fin whales. A fin whale vocalization is composed by a series of pulses with some regularity. Fin whales can also produce single pulses or irregular pulses, but these will not be considered here. Each pulse, also designated by 20-Hz pulse, is a sound wave with 1-second duration made by a sweep downward in frequency from approximately 23 to 18 Hz. An example of repeated pulses is shown in figure 4.19. For the display we converted the digital signal recorded by the hydrophone to a sound file ("wav" format), and then used the freeware application **audacity** for sound analysis. To make the sound audible we multiplied the frequency by 10 and so the time scale of the plots has also to be multiplied by 10 to get true time measurements.

The 20-Hz sound pulses are generated regularly, separated by pulse intervals. These intervals are most frequently 10 seconds but they can be longer. An example is shown in figure 4.20. A complete song is called a 20-Hz signal bout by Watkins et al. (1987). The bouts must be separated by at least 2 hours of silence. Within a bout, long intervals between pulses are called rests, if they last for 1 to 20 minutes, or they are called gaps, if they are longer than 20 minutes but shorter than 2 hours. Coincident observations and sound recordings indicate that rests are related to respiration surfacing. More details on the observation of fin whale vocalizations and their interpretation can be found in Thompson et al. (1992) or McDonald et al. (1995).

Fin whale sound recordings by the NEAREST OBS array

We examined the first 15 days of recordings of January 2008 and selected for further processing the fin whale 20-Hz bout that was recorded by OBS16 the 4th January after 12:50 UTC. The water depth at

[2] http://ec.europa.eu/environment/nature/conservation/species/ema/species/balaenoptera_physalus.htm

the OBS16 location is 2069 m. The OBS used in this experiment, provided by the AWI pool, record 4 channels: the 3 seismometer components, Z, X and Y and one hydrophone channel. The complete set of recordings for the particular 20-Hz bout selected is shown in figure 4.21.

One thing that is surprising on the 4-channel recording is that the fin-whale sound is perfectly recorded also by the horizontal components of the seismometer. And looking carefully, we see that the amplitude of the X and Y components changes in the opposite way, suggesting that the whale is moving around OBS16.

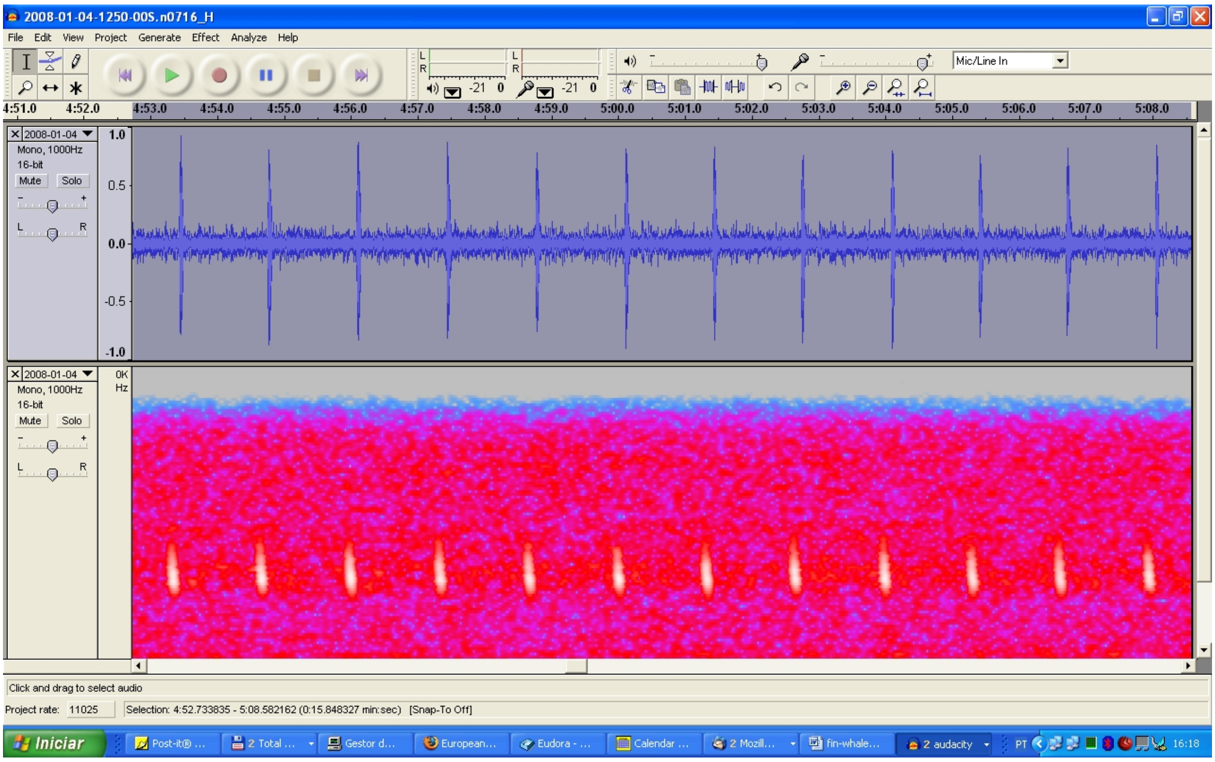

Figure 4.19 – Waveform and spectrogram of repeated pulses generated by a fin whale in the Gulf of Cadiz. The downward frequency sweep is obvious in this plot.

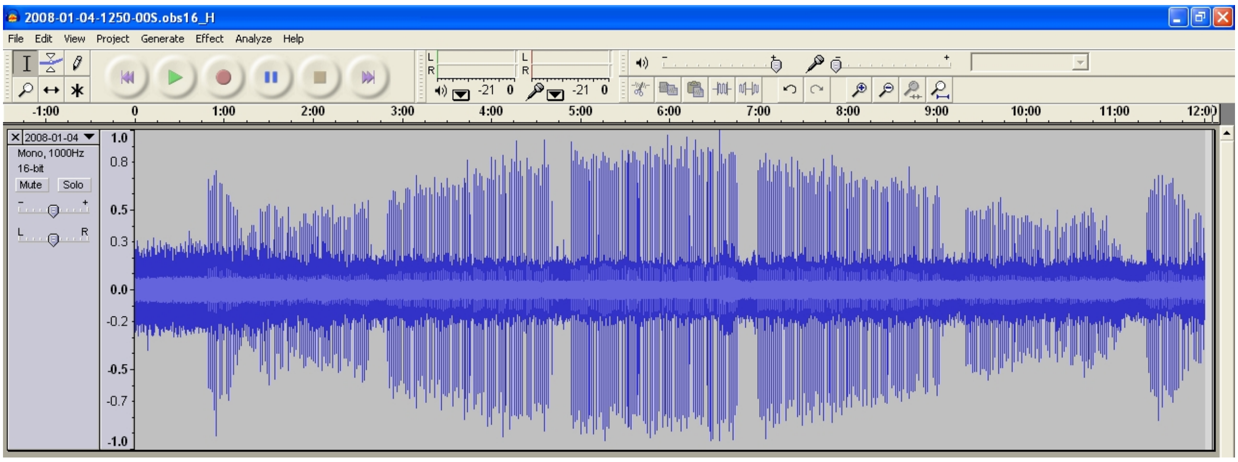

Figure 4.20 – Sequence of 20-Hz pulses separated by regular 10 second pulse intervals, and some times by longer intervals, 1 to 2 minutes. These longer intervals are called rests. The window represents a song of 2 hours duration.

When an array of sensors is used to monitor mammal vocalizations, the usual way to locate the position of the sound emitter is to use differential travel-times between the different recording instruments (e.g. McDonald et al., 1995, Rebull et al., 2006). Range to the sound source can be estimated using the knowledge of the seafloor relief and the fact that direct and reflected waves arrive at different times, according to range (ibid.). When a single instrument is available, range can also be estimated from the amplitude of the sound source (McDonald and Fox., 1999).

In the case of the NEAREST array recordings in the Gulf of Cadiz, the sensors are too far apart to record the same whale on several instruments.

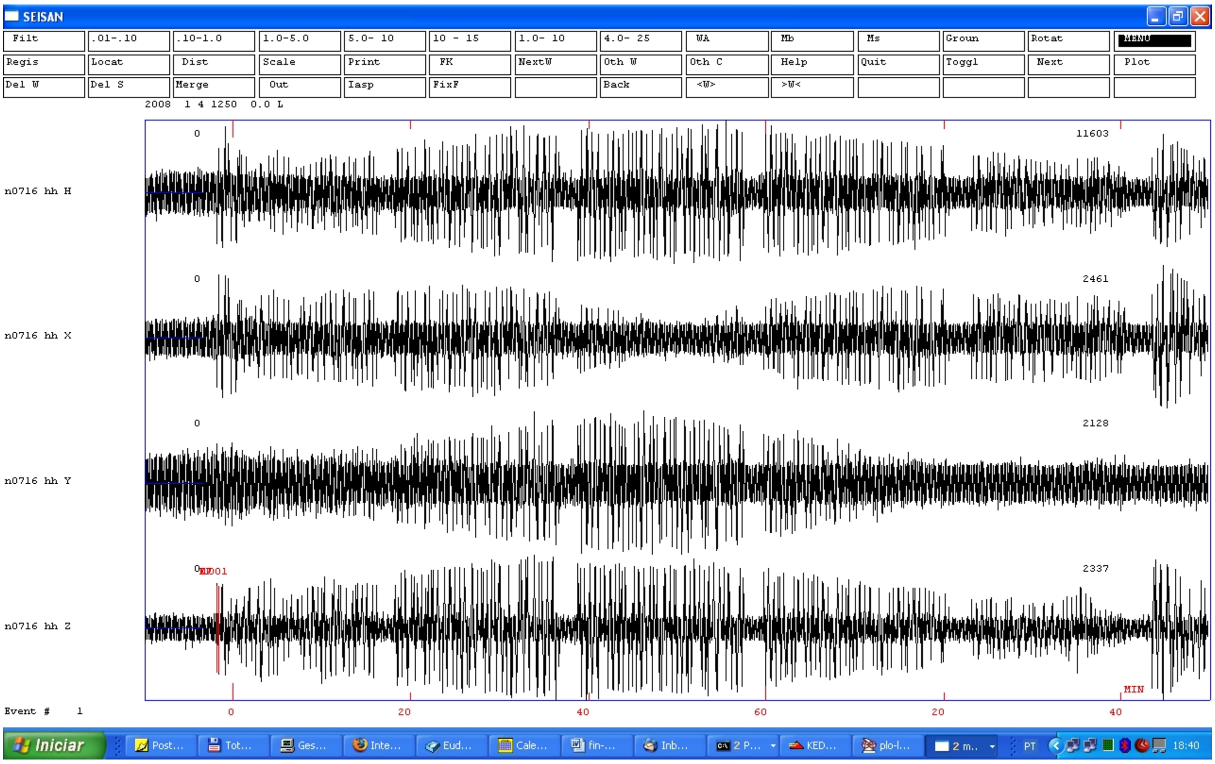

Figure 4.21 – Part of the 20-Hz pulse bout recorded by OBS16 on 4th January 2008.

4.3.3 Man-made signals recorded by the NEAREST OBS array

Besides the sounds emitted by mammals, the NEAREST OBS array also recorded other distinct signals that were detected on the spectrograms. We present below some examples that are most certainly originated by ships travelling close to the sensors. All these recordings are characterized by sharp horizontal lines on the spectrogram, with or without some frequency fluctuations. However, there is some suggestion in figures 4.22 and 4.23 that the diffuse background frequency spectrum has some frequency shift, down when approaching the sensor and up when moving away from the sensor. The reason for this strange behaviour in the spectrogram is not known yet, but it should be related to the movement of the sound source.

4.3.4 Other unknown harmonic signals

Beside the identified whale vocalizations we found further quasi-mono-frequent signals, which show similarities with whale songs. An important question is, if whale callings on seismometer components were not previously misinterpreted as harmonic tremors (related to methane release etc.) and other "interesting" seismic phenomena. We want to stress the importance to identify and characterize biological sources of seismo-acoustic signals before interpreting "unknown" types of seismic events in ocean seismic recordings.

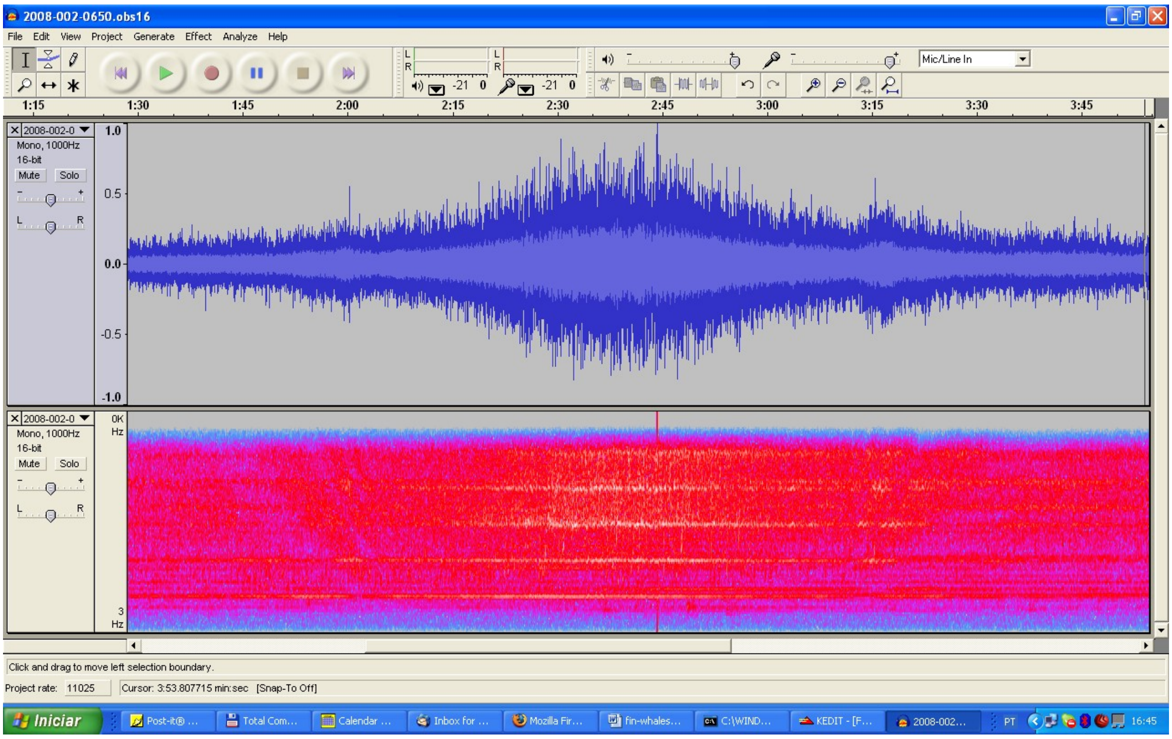

Figure 4.22 – Example of ship recording by the NEAREST array in the Gulf of Cadiz.

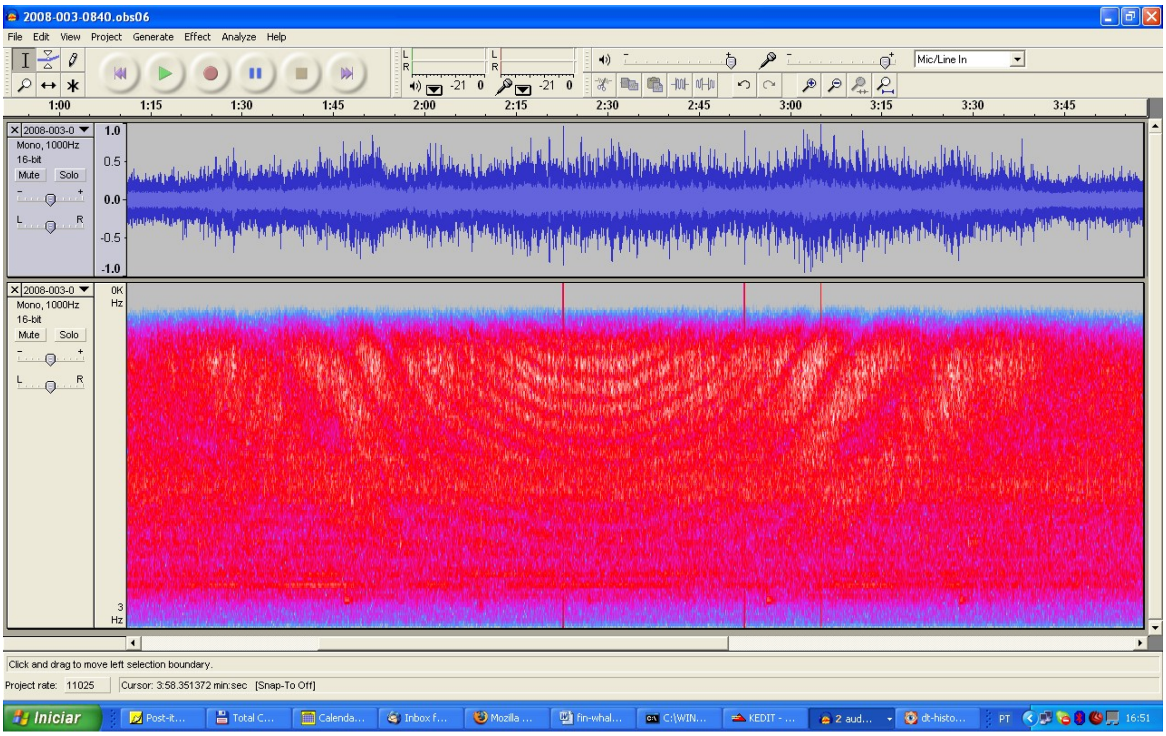

Figure 4.23 – Example of ship? recording by the NEAREST array in the Gulf of Cadiz.

There are several publications reporting monochromatic signals (harmonic tremors) and interpreting them as related to “methane release” (Pontoise & Hello, 2002), “breathing of the seafloor” (Tolstoy et al., 2002) or “hydrothermal activity” (Diaz et al., 2008). All (cited) authors agree that the observed signals are caused by movement of fluids (water, methane, ...), and not by biological sources. On the other hand, we don’t exclude a possible biological explanation for the 5-6 Hz signal.

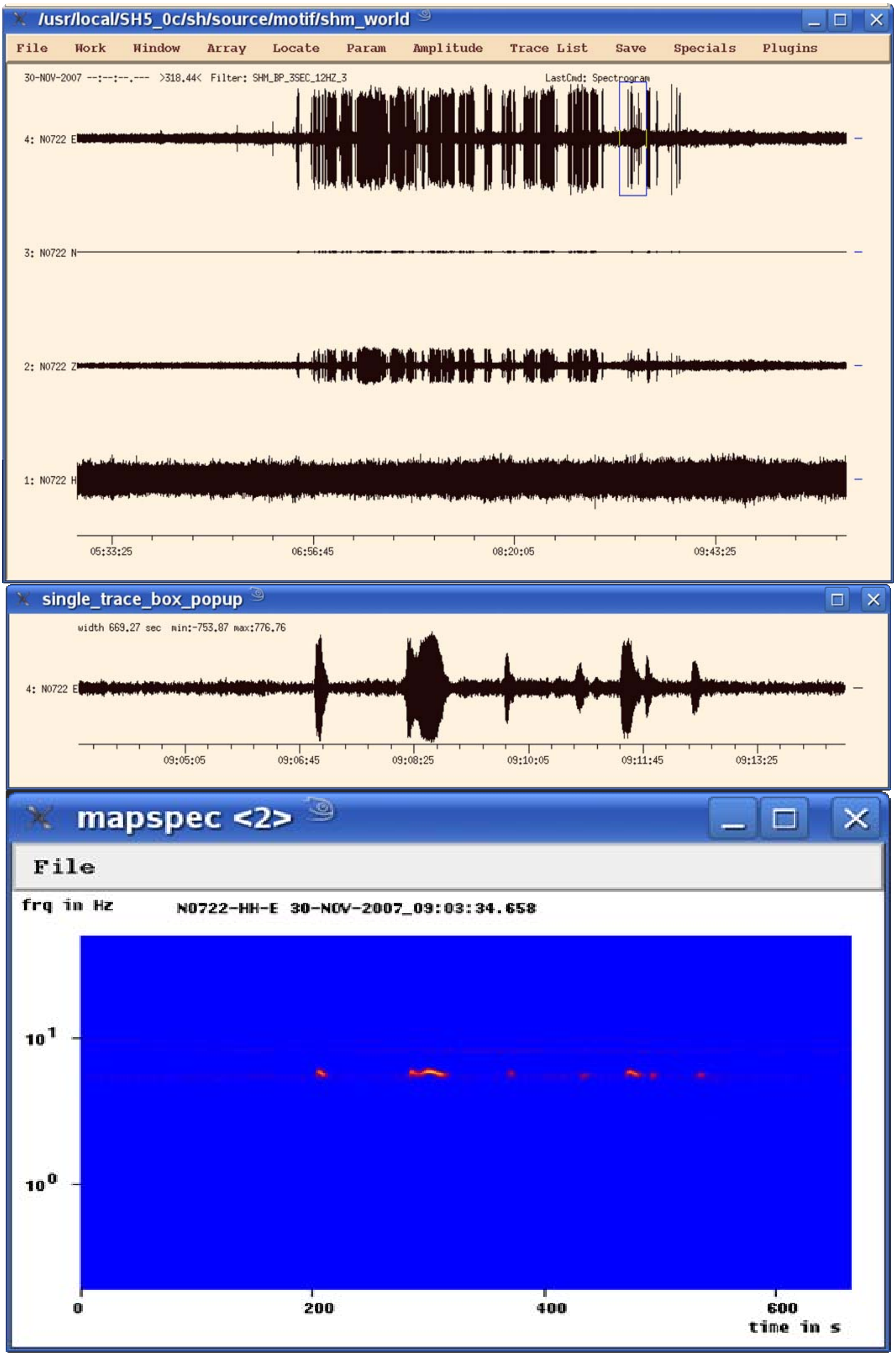

Figure 4.24 – Seismograms and spectrograms of unidentified harmonic signals.

The explanation often used by authors to favour an earth source for this tremor signal is the recording on the seismometer components, and no or weak signals on the hydrophones. In our experience it is not possible to exclude a source in the water column, and, in particular, a biological source. There seems to exist a good coupling of the acoustic signals into the ground (maybe caused by the mud layer at the sea bottom?).

5 Local seismicity

The study of local seismicity was the main goal of WP3. A major part of the WP3 activities covered the OBS deployment and data quality control. As shown before, the quality of the recorded signals provides a solid base for detailed seismicity studies in the area. So far, only a limited processing and analyses of the recorded earthquakes could be done.

5.1 Local earthquake activity in the Gulf of Cadiz 2007-2008 – trigger list

To find new earthquakes in the OBS data set, two approaches were tested. The first one is the automatic REF TEK trigger algorithm, which is a STA/LTA trigger. The second one is to manually screening of spectrograms of vertical seismometer components, which were calculated with the routine len2bmp (FORTRAN code provided by Luis Matias). The REF TEK trigger analyses the filtered data of single OBS (Z component) first. Then the trigger lists from different OBS are compared to each other to find common events which were at least triggered by a sub-set of 4 stations. The following parameters are chosen for the triggering:

The len2bmp routine of Luis Matias first converts the mseed data to ASCII format. Then it calculates daily spectrograms over a defined frequency range that can be screened by eye. Earthquakes are clearly visible in these spectrograms by the bandwidth of stimulation and their occurrence on several stations. The green lines in Figure 5.1 show the origin time of a known earthquakes published in the IM Bulletin. There is one trace for every OBS as shown in Fig. 5.1a likewise the sequence of the OBS in the bitmap. If the trace of an OBS is grey then the OBS was not yet deployed; if it is black, then the vertical component of the OBS did not level.

Table 1a – Single OBS trigger algorithm parameters

filter:	bandpass, 5 to 20 Hz
sta (**s**hort-**t**erm **a**verage) window length:	10 sec
lta (**l**ong-**t**erm **a**verage) window length:	60 sec
mean removal window length:	200 sec
trigger ratio:	3.0
detrigger ratio:	0.7

Table 1b – Network trigger algorithm parameters

network travel time (time which is allowed between first and last trigger inside the network):	15 sec
minimum number of stations with same triggered event:	4

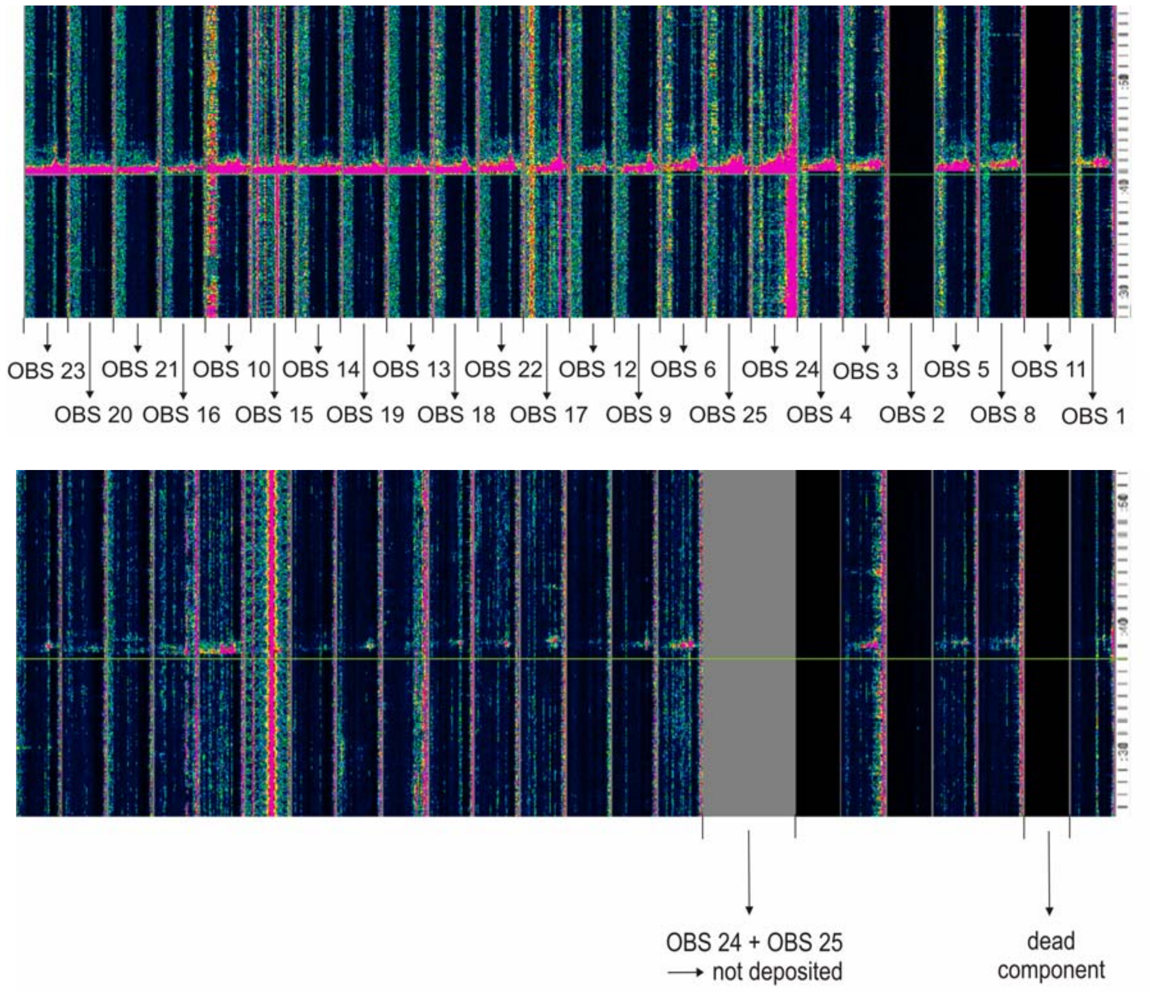

Figure 5.1 – a) Spectrogram of Z components (January 11, 2008 07:41). The origin time of a known event is marked by the green line. B) –Spectrogram of Z components (known event: September 12, 2007 04:38).

The results of the trigger algorithm and the analysis of the spectrograms are compared for several months (September 2007, January 2008, February 2008, and March 2008). The following presented results are only for September 2007, for the three other months it is similar. There are 112 triggered events with an earthquakes share of 109, and also 112 events from the spectrograms with an earthquakes share of 108. But only 97 of these events are found by both methods, 11 are found only on the spectrograms, and 12 only with the trigger algorithm (Tab. 5.2). That means, around 86 percent of the events, are detected by both methods. Almost all events that are visible in the spectrograms, but not found by the trigger in seismograms, are from lower quality (Fig. 5.2a – 5.2c) or are simply not visible in the seismograms. Because of that, and the fact that it is faster, the trigger algorithm has been chosen to isolate earthquakes from the continuous data set.

Statistics and quality checks

After extracting all triggered events from the continuous data set they are verified manually. Of 1641 triggered events are 1322 earthquakes and plus some earthquakes, which are not on the lists of the trigger algorithm (but found on spectrograms or by chance), there are in total 1354 earthquakes from August 29, 2007 till August 11, 2008 (Table 5.3). In the following all earthquakes are categorized by a quality, to have a better overview. The four categories and the criteria, which are chosen to describe the quality, are listed in Table 5.4. Furthermore, some examples of earthquakes, which are typical for one of the quality categories, are shown in Figure 5.3a – 5.3d.

Table 5.2 - Comparison trigger algorithm with spectrogram screening for September 2007

	trigger	spectrograms
number of events found:	112	112
earthquakes share:	109	108
number of events found by trigger and spectrograms:	97	

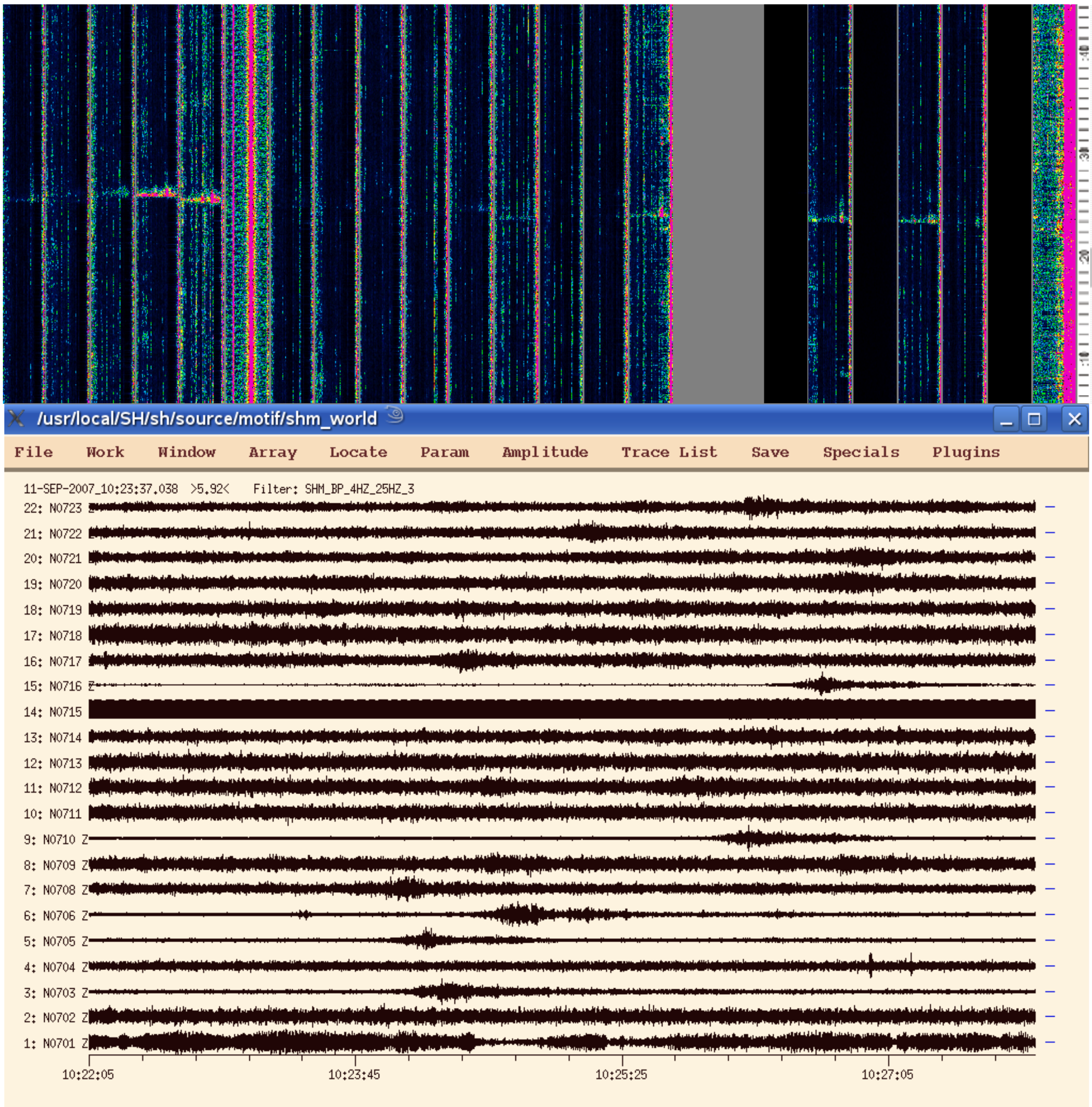

Figure 5.2a – Event from September 11, 2007 10:23 (clear bursts of energy in spectrogram, but in seismogram almost only T-phases, which are not found by the trigger algorithm because of the smooth increase in amplitude).

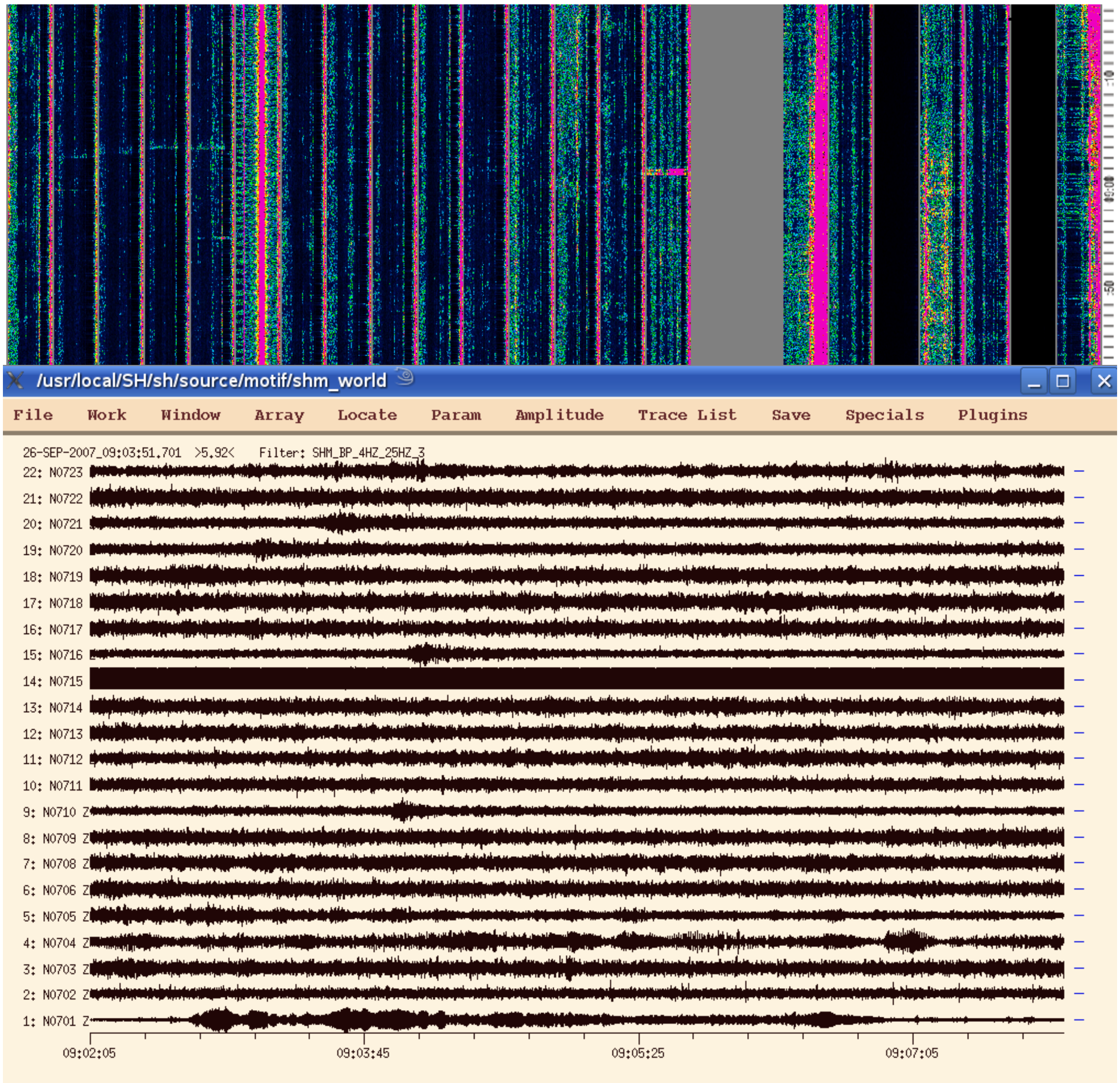

Figure 5.2b – Event from September 26, 2007 09:04, Z components.

Table 5.3 – Statistical overview of the events recorded by the NEAREST network

number of events found by trigger:	1641	
earthquakes share:	1322	≈ 80.6 %
number of earthquakes which are not on trigger list:	32	
total number of earthquakes:	1354	

Table 5.4 – Earthquake qualities

best:	earthquake visible, clear phases, **with polarities** on most of the OBS
high:	earthquake visible, phaes identifiable on **most** of the OBS
medium:	earthquake visible, phases identifiable on **some** of the OBS (minimum 3 OBS)
low:	earthquake visible, but **phases vague or not identifiable** (minimum 4 OBS)

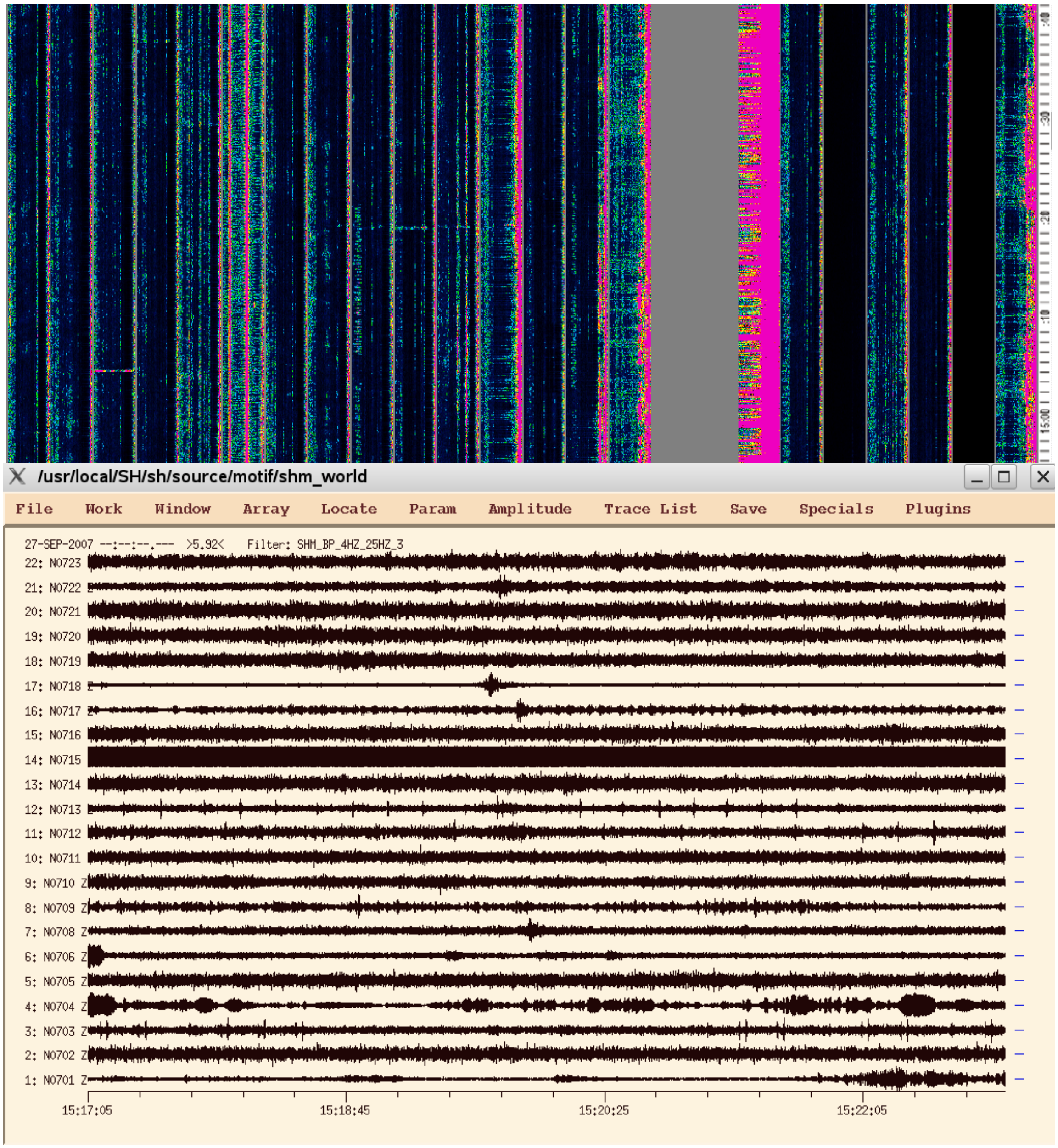

Figure 5.2c – Event from September 27, 2007 15:18 (the earthquake is clearly visible only on three OBS, that's why the trigger did not get it, because at minimum four stations are needed for a proper detection)

Table 5.5 – Statistical distribution of qualities

number of earthquakes with **best** quality:	52	≈ 3.8 %	767 --> ≈ 56.7 %
number of earthquakes with **high** quality:	154	≈ 11.4 %	
number of earthquakes with **medium** quality:	561	≈ 41.4 %	
number of earthquakes with **low** quality:	587	≈ 43.4 %	--> ≈ 43.4 %
	1354	≈ 100.0 %	

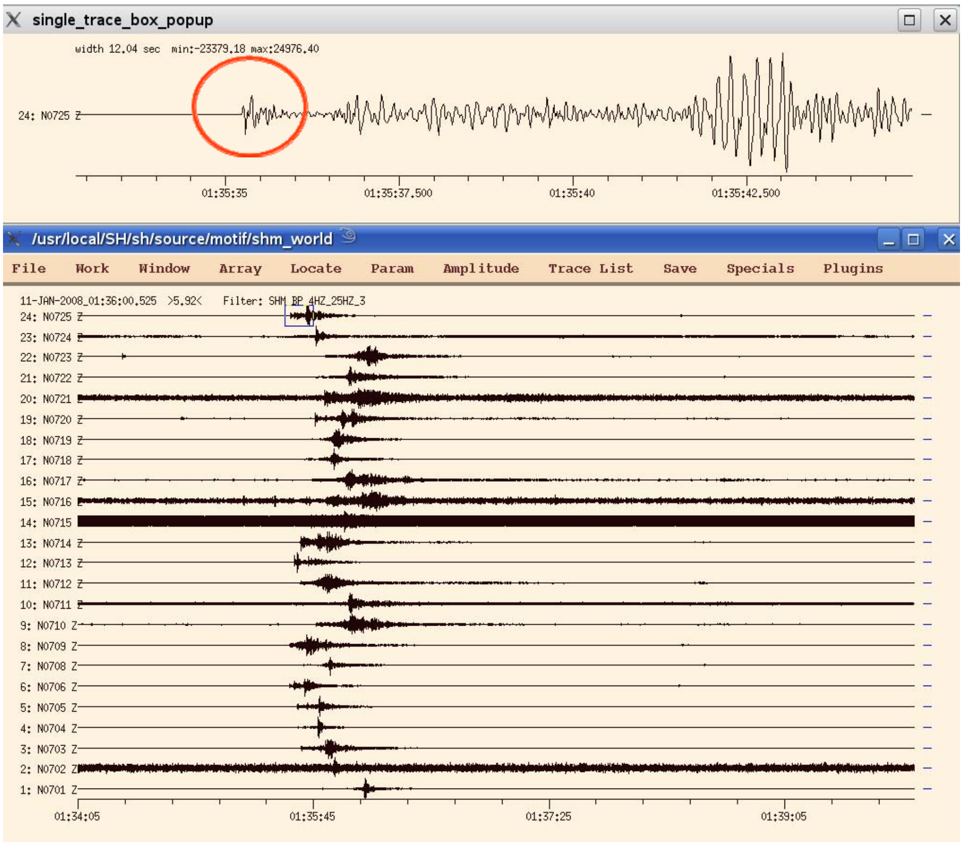

Figure 5.3a – Typical earthquake of quality "best"

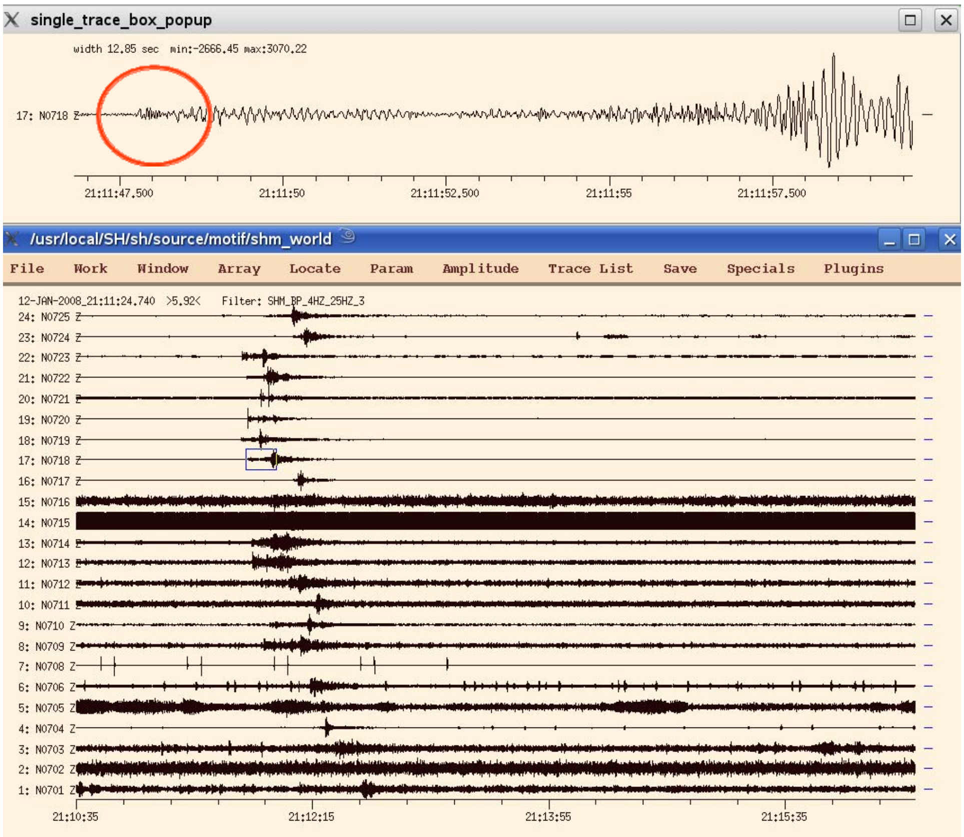

Figure 5.3b – Typical earthquake of quality "high"

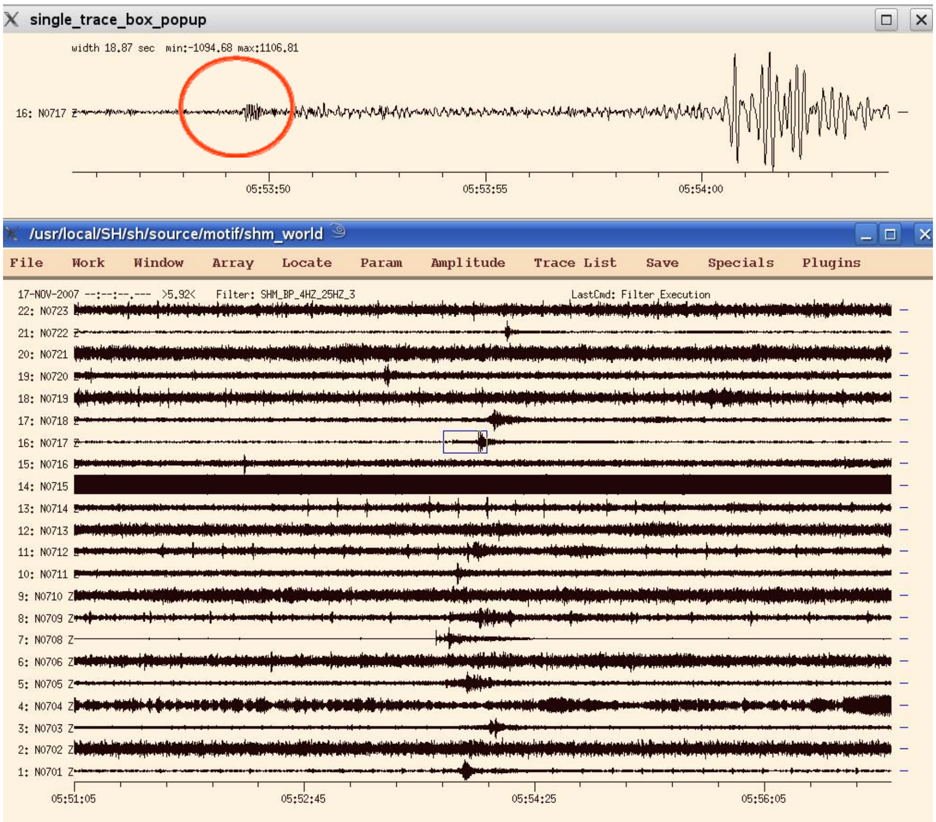

Figure 5.3c – Typical earthquake of quality "medium"

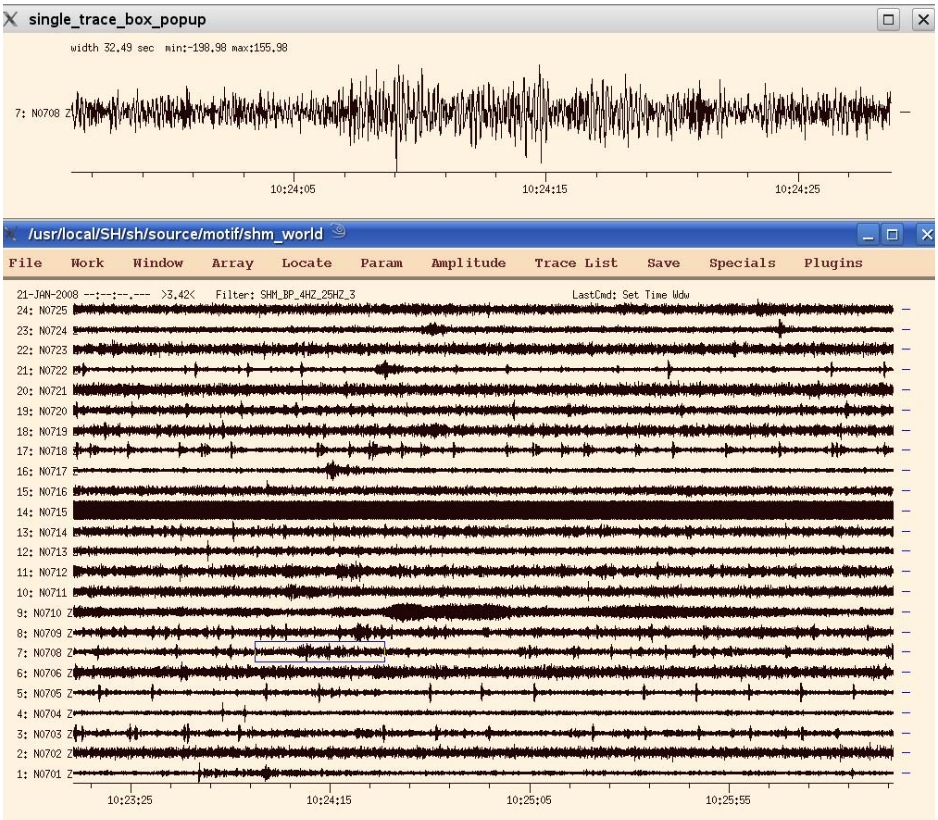

Figure 5.3d – Typical earthquake of quality "low"

At all 767 earthquakes were recorded that most probably can be located. These are more than 56 percent of all earthquakes detected by the algorithms.

Comparison of the event lists from NEAREST OBS network with IM bulletin

With the NEAREST OBS network a number of 767 earthquakes with a quality medium or higher could be recorded. For the OBS operation period the bulletin of the Meteorological Institute of Portugal (IM) containing events recorded by the land stations reports 422 located earthquakes for the area of the OBS network. That means, that the NEAREST OBS network recorded nearly two times more earthquakes with a high potential to be located.

However, table 5.6 shows also another phenomenon. 58 earthquakes in the Northeast of the OBS network, close to the Algarve coast, are detected by the land stations, but not or weakly visible in the NEAREST OBS data set (Figure 5.4).

Table 5.6 – Statistical comparison with the IM bulletin

number of earthquakes found by NEAREST network (only earthquakes with quality medium or higher):	767	
number of earthquakes found/located by land stations and the NEAREST network:	364	≈ 47.5 %
number of earthquakes not found by the NEAREST network (or on less than 4 OBS), but located by land stations:	58	
total number of earthquakes located by land stations	422	

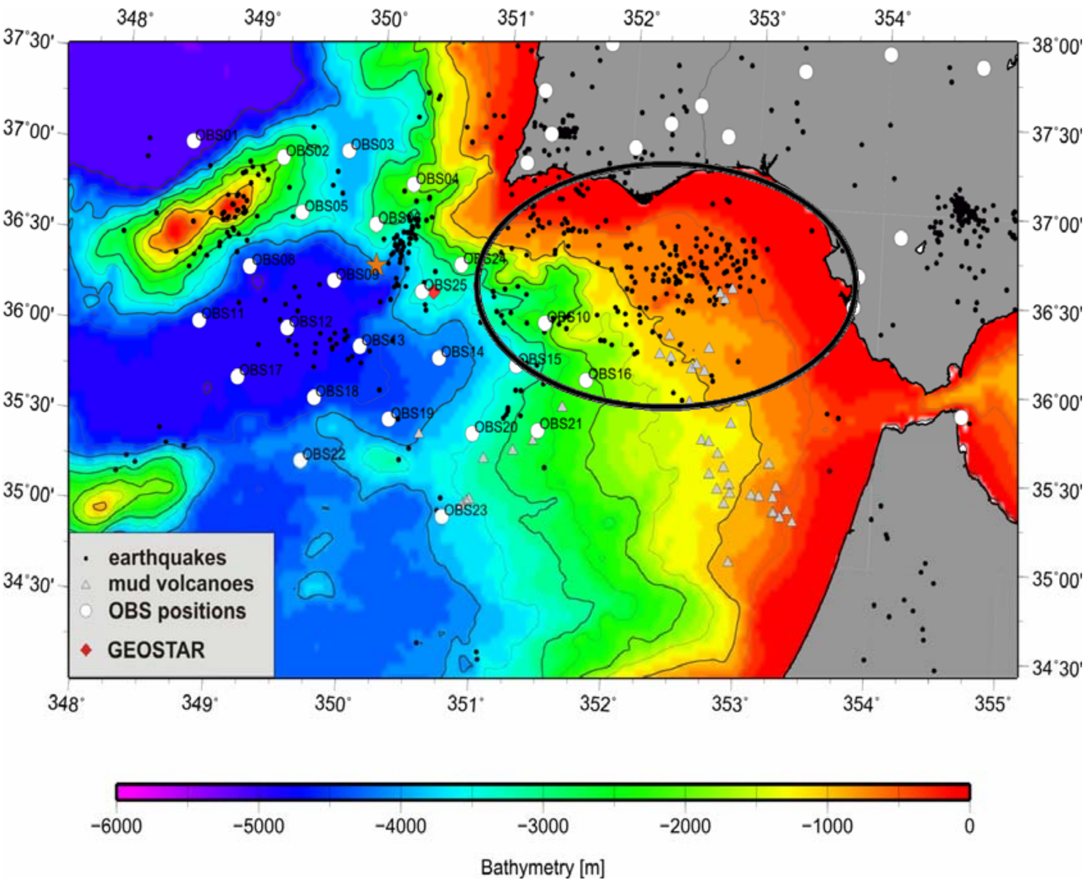

Figure 5.4 – Region from where earthquakes are recorded badly by the OBS network

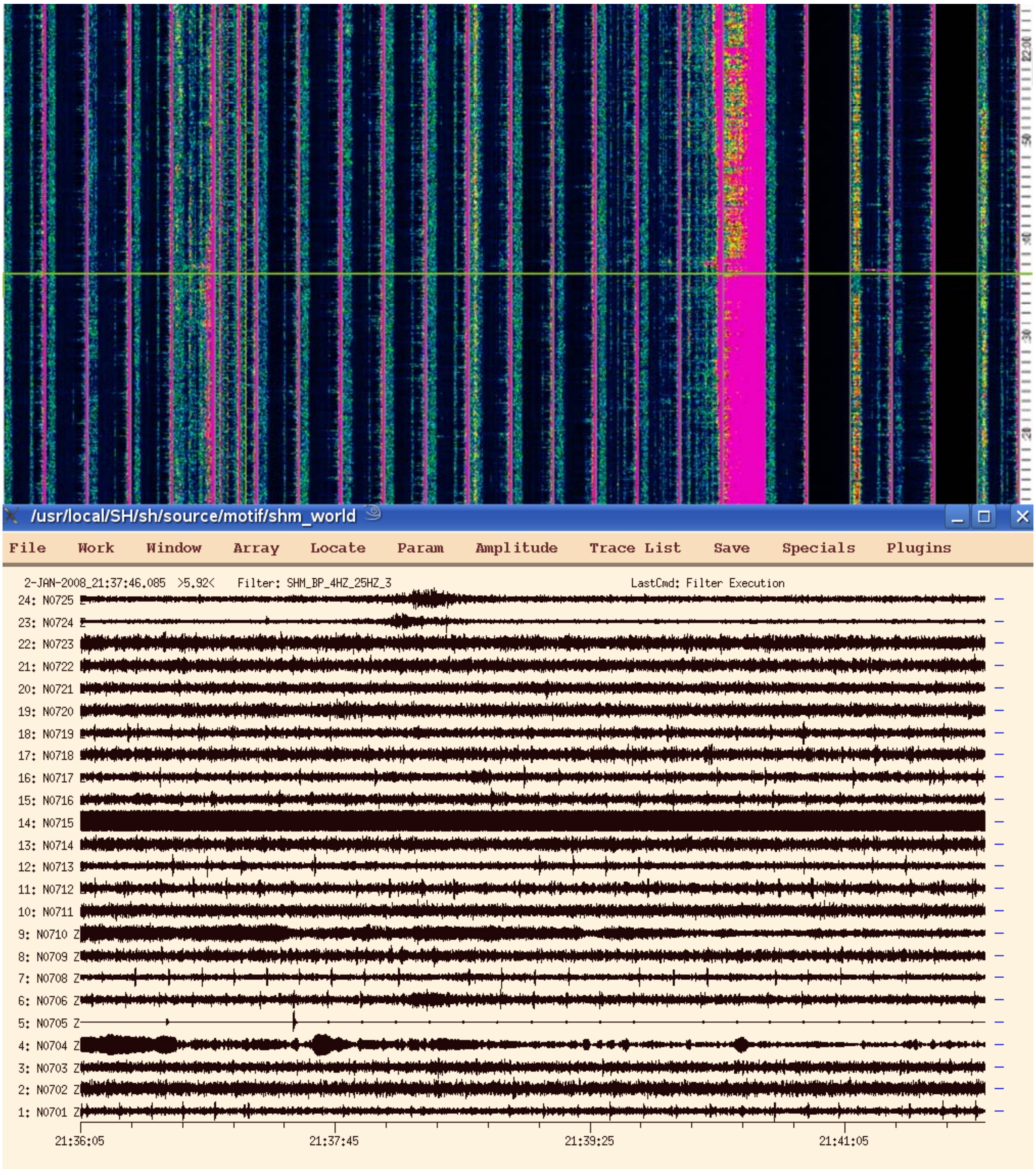

Figure 5.5a – Example of an earthquake from the Northeast of the NEAREST network (January 2, 2008 21:37). The visible amplitude is very weak; in the seismogram the event is only visible at three stations. Repeated high-frequency signals on several OBS are fin whale calls.

5.2 First evaluation of epicentres and focal mechanisms recorded by the NEAREST OBS

As a starting point 39 events recorded by the land stations inside the NEAREST network with the largest magnitude were selected (Figure 5.6). We used the SEISAN software package to analyse the waveforms and compute the earthquake locations. The velocity model used was the one described in the OBS August 2008 cruise report. After the first location, only 35 events were selected for further processing. The average station errors were used to compute station corrections that improved considerable the average event residuals (from 0.633 s to 0.445 s).

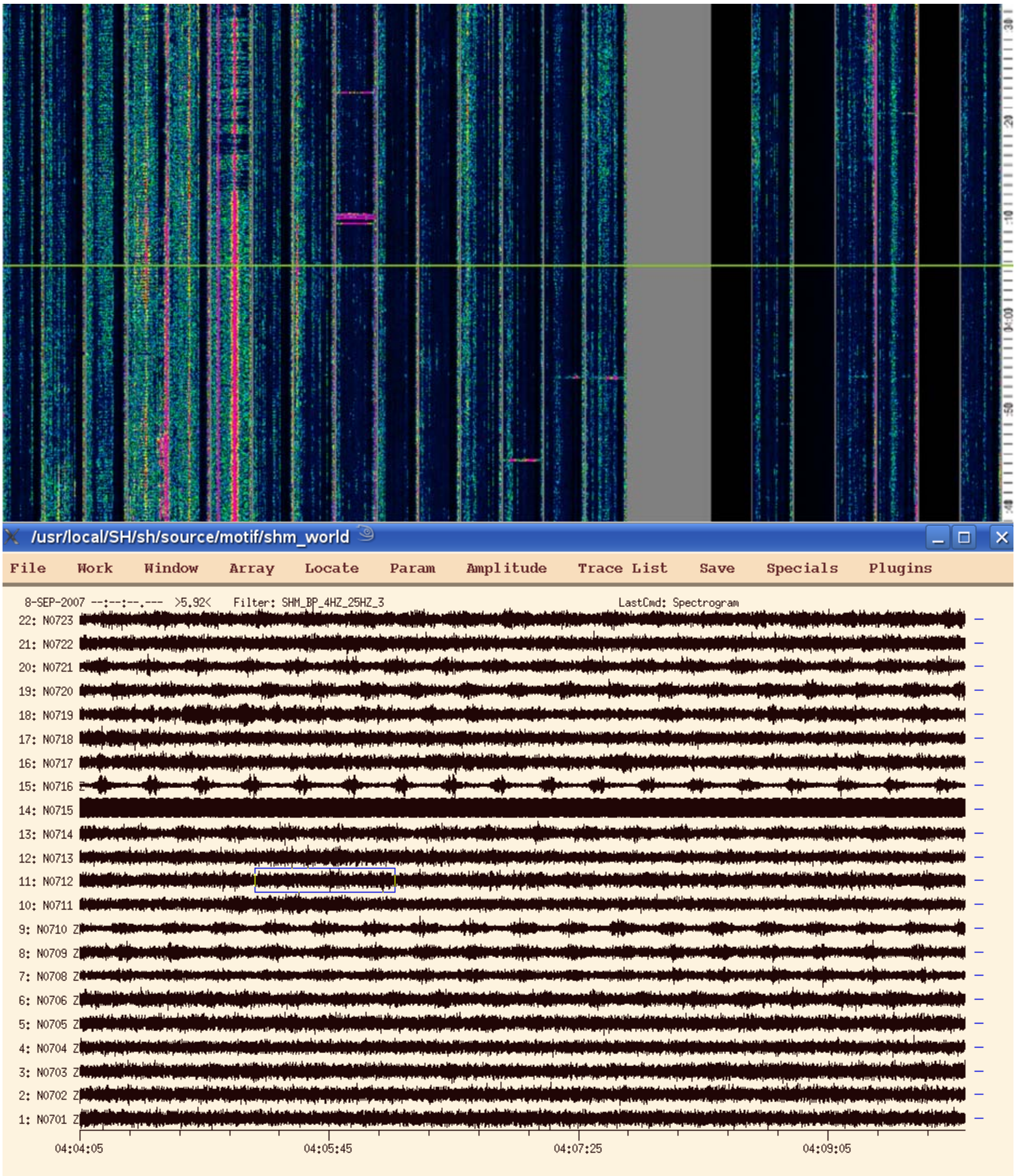

Figure 5.5b – Example of an earthquake Northeast of the NEAREST network (September 8, 2007 04:05). The blue box indicates where the earthquake should be, but in the spectrogram as well as in the seismogram no indication for an earthquake is found. Repeated signal are signals from a seismic survey in the region.

The Vp/Vs ratio was varied to find the value that best fitted the observations (1.78). The results shown were obtained using this procedure. We compare in figure 5.7 the epicentres obtained by the NEAREST network (in green) and the locations provided by IM (in red). We see that, with very few exceptions, the epicentres are displaced SW of their original location. This is confirmed by the two histograms shown in figure 5.8.

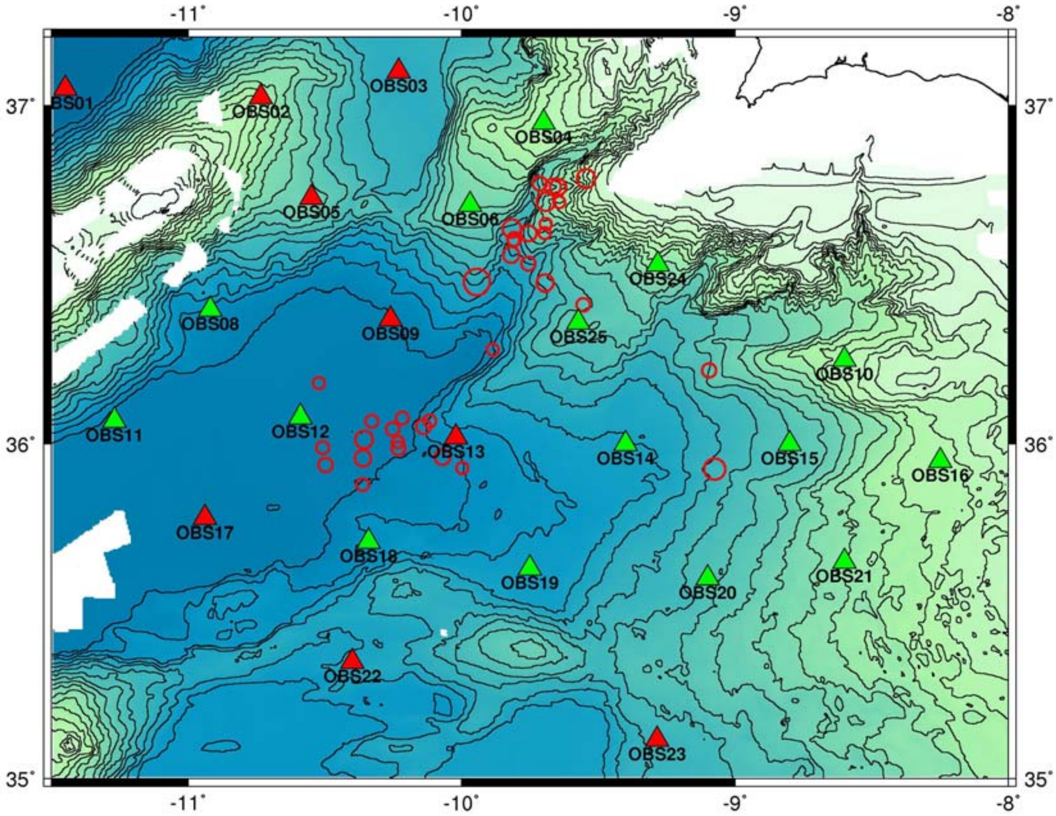

Figure 5.6 – The NEAREST OBS network with the instruments that didn't synchronize in red. The open circles show the largest magnitude events that were selected to assess the time drift.

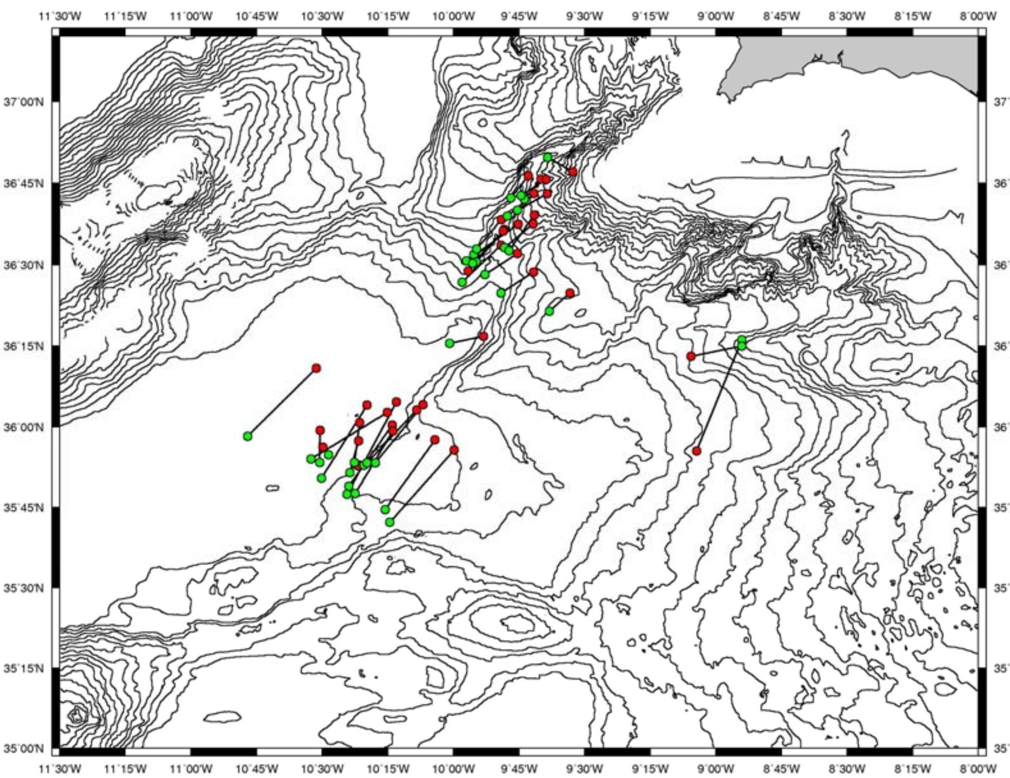

Figure 5.7 – Comparison between the locations obtained by the NEAREST network (in green) and the locations provided by IM (in red).

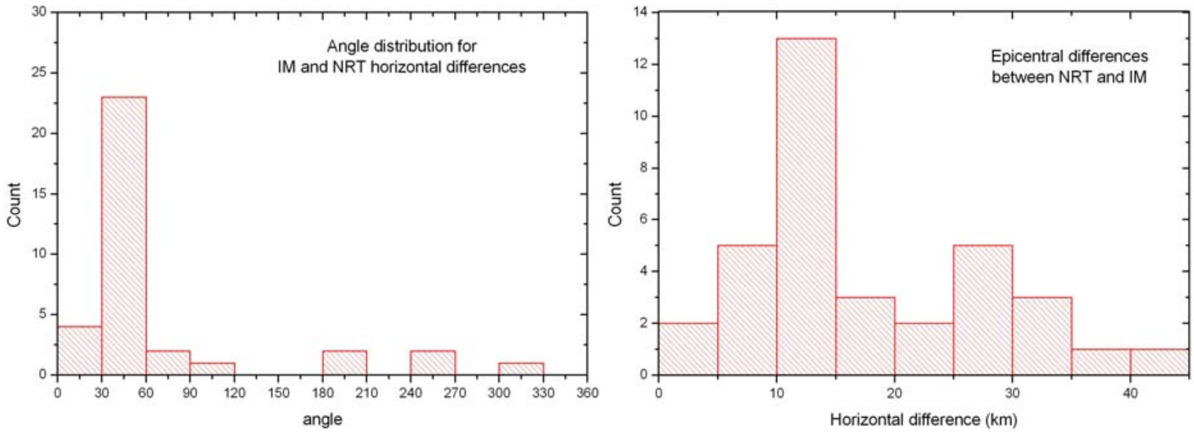

Figure 5.8 – Histograms of deviations of locations with the NEAREST OBS data from the IM Bulletin

The hypocentre depth was computed for each event and checked by a systematic search approach available in SEISAN. An example is shown in figure 5.9. Surprisingly, most of the hypocenters were found to be deep (in terms of the Gulf of Cadiz), that is, with depths greater than 40 km. These results are very different from the ones obtained by the land network and published by IM. We show a histogram on the depth comparison in figure 5.10. If we draw a depth profile on the dataset analysed (figure 5.11) the conclusion is most disturbing. The clear depth alignments present in the IM catalogue, and already published by Zitellini et al., Carrilho or Neves et al., are shown to be a geometrical feature of the network and disappear in the NEAREST data.

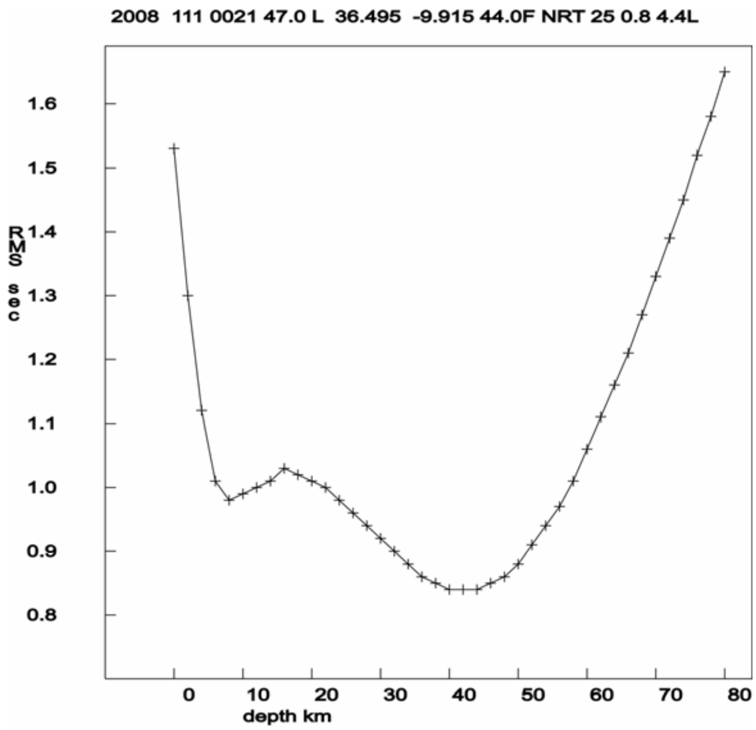

Figure 5.9 – Systematic search to test the confidence on the hypocentre depth computation.

To compute the focal mechanisms of these events we use the polarity of the P-wave interpreted on the OBS and also land station data provided by IM and IGIDL. The first solution was estimated using the FOCMEC routine. This solution was further improved using the MECSTA code (Brillinger's algorithm). We plot in figures 5.12 and 5.13 the best solutions obtained. Those selected to have more than 13 P-wave readings and a score larger than 80%.

Table 5.7 – location of the Jan 11th, 2008 00:21 event in the Gulf of Cadiz provided by different institutes.

	origin time	longitude	latitude	depth [km]	magnitude	intensity
GEOFON	00:21:45.1	9.78°W	36.54°N	10	5.4	
IM Lisbon	00:21	9.94°W	36.48°N	17	4.7	IV/V
EMSC	00:21:42.5	9.98°W	36.49°N	20f	Mw 4.4	
NEIC	00:21:48	9.80°W	36.62°N	16	4.4	
NEAREST	00:21:47	9.91°W	36.50°N	**44**	4.4	

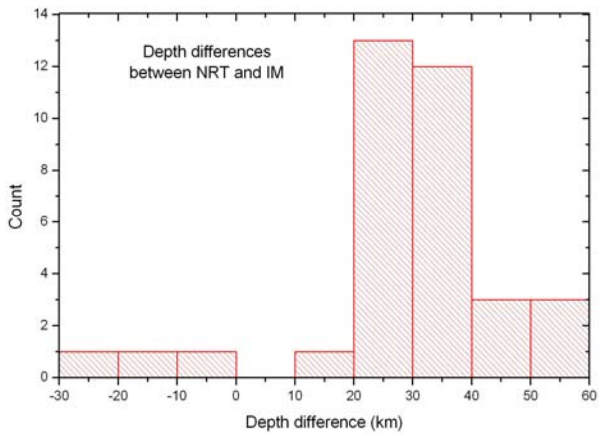

Figure 5.10 – Histogram of deviations in depth determination of NEAREST locations from IM Bulletin

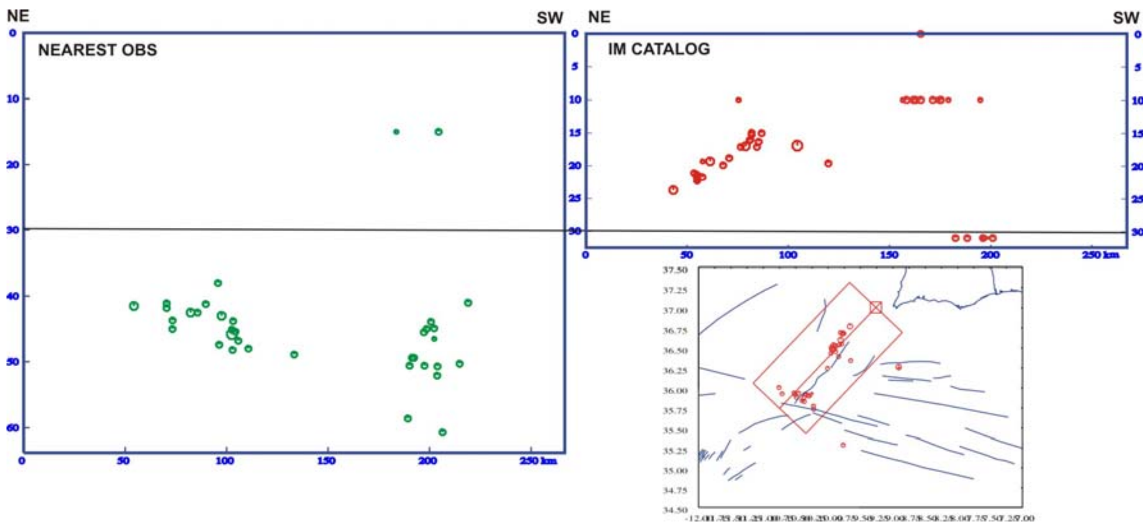

Figure 5.11 – Comparison of hypocentres depth computed by IM (right in red) and the NEAREST network (left in green). The location of the profile is shown on the right bottom. The vertical scale is the same for both sections, but the absence of events in the IM catalogue below 30 km, renders that part of the profile useless and was not plotted.

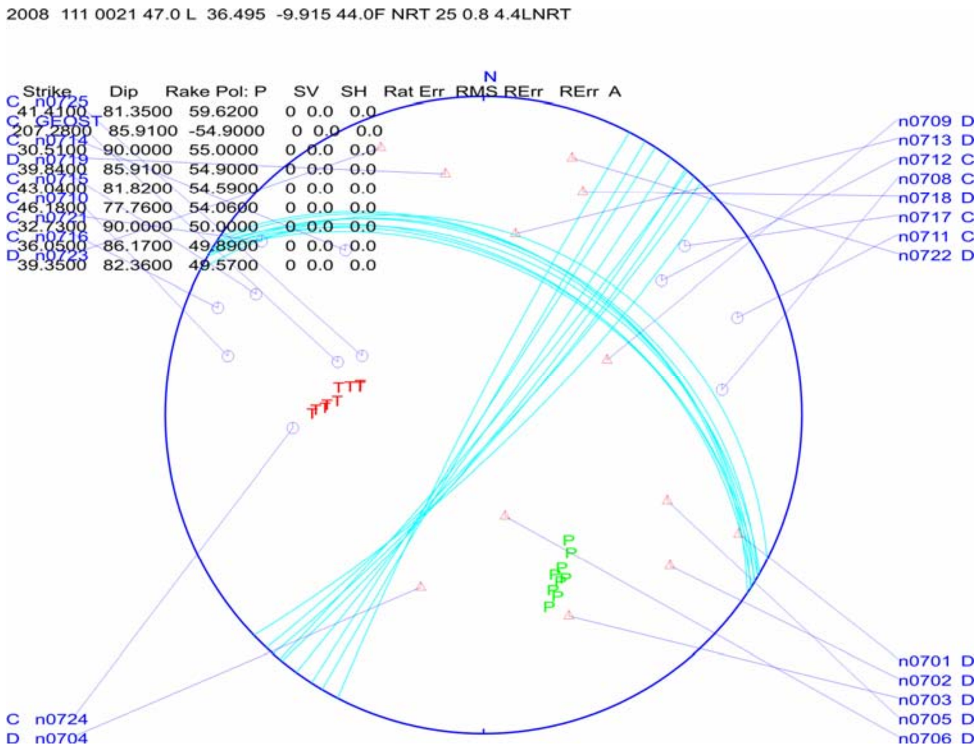

Figure 5.12 – FOCMEC solution for P wave polarities of the strongest recorded event from Jan 11th, 2008 00:21.

Tests were made to use the OBS data for waveform inversion of local earthquakes. Unfortunately, the recorded waveforms are not useful for this method, because of the mentioned transient signals after strong phases and associated steps in the data. Therefore, waveform inversion was performed using data from land stations around. The result for the strongest local event is shown in figure 5.14.

Teleseismic studies

No clear SKS phase could be recorded in the operation period of the OBS. That's why no results were achieved in the field of anisotropy studies using shear wave splitting. However, strong surface waves could be recorded, that might have the potential to reveal the S wave velocity and anisotropy structure of the lithosphere beneath the Gulf of Cadiz. First tests were done to calculate teleseismic receiver functions; however, so far there are not yet consistent results. The occurrence of deep (lithospheric) local events provides the base to use also these events to study the deep seismic velocity structure by converted waves.

6 Conclusion/summary & outlook

The data collected by the OBS network within one year show a good quality and are an excellent base for the further processing. Despite of the levelling problems of some components and the timing problems the recordings can be used for location of small magnitude events, which can give further knowledge about the seismicity and the geological structure off SW Iberia. The first look on the data gives a satisfying result and shows that with an OBS Network there is the opportunity to fill the gap of exact seismological information in the oceans.

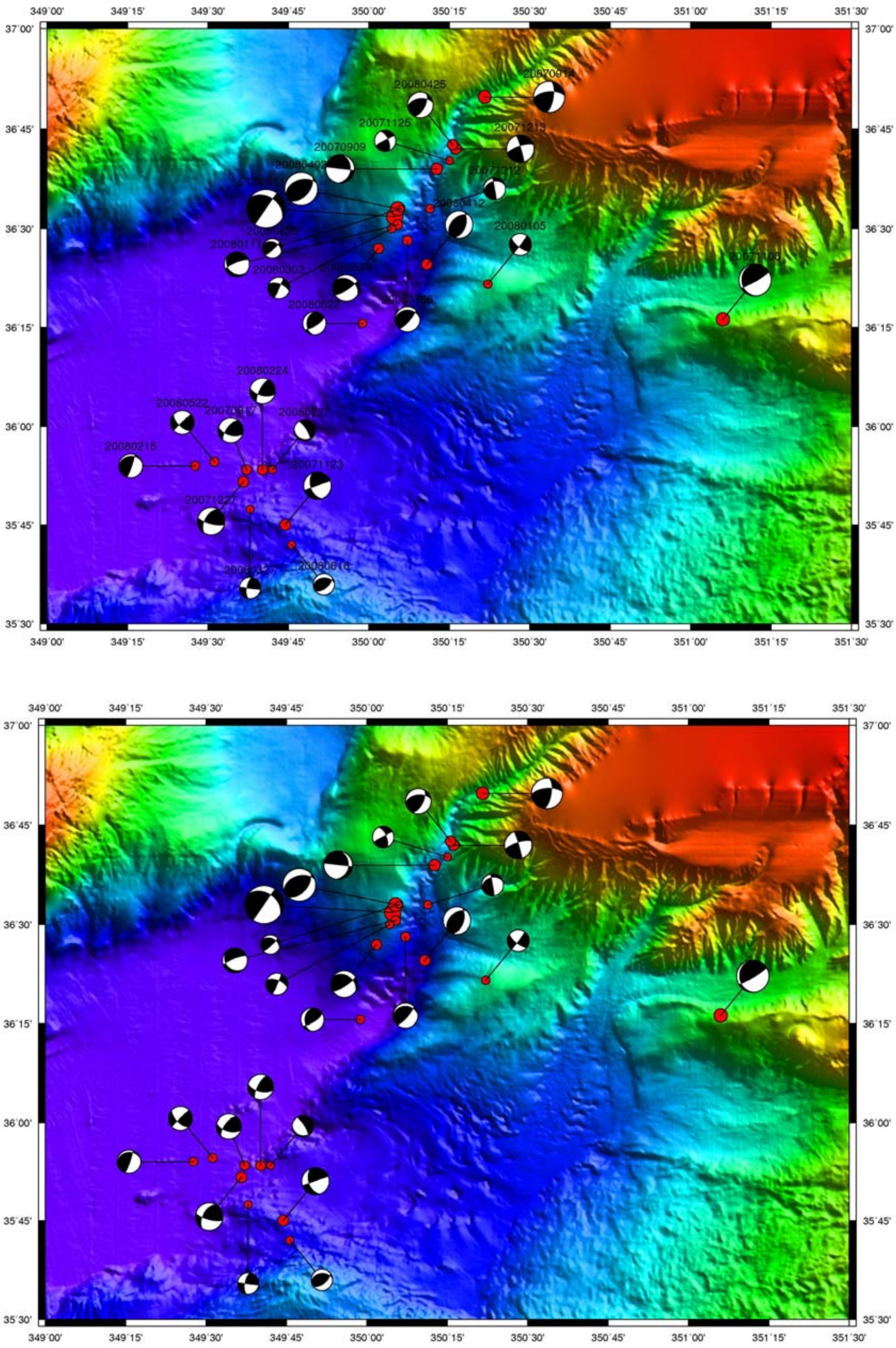

Figure 5.13 – a) standard FOCMEC solutions. b) Improved solutions using the MECSTA code (Brillinger's algorithm)

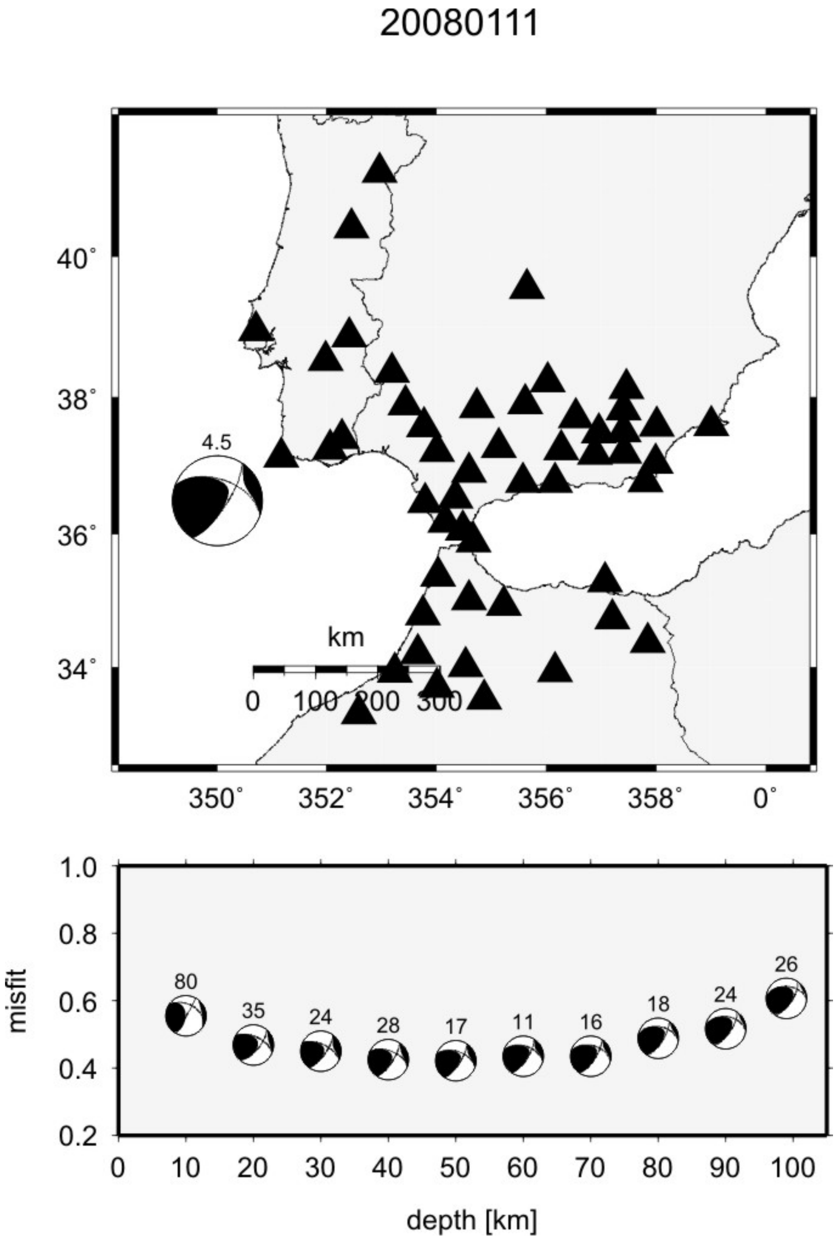

Figure 5.15 – Results from waveform inversion of the event from January 11th, 2008 00:21. Data from land stations shown in the map was used.

7 References

Carrilho, F., 2005. Estudo da Sismicidade da Zona Sudoeste de Portugal Continental, MsC Thesis, Lisbon University, 172pp.

Filloux, J., (1980). Pressure Fluctuations on the Open Ocean Floor Over a Broad Frequency Range: New Program and Early Results, J. Phys. Oceanogr., 10, 1959–1971.

Havskov, J. and Ottemöller, Lars (editors), 2005. SEISAN: The Earthquake Analysis Software for Windows, Solaris, Linux and Macosx, Version 8.1, 259pp.

Garrett, C., and W. Munk (1975). Space-Time Scales of Internal Waves: A Progress Report, J. Geophys. Res., 80, 291-297.

McDonald, M.A., Hildebrand, J.A. and Webb, S.C., 1995. Blue and fin whales observed on a seafloor array in the Northeast Pacific, J. Ac. Soc. Am. 98(2), pp 712-721.

McDonald, M.A. and C.G. Fox, 1999. Passive acoustic methods applied to fin whale population density estimation, J. Ac. Soc. Am. 105(5), pp 2643-2651.

Press, W.H., Flannery, B.P., Teukolsky, S.A. and Vetterling, W.T. (1986). Numerical Recipes: The Art of Scientific Computing, Cambridge University Press, 818pp.

Rebull, O.G., Cusi, J.D., Fernandez, M.R. and Muset, J.G., 2006. Tracking fin whale calls offshore the Galicia Margin, North East Atlantic Ocean, J. Ac. Soc. Am. 120(4), pp 2077-2085.

Roberts, R.G., Christoffersson, A., and Cassidy, F., 1989. Real time events detection, phase identification and source location estimation using single station component seismic data and a small PC, Geophysical Journal, 97, 471-480.

Somoza et al., 2007. Moundforce - Informe científico-técnico, N/O L'ATALANTE, 23 Agosto / 9 Septiembre 2007. http://tierra.rediris.es/moundforce/

Thompson, P.O., Findley, L.T. and Vidal, O., 1992. 20-Hz pulses and other vocalizations of fin whales, *Balaenoptera physalus,* in the Gulf of California, Mexico, J. Ac. Soc. Am. 92(6), pp 3051-3057.

Watkins, W. A., Tyack, P. and Moore, K. E., 1987. The 20-Hz signals of finback whales (*Balaenoptera physalus)*, J. Ac. Soc. Am. 82(6), pp 1901-1912.

Webb, S.C., 1998. Broadband Seismology and Noise Under the Ocean, *Rev. Geophys.*, 36(1), 105–142.

Webb, S.C., X. Zhang, and W. Crawford (1991). Infragravity Waves in the Deep Ocean, J. Geophys. Res., 96(C2), 2723–2736.

Zitellini, N., Chierichi, F., Torelli, L., 1999. The Tectonic Source of the 1755 Lisbon Earthquake and Tsunami, Annali di Geofisica 1999; 42:49-55.

Zitellini, N., Mendes-Victor, L.A., Cordoba, D., Danobeitia, J., Nicolich , R., Pellis, G., Ribeiro, A., Sartori, S., Torelli,L., Bartolome, R., Bortoluzzi, G., Calafato, A., Carrilho, F., Casoni, L., Chierici, F., Corela, C., Correggiari, A., Della Vedova, B., Gracia, E., Jornet, P., Landuzzi, M., Ligi, M., Magagnoli, A., Marozzi, G., Matias, L., Penitenti, D., Rodriguez, P., Rovere, M., Terrinha, P., Vigliotti, L., Zahinos Ruiz, A., 2001. Source of the 1755 Lisbon earthquake and tsunami investigated. EOS 2001; 82(26).

Appendix A

OBS dataless seed information

MCS input: 10 Vss
Guralp CMG 40T output: 4.2 Vss
System MCS + CMG 40T: 4.2 Vss

24 bits = 2^24 = 16 777 216 counts – equivalent to 10 Vss
1V = 1 677 721.6 counts

Seismometer sensitivity: 2000 V/m/s single ended → 3 355 443 200 counts/m/s

1 count = 596.04645 nV/Gain
q_vel_mod=0.29802 nm/s/Gain